Carbon-catalyzed hydrolysis of cellulose to cello-oligosaccharides

(炭素触媒によるセルロースのセロオリゴ糖への加水分解反応)

Pengru Chen

Hokkaido University

北海道大学

2020

Table of Contents

Chapter 1

General introduction

1.1 General background

Before the discovery of fossil fuels, trees and agricultural crops were the main source of chemicals and fuels. These bio-based chemicals were replaced by easily available petrochemicals over the course of two centuries.[1] The availability of these low-cost fuels and chemicals played a major role in industrializing the world and creating the modern society we know today. However, the finite nature of fossil fuel reserves has become apparent in recent dacades.[2] The continuous increase in demand for petroleum resources, combined with accumulation of carbon dioxide and other greenhouse gases in the earth's atmosphere causing increase in global temperatures,[3-5] has made it apparent that a shift towards sustainable and environmentally benign resource is required. This has renewed the interest in using bioresources as raw materials for chemical production.[6] While the shift to bio-based chemicals creates opportunities for discovery of novel compounds, it also requires a process overhaul to produce established chemical building blocks from a highly oxygenated chemical resource. Therefore, extensive research is required to understand the chemical composition of biomass derived resource and to convert them to industrially relevant chemicals.

Lignocellulosic biomass, a composite material found in plants, has been the frontrunner as an alternative resource for chemicals and carbon-based fuels.[7] It is considered as an inexhaustible and abundant carbon resource on our planet.

Lignocellulose is primarily composed of polysaccharides cellulose and hemicellulose as well as a phenylpropanoid polymer called lignin, which can be potentially refined to valuable carbon-based chemicals that possess similar or improved properties compared to those obtained from fossil fuels.[8-10] Being inedible for human beings, lignocellulose processing at large-scale for chemical synthesis will not hamper food supplies, which is an important distinction from resources such as corn and starch.[7,11] Therefore, the development of innovative enzymatic and catalytic processes for conversion of lignocellulose has the potential to create a future when chemical synthesis will be sustainable and not detrimental to the environment.

1.2 Cellulose

Cellulose is the major component of lignocellulose with its proportion varying from 35-50 % between different species of plants. It is estimated that nearly half of the organic carbon in the biosphere is present in the form of cellulose.[7] Therefore, in the context of converting lignocellulosic biomass to valuable chemicals, the utilization of cellulose is of paramount importance and is seen as an entry point for biorefinery.

Cellulose is composed solely of repeated anhydro-glucose units (AGU) linked by β-1,4-glycosidic bonds in C1 and C4 positions as shown in Figure 1.1a.[12] To accommodate the preferred bond angles of the acetal oxygen bridges, adjacent AGU ring in a cellulose chain is rotated 180^{o} in the axial plane. The lack of any bonds other than β-1,4-glycosidic linkages in cellulose gives rise to linear polymeric molecules. Each cellulose molecule has a direction since the terminal groups on the chain ends are different: nonreducing end with closed ring structure or reducing end with cyclic hemiacetals in equilibrium with aliphatic form having a carbonyl group. The chain length, termed as degree of polymerization (DP), is defined by the number of repeating AGU in cellulose molecule. Generally, the DP of cellulose ranges from about 100 to

1400 depending on the origin and treatment of raw materials and can be as high as 10,000 in materials such as cotton.[12,13]

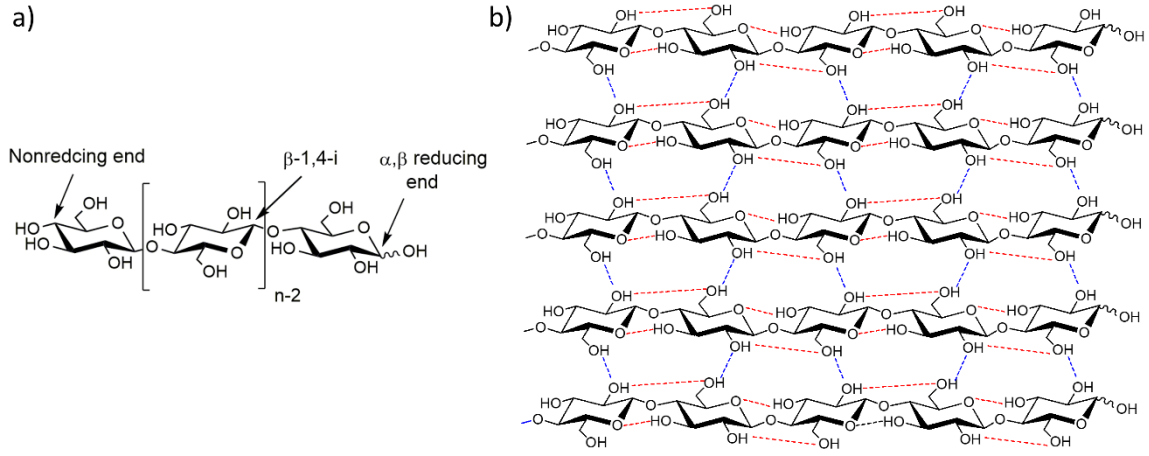

Figure 1.1. a) Elementary structure of a cellulose chain. b) Illustration showing hydrogen bonding in the extended cellulose structure.

The extended structure of cellulose is a result of hydroxyl groups arranged in equatorial position that link with neighboring AGU through inter and intra-molecular hydrogen bonds (Figure 1.1b). This ordered molecular structure imparts cellulose with its characteristic properties including, crystallinity, chirality, and insolubility, resulting in a material impermeable to mild chemical attacks.

1.3 Complete depolymerization of cellulose

Depolymerization of cellulose by hydrolysis of β-1,4-glycosidic bonds is the first step in obtaining small molecules for the synthesis of value-added chemicals. However, the closely packed structure of cellulose chains through hydrogen bonds in association with van der Waals interactions create a barrier for solvents and reactants from accessing the β-1,4-glycosidic bonds.[14,15] Therefore, only the external surface of cellulose is exposed to reactants, which severely reduces the rate of reaction. Several pretreatment methods such as partial chemical degradation,[16] mechanical comminution,[17] nonthermal atmospheric plasma technology,[18] and many others are

employed to disrupt the structural integrity of cellulose and increase its reactivity.[19,20]

1.3.1 Catalytic conversion of cellulose to glucose

The transformation of cellulose to glucose is a pre-requisite for a synthesis of wide range of valuable chemicals and biofuels (Figure 1.2).[21] Glucose is synthesized during the decomposition of cellulose by complete cleavage of β-1,4-glycosidic linkages through enzymatic or catalytic treatment. The hydrolysis of cellulose through enzymes can limit the formation of unwanted byproducts.[17] Enzymes such as cellulases and β-glycosidase are usually employed for the production of glucose from cellulose. They can bind with the cellulose molecules through CH-π and hydrophobic interaction with aromatic residues.[22,23] The enzymatic hydrolysis of cellulose is concomitant with pre-treatment using ionic liquid (IL), for example [BMIM]Cl, to enhance the dissolution of cellulose. It was reported that celluloses regenerated from IL solutions are subject to faster conversion than untreated substrates.[24] Adding IL into reaction solvent (usually water) resulted in over 70% of the microcrystalline cellulose conversion to glucose.[25] However, ILs are toxic and so far the use of enzymes is not economical for a large-scale operation.

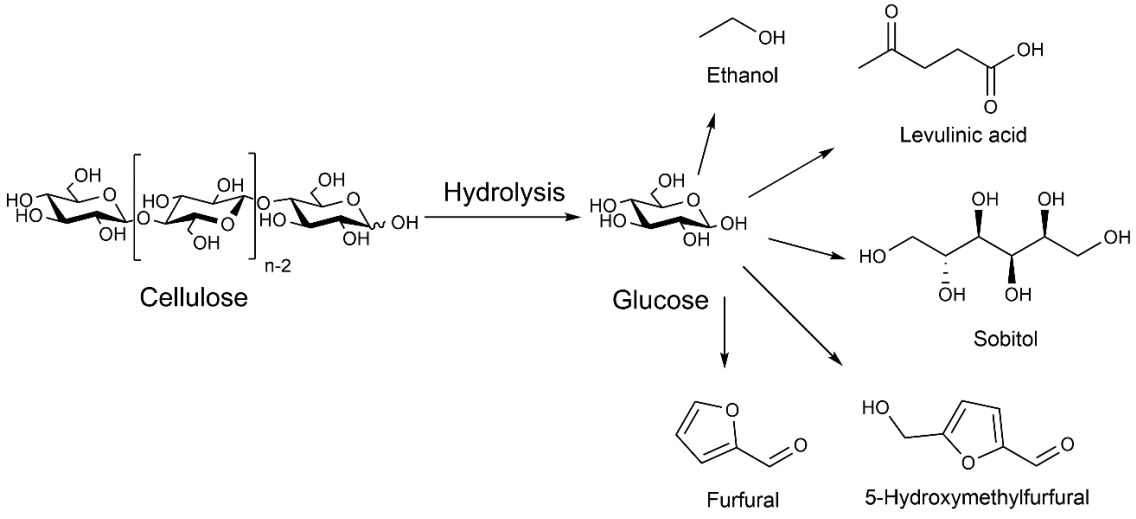

Figure 1.2. Hydrolysis of cellulose to glucose and its subsequent conversion of value-added chemicals.

Mineral acids are conventional homogeneous catalysts for transforming cellulose to sugars.[26,27] For example, sulfuric acid (H_2SO_4) has received considerable attention for catalyzing hydrolysis of cellulose and has been implemented on relatively large scales in industries.[28,29] However, during this process, further degradation or dehydration of glucose is an issue because the activation energy for degradation is similar to the energy for the hydrolysis of cellulose.[30] It has been reported that more than 50 % of glucose can be obtained in a plug flow reactor by using H_2SO_4 (1 wt%) aqueous solution.[31] Cellulose breakdowns into glucose in concentrated (12 M) HCl at room temperature without the formation of excess byproducts.[29] In a dilute solution, up to 85 % yield of glucose was obtained by the catalysis of HCl combined with $CaCl_2$ or LiCl, which was explained by the swelling effect in the cellulosic fibers. While these examples show that mineral acids act as highly active catalysts for cellulose utilization, their use is often energy-inefficient and riddled with problems of separation, recycling, and waste neutralization.

Use of heterogeneous catalyst for cellulose hydrolysis has been the topic of intense research in the past 15 years.[32,33] Efficient catalysts require a high density of accessible and strong Brønsted acid sites with high stability in aqueous environments.[34] Hara and Onda et al. used sulfonated carbon catalysts prepared by sulfonating activated carbon materials with sulfuric acid for complete hydrolysis of cellulose to glucose.[35-37] Glucose yield of 41 % was achieved over this carbon catalyst (AC-SO_3H) at 423 K for 24 h.[37] Mesoporous carbon CMK-3 treated by sulfonic acid also showed high activity, giving a 75 % yield of glucose.[38] Furthermore, sulfonated silica / carbon nanocomposites have also been demonstrated to hydrolyze cellulose with high yield of glucose.[32] Weakly oxygenated functional groups on carbon surface such as carboxyl and phenolic groups also show high activity when there is good contact between

substrate and catalyst. Carbon catalyst with oxygenated functional groups will be discussed in detail in Section 1.4.

1.3.2 Catalytic conversion of cellulose to other valuable chemicals

Promising routes for utilization of cellulose to synthesize other valuable chemicals are also emerging such as complete conversion to sorbitol, methyl glycosides, ethylene glycol, and 5-HMF.[39-41] Apart from reducing the process costs, direct conversion of cellulose to these compounds can also increase product selectivity owing to the rapid secondary conversion of glucose, which can decompose to byproducts.

Sorbitol is thermally more stable than glucose and the first monomeric compound to be produced from cellulose using heterogeneous catalysts (Figure 1.3). The hydrolytic hydrogenation of cellulose using Pt/γ-Al_2O_3 catalyst produced sorbitol in 25 % yield under reducing reaction conditions.[42] In this reaction, cellulose underwent hydrolysis to glucose followed by rapid hydrogenation to sorbitol. However, the Al_2O_3 was not durable in hot water, causing aggregation of metal nanoparticles.[43] Ru/CNT catalyst was water tolerant and showed high activity with 40 % yield of sugar alcohols from microcrystalline cellulose. The sugar alcohol yield was improved to 73 % when cellulose was pretreated using H_3PO_4.[44] Pt when supported on a carbon black BP2000 was also selective and durable catalyst, resulting in 58-65% yield of sugar alcohols.[45] Kinetic analysis showed that Pt catalyst promoted both the hydrolysis and the hydrogenation reaction and the rate-determining step was the hydrolysis of cellulose. Use of Ni can reduce the cost of catalyst preparation from precious metals and catalysts, such as Ni/CNF,[46] Ni_2P[47] and Ni/KB[48] have been reported. Large particle size of Ni was essential for durability of Ni catalyst, which is contrary to the conventional notion that small metal particles are better catalysts. Nevertheless, carbon supports were most effective owing to their high surface area, stability and strong metal support interaction.

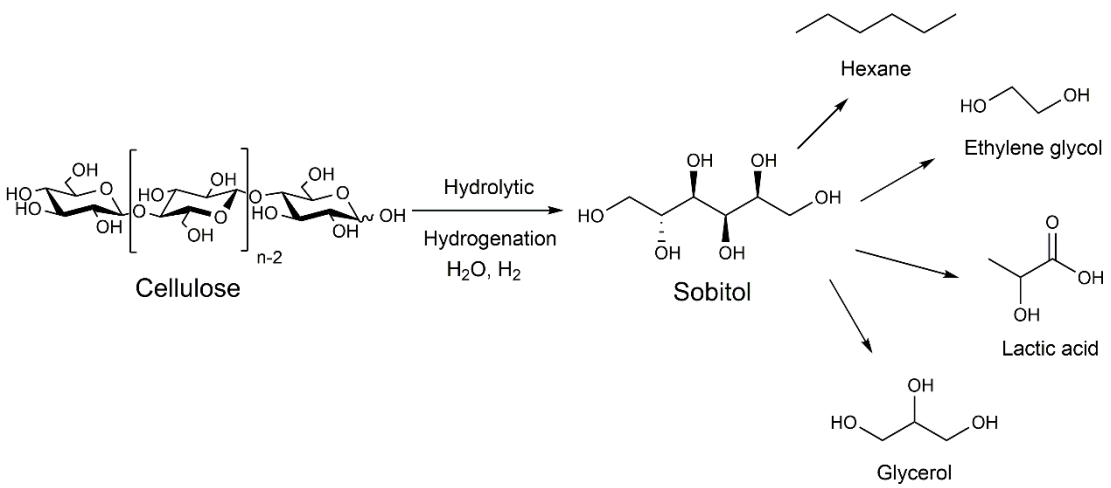

Figure 1.3. Hydrolytic hydrogenation of cellulose to sorbitol and its subsequent conversion of other chemicals.

Methyl glycosides are raw materials for producing non-ionic surfactants, detergents, and cosmetics. They can be obtained by depolymerization of cellulose in supercritical methanol instead of water. Acid catalysts are used to aid the cleavage of β-1,4-glycosidic bonds. The methyl group is then replaced with larger alkyl groups such as n-butanol[49] or n-dodecanol[50] to produce amphiphilic alkyl glycosides.

Other notable chemicals that can be directly produced from cellulose include ethylene glycol and 5-HMF (Figure 1.4). One-pot catalytic hydrocracking of cellulose by carbon supported Ni-W_2C catalyst produces ethylene glycol with up to 61% yield under 6 MPa of H_2 in 30 min.[51] While the direct synthesis of 5-HMF from cellulose is highly attractive, the low thermal stability of 5-HMF requires separation of hydrolysis and 5-HMF synthesis steps.[52]

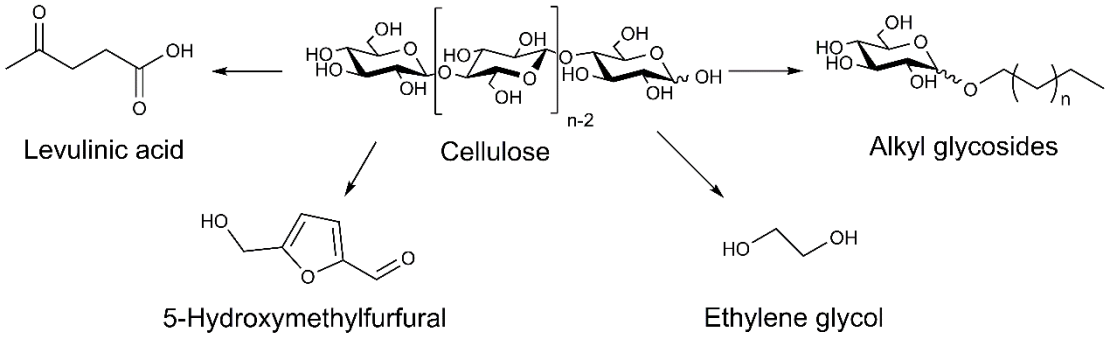

Figure 1.4. Direct transformation of cellulose to platform chemicals.

1.4 Partial depolymerization of cellulose to oligosaccharides

Although, the complete depolymerization of cellulose acts as a gateway to several value-added chemicals, partial hydrolysis of β-1,4-glycosidic bonds can produce carbohydrate with favorable properties and high value (Figure 1.5). Partial hydrolysis produces water-soluble carbohydrates with low molecular weight that mimic the repeating structure of cellulose. These glucans are called oligosaccharides and they have a degree of polymerization typically lower than 15. They are present as intermediates during the acid catalyzed transformation of cellulose to glucose. Even though cellulose only consists of β-1,4-glycosidic linkages, the oligosaccharides derived from it can contain other linkages as a result of glycosylation during the reaction. Examples of such linkages are *α*-1,4, α/β-1,3, α/β-1,6, and α/β-1,2-glycosidic linkages, with α-1,6 being the most abundant secondary linkage. The relatively lower degree of polymerization causes the oligosaccharides to be soluble in water and increases their reactivity. These oligosaccharides are sometimes used as alternative to glucose for downstream synthesis of chemical such as sorbitol[53] or 5-HMF.[54]

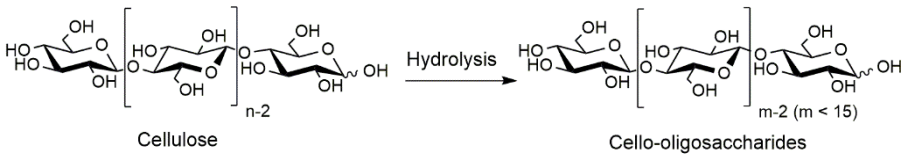

Figure 1.5. Partial hydrolysis of cellulose to water-soluble cello-oligosaccharides.

1.4.1 Influence of oligosaccharides on physiology

Oligosaccharides are biologically active molecules with physiological properties that benefits health of humans, animals and plants. One of the most glaring examples is that oligosaccharide is potential candidate as a functional food for human consumption. Unlike starch and simple sugars, oligosaccharides are classified as non-digestible carbohydrates due to the lack of enzymes required to digest them.[55] Therefore, they can be used as a non-calorific sweetener and texture enhancer in food products.[56] The sweetness is related with the size of the oligosaccharides DP, making them quite favorable in various food production than conventional sweetners.[57] Moreover, oligosaccharides influence the metabolism of bacteria in the human gut as they are not digested in the upper gastrointestinal tract.[58] Some oligosaccharides can stimulate the growth and metabolic activity of bacteria species beneficial for health. This prebiotic effect improves the composition of gut-microbiome, resulting in various health benefits.[59,60]

The physiological properties of oligosaccharides are also prominent in animal husbandries such as farming of pigs and calves. It was reported that dietary supplementation with cello-oligosaccharides (oligosaccharide with only β-1,4 linkages) improved the growth of weanling pigs, leading to higher productivity.[61] A similar study concluded that co-feeding cello-oligosaccharides to calves reduced the instances of diarrhea and decreased the use of antibiotics.[62]

Another important application of oligosaccharides is in the field of eco-friendly agriculture.[63] Cellulose-derived oligosaccharides are perceived as signal molecules in plant and their presence triggers the cell wall surveillance system for signs of danger. Consequently, a low-concentration dose of oligosaccharides to plant can induce an immune response and provides natural protection against pathogens, resulting in higher

yield of crops.[64]

The multitude of applications for oligosaccharides in healthcare and other industries has generated interest in their synthesis and accurate characterization. In addition, cello-oligosaccharides also serve as model compounds for cellulose and provide fundamental insight on crystallinity, solubility, and hydrolysis. However, the application and research in use of oligosaccharides is severely limited by their availability and high cost. In this work we have devoted our attention towards oligosaccharides derived from cellulose. Currently, cellobiose, a dimer, is the only commercially available cello-oligosaccharide. Higher oligosaccharides are available in small amounts and are difficult to produce as the chain length increases.

1.4.2 Enzymatic depolymerization

Various efforts have been made to develop pathways for synthesis of cello-oligosaccharides. In general, there are two main strategies, namely, enzyme-based and acid-based hydrolysis of cellulose. Enzymatic hydrolysis is considered attractive due to the relatively mild reaction condition, resulting in less byproducts formation. Although the research in enzymatic hydrolysis of cellulose is focused on production of glucose, this strategy has been modified to produce cello-oligosaccharides. Sasaki et al. used cellulase for enzymatic hydrolysis of cellulose and activated carbon as an adsorbent for cello-oligosaccharides. In their research, cellobiose and cellotriose were main products except glucose.[65] However, secondary hydrolysis of cello-oligosaccharides over β-glucosidase is a major drawback in this process. Therefore, in order to increase cello-oligosaccharides yield, β-glucosidase should be removed from cellulase mixture while retaining endo-glucanases, which randomly cleave the cellulose chains to release short chain cello-oligosaccharides (Figure 1.6).[66] β-Glucosidase has a low binding affinity to cellulosic substrates due to the lack of cellulose-binding domain in its structure.

Consequently, it can be separated by filtration after adsorption cellulase enzymes over the surface of cellulose.[67]

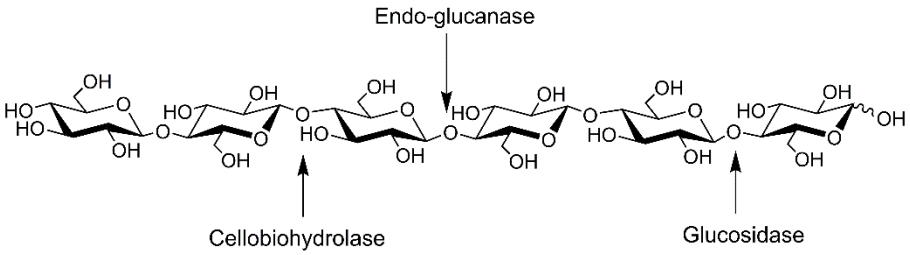

Figure 1.6. Scheme showing glycosidic bonds targeted by different enzymes during cellulose hydrolysis.

This strategy runs into another problem as the accumulation of synthesized cello-oligosaccharides, especially cellobiose, forms an enzyme-saccharide complex and inhibits the activity of endo-glucanases.[68,69] Multi-stage reaction system can overcome this problem by removing the product from the reaction media to prevent inhibition.[70,71] Yong et al. used a three-stage process for enzymatic hydrolysis of corncob residues with the β-glucosidase deficient cellulase. They could obtain cello-oligosaccharides with 52 % yield after this three-stages hydrolysis of 6 h/6 h/12 h, whereas only 25 % yield of cello-oligosaccharides was obtained in a single-stage process under the same reaction condition.[72] However, enzymatic process suffers from issues such as the high cost of enzymes, relatively long hydrolysis time and limited potential for scaleup.

1.4.3 Acidic depolymerization

Partial depolymerization of cellulose by acid-catalyzed processes is also an attractive approach to synthesize oligosaccharides. The acid catalyzed hydrolysis of cellulose follows the same basic mechanism irrespective of the choice between homogeneous and heterogeneous catalysts (Figure 1.7).[30] In the first step, oxygen atom in the glycosidic bond is protonated by the acid catalyst, resulting in cleavage of the bond. This is followed by the formation of a cyclic carbocation requiring conformational change of the tetrahydropyran ring. Finally, a water molecule reacts

with the carbocation to reestablish the anomeric center and complete the catalytic cycle.

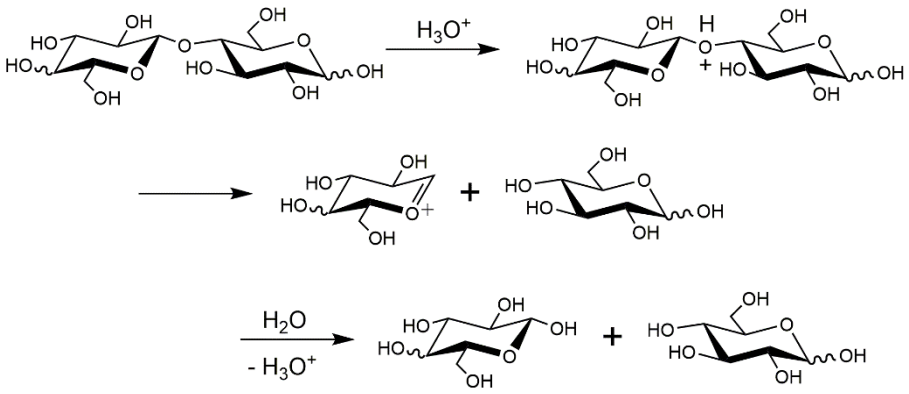

Figure 1.7. Mechanism of acid catalyzed hydrolysis of cellulose.

1.4.3.1 Homogeneous acidic hydrolysis

The use of homogeneous acid catalysts for hydrolysis of cellulose was first reported about a century ago. From early days it is known that the rate of hydrolysis depends on the pK_a of the acids as strong acids are more effective in protonating the glycosidic oxygen. Therefore, sulfuric acid and hydrochloric acid with strong acidity are the obvious candidates for this process.[73,74] Liebert et al. reported a process that combined the treatment of cellulose in 85 % phosphoric acid for 30 minutes at room temperature followed by further hydrolysis for 20 hours at 55 ^oC as an efficient method for cello-oligosaccharide synthesis.[75] They obtained a yield of 53 % of oligosaccharides with an average DP of 7.5 and a polydispersity index of 1.7. HF-SbF_5, a superacid, was also able to selectively depolymerize cellulose to water-soluble glucans (DP<13) at 0 °C, avoiding the formation of byproducts.[76] It was asserted that the DP of oligosaccharides could be adjusted according to the amount of SbF_5 used. A common problem faced under homogeneous reaction conditions is that the oligosaccharides obtained can rapidly undergo further hydrolysis to glucose if the reaction conditions are not precisely controlled. In addition, issues such as catalyst separation, waste disposal

and toxicity limited the application of these methods in food and agricultural industries.

1.4.3.2 Heterogeneous acidic hydrolysis

The difficulties in homogeneous process has led to development of solid acid catalytic systems for selective depolymerization of cellulose to oligosaccharides.[77] Amberlyst 15, an acid resin functionalized with sulfonic groups (-SO_3H) was reported as a promising catalyst for selective depolymerization of cellulose dissolved in ionic liquids (BMIMCl).[78] The reaction resulted in formation of water-soluble oligosaccharides with negligible production of mono- and disaccharides. A large external surface area of catalyst was essential to obtain high activity. In the case of solid acid zeolites, the acid sites are located within the micropores and are inaccessible to cellulose chains. For this reason, zeolites have generally shown inferior performance in cellulose hydrolysis.[44] Other oxide supports such as $HNbMoO_6$, having a layered transition-metal oxide, can exhibit strong Brønsted acidity attributed to bridged –OH groups formed on nanosheets.[79,80] While these catalysts are active for hydrolysis of cellulose, controlling the reaction to selectively obtain cello-oligosaccharides remains a challenge.

Heterogeneous carbon catalysts emerged a decade ago for sustainable depolymerization of cellulose to glucose and have shown promise for cellulose hydrolysis to cello-oligosaccharides.[81] Carbon based catalysts are relatively stable under hydrothermal conditions, an essential attribute in cellulose hydrolysis process.[82,83] In addition, carbon catalyst have large surface areas along with ability to adsorb cellulose. During heterogeneous reaction, good contact between cellulose and catalyst is essential because both of them are insoluble in water. The polyaromatic surface of carbon can adsorb glucans through CH-π and hydrophobic interactions, a behavior analogous to cellulose hydrolyzing enzymes (Figure 1.8a).[84-86] Following

adsorption, the glycosidic bonds can be hydrolyzed by acid sites on the carbon surface. Onda et al. firstly described the cellulose hydrolysis by using carbon catalyst functionalized with sulfonic groups (-SO_3H).[37,87] They obtained glucose as the main product owing to rapid degradation of oligosaccharides under the strong acidic environment. Suganuma et al. also prepared an amorphous carbon catalyst through carbonization of cellulose with strong (SO_3H) and weak acid (COOH and OH) functional groups. [35,88] This catalyst showed a preference for the conversion of long cellulose chains to water-soluble β-1,4 glucan with a yield of 64 %.

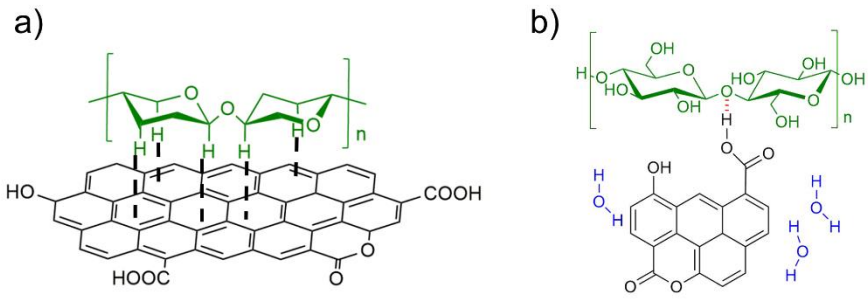

Figure 1.8. Hydrolysis of cellulose over carbon catalysts, a) Adsorption of cellulose molecule on carbon surface, b) Hydrolysis of β-1,4-glycosidic bonds by acid sites.

Soon it was realized that porous carbons can show hydrolysis activity even when strong acid (SO_3H) functional groups were not present.[38,89,90] CMK-3, a mesoporous carbon material, was able to selectively hydrolyze cellulose to oligosaccharides with 24 % yield.[32] Weakly acidic functional groups, such as carboxyl and phenolic groups (COOH and OH) acted as the active sites (Figure 1.8b). These functional groups are more durable than the sulfonic groups (SO_3H), which are liable to leach out under hydrothermal condition.[91,92] K26, an alkali activated carbon with oxygenated functional groups, when ball milled with cellulose before hydrolysis, gave 70 % yield of cello-oligosaccharides with a DP in the range of 2 to 6.[93] Another carbon catalyst prepared by air-oxidation of activated carbon showed good activity for cellulose hydrolysis with

96 % conversion and 62 % yield of cello-oligosaccharides.[94] These results show that carbon materials have the potential to be a stable and environmentally benign catalyst for cello-oligosaccharide synthesis.

1.4.4 Mechanocatalysis

Recently, mechanocatalytic depolymerization of cellulose in the absence of solvents has emerged as a promising approach to convert recalcitrant cellulose into water-soluble products. This process is based on a synergistic effect between acid catalysts and mechanical forces. Mechanocatalysis can facilitate the conformational change of the pyranose ring followed by protonation and cleavage of the β-1,4 glycosidic bond.[95] Blair et al. first reported the mechanocatalytic depolymerization of cellulose in the presence of a solid kaolinite catalyst to water-soluble fractions.[96] However, monomers were the main products in their reaction. Schüth group demonstrated that ball milling HCl impregnated cellulose in a solvent-free environment was capable of converting cellulose into water-soluble oligosaccharides within 2 h.[56,97] Main products obtained in this case were low molecular weight glucans with a degree of polymerization ranging from 2 to 7. Lignocellulosic materials, for example sugarcane bagasse, beechwood, and pinewood, were also transformed by this mechanocatalytic method into soluble products within 2-3 h. Their further studies on depolymerization of HCl-impregnated beechwood by mechanocatalytic method showed the formation of water-soluble products with 74 % yield after a milling for a similar duration of 2 h.[98]

Structural analysis of soluble oligosaccharides obtained from mechanocatalysis revealed a non-linear structure. Beltramini et al. employed high resolution NMR spectroscopy to elucidate that besides β-1,4 linkages, the α-1,6 linkages were also present, which contributed to increased solubility of products in water.[99] Formation of

branches was ascribed to acid-catalyzed repolymerization of glucose and other small molecules produced during the milling process. Lack of solvent was crucial for faster hydrolysis rate and was also responsible for branch formation. Fan et al. co-impregnate glucose during mechanocatalysis to facilitate formation of α-1,6 branches which resulting in an increase in the yield of water-soluble oligosaccharides.[100] Although, mechanocatalysis has several advantages over conventional processes, the branching in oligosaccharide structure is detrimental for application in healthcare industry. This issue also raises the crucial point of rigorous analysis of oligosaccharide structure to screen them for unwanted branch formation.

1.4.4 Other non-catalytic methods

A few other methods have also been successful in obtaining oligosaccharides from cellulose. Flash pyrolysis of cellulose can produce anhydro-oligosaccharides, containing a dehydrated reducing end. Products in the range of cellobiose to celloheptaose were detected in this method.[101] Non-thermal atmospheric plasma (NTAP) technology has also been used to produce oligosaccharides with controlled distribution.[102] Jérôme group claimed that the NTAP treatment can selectively cleave the β-1,4 glycosidic bond in cellulose without the assistance of any catalyst or solvent, decreasing the DP from 250 to 120 within a few minutes.[103] Their further study demonstrates that NTAP promotes the partial cleavage of the β-1,4 glycosidic bond of cellulose leading to the release of short-chain cellodextrins.[104] Sub-and supercritical water also has the ability to hydrolyze cellulose with a 40 % yield formation of oligosaccharides.[105,106]

1.5 Objective of this work

Cello-oligosaccharides are water soluble linear polymers of glucose linked by β-1,4-glycosidic bonds. They are biologically active with broad application in the

agricultural and healthcare industries. However, their industrial synthesis faces many hurdles encompassing lack of suitable technology and poor understanding of their reactivity. From an environmental point of view, it is sensible to produce cello-oligosaccharides from cellulose, a renewable and sustainable chemical feedstock. Therefore, the aim of this work is to selectively synthesize cello-oligosaccharides using catalytic hydrolysis of cellulose. The work aims at technology development for synthesis and characterization of cello-oligosaccharides, mechanistic insight into the hydrolysis reaction and designing novel catalyst based on generated knowledge.

In order to selectively produce cello-oligosaccharides via the depolymerization of cellulose, a heterogeneous carbon catalyst was prepared with weakly acidic functional groups on the surface. Furthermore, new carbon catalysts with higher concentration of acidic function groups were synthesized to improve the hydrolysis activity. The applications of cello-oligosaccharides depend on their degree of polymerization. Therefore, I plan to develop a method to quantify individual cello-oligosaccharides and try to control the distribution of products.

1.6 Outline of the thesis

The thesis starts with a focus on efficient synthesis of cello-oligosaccharides (DP more than 3) from cellulose using an existing carbon catalyst (Chapter 2). Cello-oligosaccharides are more reactive than cellulose and a major challenge in this method was to prevent their further degradation during the hydrolysis reaction. My strategy involved use of a carbon catalyst that shows high cellulose hydrolysis activity in combination with a semi-flow reactor, in which the products can be rapidly removed from reaction system to achieve high cello-oligosaccharide yield. The effect of pretreatment method, reaction temperature and mix-milling duration were also investigated. In addition, a method for quantitative analysis of individual cello-

oligosaccharides in the product mixture was developed by using MALDI-TOF MS method. The quantification holds significance in the cello-oligosaccharide research to evaluate their efficacy based on their chain length. Furthermore, the distribution of products was adjusted by changing the space velocity of the reactor.

Chapter 3 is aimed at understanding the mechanism of hydrolysis of β-1,4-glycosidic bond in cellulose over carbon catalysts. Cello-oligosaccharides were used as model compounds to evaluate the change in rate of hydrolysis with respect to molecule size and elucidate the underlying factors from a mechanistic perspective. The hydrolysis over other heterogeneous catalysts and homogeneous H_2SO_4 were also performed to compare with carbon catalyst. The adsorption capacity and activation energy during the hydrolysis were evaluated and a plausible mechanism was proposed for the reaction leading to high cello-oligosaccharide yield.

Based on the results from Chapters 2 and 3, it is deduced that cello-oligosaccharide yield can be improved by designing a catalyst with very high density of functional groups. Chapter 4 aims to create such a catalyst by using chemical oxidation methods to introduce high density of oxygenated functional groups. Different kind of activated carbon were used to compare their hydrolysis performance on cellulose hydrolysis. The synthesized catalysts were analyzed by XPS, FTIR, N_2 adsorption and TPD to characterize the properties and correlate the catalytic properties with cello-oligosaccharide yield and distribution.

Finally, this work is summarized and an outlook on future challenges along with possible approaches to overcome them is included.

References

1. A. J. Ragauskas, C. K. Williams, B. H. Davison, G. Britovsek, J. Cairney, C. A. Eckert, W. J. Frederick, Jr., J. P. Hallett, D. J. Leak, C. L. Liotta, J. R. Mielenz, R. Murphy, R.

Templer and T. Tschaplinski, *Science*, 2006, **311**, 484-489.

2. T. E. Amidon and S. Liu, *Biotechnol. Adv.*, 2009, **27**, 542-550.
3. M. I. Hoffert, K. Caldeira, G. Benford, D. R. Criswell, C. Green, H. Herzog, A. K. Jain, H. S. Kheshgi, K. S. Lackner, J. S. Lewis, H. D. Lightfoot, W. Manheimer, J. C. Mankins, M. E. Mauel, L. J. Perkins, M. E. Schlesinger, T. Volk and T. M. L. Wigley, *Science*, 2002, **298**, 981-987.
4. M. a. R. Rodríguez, J. D. Ruyck, P. R. Díaz, V. K. Verma and S. Bram, *Appl. Energy*, 2011, **88**, 630-635.
5. W. P. Nel and C. J. Cooper, *Energy Policy*, 2009, **37**, 166-180.
6. J. P. H. V. Wyk, *Trends Biotechnol.*, 2001, **19**, 172-177.
7. C.-H. Zhou, X. Xia, C.-X. Lin, D.-S. Tong and J. Beltramini, *Chem. Soc. Rev.*, 2011, **40**, 5588-5617.
8. C. Li, X. Zhao, A. Wang, G. W. Huber and T. Zhang, *Chem. Rev*, 2015, **115**, 11559-11624.
9. G. W. Huber, S. Iborra and A. Corma, *Chem. Rev.*, 2006, **106**, 4044-4098.
10. L. S. T. Mika, E. CséFalvay and A. R. NéMeth, *Chem. Rev.*, 2018, **118**, 505-613.
11. M. R. Schmer, K. P. Vogel, R. B. Mitchell and R. K. Perrin, *Proc. Natl. Acad. Sci. U. S. A.*, 2008, **105**, 464-469.
12. D. Klemm, B. Heublein, H.-P. Fink and A. Bohn, *Angew. Chem. Int. Ed.*, 2005, **44**, 3358-3393.
13. S. Kobayashi, J. Sakamoto and S. Kimura, *Prog. Polym. Sci.*, 2001, **26**, 1525-1560.
14. H. Zhao, J. E. Holladay, J. H. Kwak and Z. C. Zhang, *J. Phys. Chem. B*, 2007, **111**, 5295-5300.
15. C. Loerbroks, R. Rinaldi and W. Thiel, *Chem. Eur. J*, 2013, **19**, 16282-16294.
16. Y. Sun and J. Cheng, *Bioresour. Technol.*, 2002, **83**, 1-11.
17. P. Kumar, D. M. Barrett, M. J. Delwiche and P. Stroeve, *Ind. Eng. Chem. Res.*, 2009, **48**, 3713–3729.
18. M. Benoit, A. Rodrigues, Q. Zhang, E. Fourré, K. D. O. Vigier, J. M. Tatibouët and F. Jérôme, *Angew. Chem. Int. Ed.*, 2011, **50**, 8964-8967.
19. M. J. Taherzadeh and K. Karimi, *Int. J. Mol. Sci.*, 2008, **9**, 1621-1651.
20. X. Zhao, K. Cheng and D. Liu, *Appl. Microbiol. Biotechnol.*, 2009, **82**, 815-827.
21. D. M. Alonso, J. Q. Bond and J. A. Dumesic, *Green Chem.*, 2010, **12**, 1493-1513.
22. G. Zolotnitsky, U. Cogan, N. Adirt, V. Solomon, G. Shoham and Y. Shoham, *Proc. Natl. Acad. Sci. U. S. A.*, 2004, **101**, 11275-11280.
23. W. Chen, S. Enck, J. L. Price, D. L. Powers, E. T. Powers, C.-H. Wong, H. J. Dyson and J. W. Kelly, *J. Am. Chem. Soc.*, 2013, **135**, 9877-9884.

24. H. Zhao, C. L. Jones, G. A. Baker, S. Xia, O. Olubajo and V. N. Person, *J. Biotechnol.*, 2009, **139**, 47-54.
25. N. Kamiya, Y. Matsushita, M. Hanaki, K. Nakashima, M. Narita, M. Goto and H. Takahashi, *Biotechnol. Lett.*, 2008, **30**, 1037-1040.
26. K.-I. Shimizu, H. Furukawa, N. Kobayashi, Y. Itaya and A. Satsuma, *Green Chem.*, 2009, **11**, 1627-1632.
27. Y. Ogasawara, S. Itagaki, K. Yamaguchi and N. Mizuno, *ChemSusChem*, 2011, **4**, 519-525.
28. E. E. Harris and E. Beglinger, *Ind. Eng. Chem. Res.*, 1946, **38**.
20. F. Bergius, *Ind. Eng. Chem. Res.*, 1937, **29**, 247-253.
30. R. Rinaldi and F. Schüth, *ChemSusChem*, 2009, **2**, 1096-1107.
31. D. R. Thompson and H. E. Grethlein, *Ind. Eng. Chem. Prod. Res. Dev.*, 1979, **18**, 166-169.
32. S. V. D. Vyver, L. Peng, J. Geboers, H. Schepers, F. D. Clippel, C. J. Gommes, B. Goderis, P. A. Jacobs and B. F. Sels, *Green Chem.*, 2010, **12**, 1560-1563.
33. T. Komanoya, H. Kobayashi, K. Hara, W.-J. Chun and A. Fukuoka, *Appl. Catal. A*, 2011, **407**, 188-194.
34. R. Rinaldi and F. Schüth, *Energy Environ. Sci.*, 2009, **2**, 610-626.
35. D. Yamaguchi, M. Kitano, S. Suganuma, K. Nakajima, H. Kato and M. Hara, *J. Phys. Chem. C*, 2009, **113**, 3181–3188.
36. K. Fukuhara, K. Nakajima, M. Kitano, H. Kato, S. Hayashi and M. Hara, *ChemSusChem*, 2011, **4**, 778-784.
37. A. Onda, T. Ochi and K. Yanagisawa, *Green Chem.*, 2008, **10**, 1033-1037.
38. J. Pang, A. Wang, M. Zheng and T. Zhang, *Chem. commun.*, 2010, **46**, 6935-6937.
39. Y. Liu, G. Li, Y. Hu, A. Wang, F. Lu, J.-J. Zou, Y. Cong, N. Li and T. Zhang, *Joule*, 2019, **3**, 1028-1036.
40. X. Liu, X. Liu, G. Xu, Y. Zhang, C. Wang, Q. Lu and L. Ma, *Green Chem.*, 2019, **21**, 5647-5656.
41. Y.-B. Huang, T. Yang, Y.-T. Lin, Y.-Z. Zhu, L.-C. Li and H. Pan, *Green Chem.*, 2018, **20**, 1323-1334.
42. A. Fukuoka and P. L. Dhepe, *Angew. Chem. Int. Ed.*, 2006, **45**, 5161-5163.
43. R. M. Ravenelle, J. R. Copeland, W.-G. Kim, J. C. Crittenden and C. Sievers, *ACS Catal.*, 2011, **1**, 552-561.
44. W. Deng, X. Tan, W. Fang, Q. Zhang and Y. Wang, *Catal. Lett.*, 2009, **133**, 167-174.
45. H. Kobayashi, Y. Ito, T. Komanoya, Y. Hosaka, P. L. Dhepe, K. Kasai, K. Hara and A. Fukuoka, *Green Chem.*, 2011, **13**, 326-333.

46. S. V. D. Vyver, J. Geboers, M. Dusselier, H. Schepers, T. Vosch, L. Zhang, G. V. Tendeloo, P. A. Jacobs and B. F. Sels, *ChemSusChem*, 2010, **3**, 698-701.
47. L.-N. Ding, A.-Q. Wang, M.-Y. Zheng and T. Zhang, *ChemSusChem*, 2010, **3**, 818-821.
48. H. Kobayashi, Y. Hosaka, K. Hara, B. Feng, Y. Hirosakia and A. Fukuoka, *Green Chem.*, 2014, **16**, 637-644.
49. F. Boissou, N. Sayoud, V. K. D. Oliveira, A. Barakat, S. Marinkovic, B. Estrine and F. Jérôme, *ChemSusChem*, 2015, **8**, 3263-3269.
50. A. Karam, K. D. O. Vigier, S. Marinkovic, B. Estrine, C. Oldani and F. Jérôme, *ChemSusChem*, 2017, **10**, 3604-3610.
51. C. Li, M. Zheng, A. Wang and T. Zhang, *Energy Environ. Sci.*, 2012, **5**, 6383-6390.
52. H. Zhao, J. E. Holladay, H. Brown and Z. C. Zhang, *Science*, 2007, **316**, 1597-1600.
53. J. Hilgert, N. Meine, R. Rinaldi and F. Schüth, *Energy Environ. Sci.*, 2013, **6**, 92-96.
54. R. Carrasquillo-Flores, M. Käldström, F. Schüth, J. A. Dumesic and R. Rinaldi, *ACS Catal.*, 2013, **3**, 993-997.
55. S. I. Mussatto and I. M. Mancilha, *Carbohydr. Polym.*, 2007, **68**, 587-597.
56. H. J. Flint, E. A. Bayer, M. T. Rincon, R. Lamed and B. A. White, *Nat. Rev. Microbiol.*, 2008, **6**, 121-131.
57. M. Roberfroid and J. Slavin, *Crit. Rev. Food Sci. Nutr.*, 2000, **40**, 461-480.
58. N.M.Delzenne and M.R.Roberfroid, *LWT - Food Sci. Technol.*, 1994, **27**, 1-6.
59. L. V. Hooper, M. H. Wong, A. Thelin, L. Hansson, P. G. Falk and J. I. Gordon, *Science*, 2001, **291**, 881-884.
60. M. Rivero-Urgell and A. Santamaria-Orleans, *Early Hum. Dev.*, 2001, **65**, S43–S52.
61. M. Otsuka, A. Ishida, Y. Nakayama, M. Saito, M. Yamazaki, H. Murakami, Y. Nakamura, M. Matsumoto, K. Mamoto and R. Takada, *Anim. Sci. J.*, 2004, **75**, 225–229.
62. T. Hasunuma, K. Kawashima, H. Nakayama, T. Murakami, H. Kanagawa, T. Ishii, K. Akiyama, K. Yasuda, F. Terada and S. Kushibiki, *Anim. Sci. J.*, 2011, **82**, 543-548.
63. A. A. Gust, R. Pruitt and T. Nürnberger, *Trends Plant Sci.*, 2017, **22**, 779-791.
64. C. D. A. Souza, S. Li, A. Z. Lin, F. Boutrot, G. Grossmann, C. Zipfel and S. C. Somerville, *Plant Physiol.*, 2017, **173**, 2383-2398.
65. Y. Kuba, Y. Kashiwagi, G. Okada and T. Sasaki, *Enzyme Microb. Technol.*, 1990, **12**, 72-75.
66. T. Homma, M. Fujii, J. I. Mori, T. Kawakami, K. Kuroda and M. Taniguchi, *Biotechnol. Bioeng.*, 1993, **41**, 405-510.
67. Q. Zhang and L.-K. Ju, *Enzyme Microb. Technol.*, 2011, **48**, 175-180.
68. J. S. V. Dyk and B. I. Pletschke, *Biotechnol. Adv.*, 2012, **30**, 1458-1480.

69. R. Kumar and C. E.Wyman, *Enzyme Microb. Technol.*, 2008, **42**, 426-433.
70. Z. Yu, H. Jameel, H.-M. Chang, R. Philips and S. Park, *Biotechnol. Bioeng.*, 2012, **109**, 1131-1139.
71. J. Yang, X. Zhang, Q. Yong and S. Yu, *Bioresour. Technol.*, 2010, **101**, 4930-4935.
72. Q. Chu, X. Li, Y. Xu, Z. Wang, J. Huang, S. Yu and Q. Yong, *Process Biochem.*, 2014, **49**, 1217-1222.
73. Q. Xiang, J. S. Kim and Y. Y. Lee, *Appl. Biochem. Biotechnol.*, 2003, **106**, 337-352.
74. D. J. Hayes, *Catal. Today*, 2009, **145**, 138-151.
75. T. Liebert, M. Seifert and T. Heinze, *Macromol. Symp.*, 2008, **262**, 140-149.
76. A. Martin-Mingot, K. D. O. Vigier, F. Jérômeb and S. Thibaudeau, *Org. Biomol. Chem.*, 2012, **10**, 2521-2524.
77. Y.-B. Huang and Y. Fu, *Green Chem.*, 2013, **15**, 1095-1111.
78. R. Rinaldi, R. Palkovits and F. Schüth, *Angew. Chem. Int. Ed.*, 2008, **47**, 8047-8050.
79. A. Takagaki, C. Tagusagawa and K. Domen, *Chem. Commun.*, 2008, DOI: 10.1039/b810346a, 5363-5365.
80. A. Takagaki, C. Tagusagawa, S. Hayashi, M. Harad and K. Domen, *Energy Environ. Sci.*, 2010, **3**, 82-93.
81. A. W. Heinen, J. A. Peters and H. V. Bekkum, *Carbohydr. Res.*, 2001, **330**, 381-390.
82. H. Nishihara and T. Kyotani, *Adv. Mater.*, 2012, **24**, 4473-4498.
83. M. Yabushita, K. Techikawara, H. Kobayashi, A. Fukuoka and A. Katz, *ACS Sustainable Chem. Eng.*, 2016, **4**, 6844-6851.
84. M. Yabushita, H. Kobayashi, J.-Y. Hasegawa, K. Hara and A. Fukuoka, *ChemSusChem*, 2014, **7**, 1443-1450.
85. J. D. Mccarter and S. G. Withers, *Curr. Opin. Struct. Biol.*, 1994, **4**, 885-892.
86. C. S. Rye and S. G. Withers, *Curr. Opin. Chem. Biol.*, 2000, **4**, 573-580.
87. A. Onda, T. Ochi and K. Yanagisawa, *Top. Catal.*, 2009, **52**, 801-807.
88. S. Suganuma, K. Nakajima, M. Kitano, D. Yamaguchi, H. Kato, S. Hayashi and M. Hara, *J. Am. Chem. Soc.*, 2008, **130**, 12787-12793.
89. J. Pang, A. Wang, M. Zheng, Y. Zhang, Y. Huang, X. Chen and T. Zhang, *Green Chem.*, 2012, **14**, 614-617.
90. A. Charmot, P.-W. Chung and A. Katz, *ACS Sustainable Chem. Eng.*, 2014, **2**, 2866-2872.
91. A. H. V. Pelt, O. A. Simakova, S. M. Schimming, J. L. Ewbank, G. S. Foo, E. A. Pidko, E. J. M. Hensen and C. Sievers, *Carbon*, 2014, **77**, 143-154.
92. P.-W. Chung, A. Charmot, O. A. Olatunji-Ojo, K. A. Durkin and A. Katz, *ACS Catal.*, 2013, **4**, 302-310.

93. H. Kobayashi, M. Yabushita, T. Komanoya, K. Hara, I. Fujita and A. Fukuoka, *ACS Catal.*, 2013, **3**, 581-587.
94. A. Shrotri, H. Kobayashi and A. Fukuoka, *ChemSusChem*, 2016, **9**, 1299-1303.
95. E. J. Cocinero, P. Çarçabal, T. D. Vaden, J. P. Simons and B. G. Davis, *Nature*, 2011, **469**, 76-79.
96. S. Hick, C. Griebel, D. T. Restrepo, J. H. Truitt, E. J. Buker, C. Bylda and R. G. Blair, *Green Chem.*, 2010, **12**, 468-474.
97. N. Meine, R. Rinaldi and F. Schüth, *ChemSusChem*, 2012, **5**, 1449-1454.
98. M. Käldström, N. Meine, C. Farès, F. Schüth and R. Rinaldi, *Green Chem.*, 2014, **16**, 3528-3538.
99. A. Shrotri, L. K. Lambert, A. Tanksale and J. Beltramini, *Green Chem.*, 2013, **15**, 2761-2768.
100. P. Dornath, H. J. Cho, A. Paulsen, P. Dauenhauer and W. Fan, *Green Chem.*, 2015, **17**, 769-775.
101. J. Piskorz, P. Majerski, D. S. Scott, A. Vladars-Usas and D. Radlein, *J. Anal. Appl. Pyrol.*, 2000, **56** 145-166.
102. F. Jérôme, *Curr. Opin. Green Sustain. Chem.*, 2016, **2**, 10-14.
103. M. Benoit, A. Rodrigues, K. D. O. Vigier, E. Fourré, J. Barrault, J.-M. Tatibouët and F. Jérôme, *Green Chem.*, 2012, **14**, 2212-2215.
104. J. Delaux, C. Ortizmellet, C. Canaff, E. Fourré, C. Gaillard, A. Barakat, J. M. García, J.-M. Tatibouët and F. Jérôme, *Chemistry*, 2016, **22**, 16522-16530.
105. D. A. Cantero, L. Vaquerizo, F. Mato, M. D. Bermejo and M. J. Cocero, *Bioresour. Technol.*, 2015, **179**, 136-143.
106. Y. Zhao, W.-J. Lu, and H.-T. Wang, *Chem. Eng. J.*, 2009, **150**, 411-417.

Chapter 2

Soluble cello-oligosaccharides produced by carbon-catalyzed hydrolysis of cellulose

Abstract

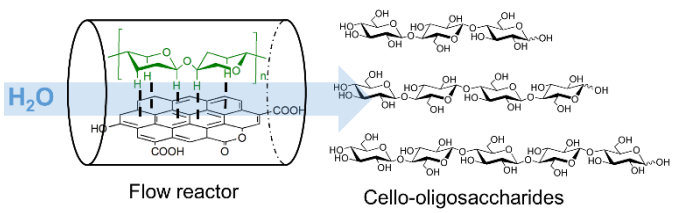

Cellulose is less reactive than water-soluble cello-oligosaccharides. Therefore, to achieve high yield of cello-oligosaccharides, it is essential to remove them from the reaction environment as soon as they are formed. This chapter focuses on maximizing the yield of water-soluble cello-oligosaccharides by preventing their further hydrolysis to cellobiose or glucose. To accomplish this goal, the hydrolysis of cellulose was performed over a carbon catalyst in a semi-flow reactor, resulting in high yield of cello-oligosaccharides (72 %). The excellent activity of the oxidized carbon catalyst, the adsorption of cellulose on the catalyst, and the high space velocity of products in the reactor were essential. Moreover, a method for quantification of individual cello-oligosaccharides was developed, which suggested a reduction in the rate of hydrolysis with a reduction in chain length.

2.1 Introduction

Cello-oligosaccharides are short-chain linear polymers of glucose linked by β-1,4-glycosidic bonds. They are biologically active molecules with physiological properties that can benefit the health and growth of plants, animals, and humans.[1,2] A low-concentration dose of cello-oligosaccharides to plant elicits an immune response and increases resistance towards diseases.[3,4] Animal studies have shown that adding cello-oligosaccharides to the feed of calves causes fewer incidences of gastrointestinal infections and reduces the use of antibiotics.[5] Cello-oligosaccharides also have the potential to act as a nondigestible prebiotic that can reduce the risk of lifestyle diseases in humans by promoting the growth of beneficial bacteria and inhibiting pathogenic bacterial species in the gastrointestinal tract.[2,6] Thus, cello-oligosaccharides can provide multiple benefits to the agricultural and healthcare industries.

Research for studying the benefits and application of cello-oligosaccharides is hindered by their limited availability. Cellobiose, containing two glucose units, is the only commercially available cello-oligosaccharide. Higher cello-oligosaccharides are produced in small amounts and are up to 500 times more expensive.[6] Commercial application of cello-oligosaccharides is not feasible until a cost-effective process is developed for their synthesis.

Cello-oligosaccharides can be produced by partial hydrolysis of cellulose, an abundant polysaccharide made up of β-1,4-linked glucose units.[7,8] However, the packed crystalline structure of cellulose and the presence of hydrogen bonds make it resistant to chemical attack.[9-11] Severe reaction conditions are required to overcome these barriers and cleave the β-1,4-glycosidic bonds by hydrolysis.[12] As a result, cello-oligosaccharides are only obtained as intermediates that rapidly hydrolyze to glucose during the reaction (Figure 2.1).

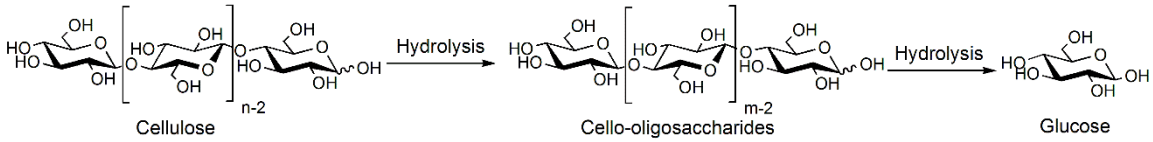

Figure 2.1. Cello-oligosaccharides are formed as intermediates in cellulose hydrolysis.

Previously, the enzymatic hydrolysis of cellulose was modified by removing β-glucosidase from the enzyme mixture to produce cellobiose from cellulose.[13] However, higher oligosaccharides cannot be obtained by this method. Homogeneous catalysts such as 3.8 % HF/SbF_5[14] and 85 % H_3PO_4[15] could dissolve and hydrolyze cellulose, resulting in cello-oligosaccharides with high degrees of polymerization (DP). Issues such as catalyst separation and toxicity limited the application of these methods in food and agricultural industries. Recently, depolymerization of cellulose was achieved by solvent-free mechanocatalysis.[16,17] Although cellulose was completely converted to water-soluble oligosaccharides, 70 % of them contained α-1,6 linkages formed by glycosylation of small sugar molecules.[18,19] These reports also highlight the importance of characterization of oligosaccharides to detect undesired functionalization.

Carbon materials containing oxygenated functional groups are potential heterogeneous catalysts for the synthesis of cello-oligosaccharides from cellulose.[9,20,21] These functional groups are stable under the ball-milling and hydrothermal conditions required for cellulose hydrolysis.[22,23] During the reaction, cellulose adsorbs on the carbon surface by CH-π and hydrophobic interactions,[24] and then the β-1,4-glycosidic bonds are hydrolyzed by the acidic functional group present on the catalyst surface.[25,26] Therefore, this work reports the use of carbon catalyst for hydrolysis of cellulose in a semi-flow reactor to obtain high yields of cello-oligosaccharides that can be readily used in food and agricultural industries.

2.2 Experimental Methods

2.2.1 Materials

Microcrystalline cellulose (Avicell PH-101) was purchased from Sigma Aldrich. Activated carbon (denoted AC) was supplied from Ajinomoto Fine-Techno. Distilled water and ethanol (99.5 %) were purchased from Wako Pure Chemical Industries. Granular SiO_2 (Q30, 100 - 200 mesh) was supplied from Fuji Silysia Chemical Ltd. Cellotriose (95 %), cellotetraose (95 %), cellopentaose (95 %) and cellohexaose (94 %) were purchased from Megazyme. Glucose and cellobiose were purchased from Kanto Chemical Industries. D_2O and DMSO-d_6 for proton nuclear magnetic resonance (^{1}H NMR) analysis was obtained from Sigma Aldrich.

2.2.2 Air-oxidation and characterization of carbon catalyst

For the preparation of carbon catalyst, activated carbon AC (4.0 g) was spread on a Pyrex dish of diameter 130 mm with a uniform thickness. The sample was then heated in an electric furnace under air with the following program: heating from 298 K to 393 K at a rate of 10 K min^{-1} and then maintaining at 393 K for 2 h to remove the physisorbed water, followed by heating to 698 K at a rate of 4 K min^{-1} and then maintaining at 698 K for a further 10 h. The obtained oxidized carbon catalyst was denoted as AC-Air (1.9 g, yield: 47.5 %). Specific surface area of carbon catalyst was determined by N_2 adsorption-desorption measurement (BEL Japan, BELSORP-min) after vacuum drying at 393 K for 3 h. Fourier transform infrared spectroscopy (FTIR) spectra of carbon catalyst was measured by making a KBr pellet containing 0.1 wt. % of sample, followed by using a PerkinElmer Spectrum 100 FTIR Spectrometer.

2.2.3 Ball-milling treatment

Mix-milling: 5.0 g substrate (microcrystalline cellulose, paper or eucalyptus) and 0.77 g AC-Air were milled together in an alumina pot with 200 g alumina balls of 5

mm diameter at 500 rpm in a Fritsch P-6 planetary ball mill. One milling cycle included 10 minutes of milling followed by 10 minutes of pause to allow dissipation of heat. Unless explicitly mentioned, all samples were milled for 6 cycles to give a total milling time of 1 h. After milling, the mixture was separated by sieving, followed by drying under vacuum at 393 K for 3 h. Mix-milled cellulose is denoted as MMC (S/C = 6.5). Single milling: 5.0 g microcrystalline cellulose was milled under same condition for 1 h without the addition of carbon catalyst.

2.2.4 Hydrolysis reaction

Hydrolysis experiments were done in a semi-flow reactor shown in Figure 2. 2. The reactor was made from stainless steel tube with length of 52 mm and diameter of 4 mm, and it was housed in a heater. A piston sensing back-pressure regulator was used to maintain the system pressure at 3 MPa. For a typical reaction, a mixture of substrate (MMC or ball-milled cellulose) and Granular SiO_2 (Q30) was prepared by physically mixing 0.175 g substrate and 0.175 g SiO_2 (0.553 g and 0.952 g MMC in the case of space velocity (SV) of 20 h^{-1} and 13 h^{-1}, respectively, to reduce the pressure drop across the reactor. Then the mixture was packed into the reactor and attached to the semi-flow system. The setup was pressurized and purged with water (0.75 mL min^{-1}) at room temperature for 10 min. After purging, heating was started, and the reactor was allowed to reach the desired temperature in about 20 min. The reaction was continued for another 20 min at this temperature and the product was collected for the whole 40 min reaction. The product was filtered with a 0.2 micron PTFE filter paper before analysis. Oligosaccharides yield was calculated as follows (Equation 2.1):

$$\text{Yield of oligosaccharides (\%)} = \frac{\text{Moles of carbon in oligosaccharides}}{\text{Moles of carbon in cellulose}} \times 100 \qquad (2.1)$$

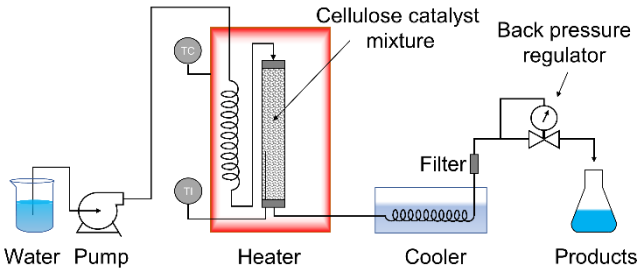

Figure 2.2. Scheme showing the design of semi flow process for hydrolysis of cellulose.

2.2.5 Precipitation of cello-oligosaccharides

The product solution was added dropwise to a beaker containing twice the volume of ethanol. This mixture was stirred for 1 h and then allowed to stand for another 2 h. The precipitate was recovered by centrifugation and washed with 5 mL of pure ethanol, followed by drying under ambient condition for 24 h and then vacuum drying for further 4 h at room temperature.

2.2.6 Characterization of cello-oligosaccharide mixture

Freshly obtained product solution was analyzed using high performance liquid chromatography (HPLC) systems equipped with a refractive index detector (Shimadzu LC 10-ATVP). A Shodex Sugar SH-1011 column (ø 8 × 300 mm; eluent, water at 0.5 mL min^{-1}; 323 K), a Phenomenex Rezex RPM-Monosaccharide Pb++ column (ø 7.8 × 300 mm, eluent: water at 0.6 mL min^{-1}, 343 K) and a Shodex Asahipak NH 2P-40E 30 column (ø 3 × 250 mm; eluent, water/acetonitrile (2:3 by vol.) at 0.3 mL min^{-1}; 318 K) were used for the detection of cello-oligosaccharides. Matrix assisted laser desorption / ionization – time of flight mass spectroscopy (MALDI-TOF MS) analysis of the freshly obtained product solution was performed using a Bruker Dal-tonics Autoflex-III smartbeam instrument. Sample was prepared by placing a 1 μL mixture of cello-oligosaccharides solution and matrix (2,5-dihydroxybenzoic acid solution) onto the MTP 384 Massive Target T plate followed by drying. FTIR spectra of precipitated oligosaccharides and cellulose were measured by making a KBr pellet containing 0.1

wt. % of sample. The pellet was analyzed by using a PerkinElmer Spectrum 100 FTIR Spectrometer. ^{1}H NMR measurements were performed using a JEOL ECX-600, ^{1}H 600 MHz instrument. NMR sample was prepared by dissolving 5 mg of precipitated sample in 1.1 mL of DMSO-d_6 containing 0.1 mg of 4,4-dimethyl-4-silapentane-1-sulfonic acid (DSS) and sonicating for 20 minutes.

2.2.7 Separation and characterization of individual cello-oligosaccharides

The separation of individual cello-oligosaccharides from the product solution was performed by using an HPLC equipped with a fraction collector (Shimadzu). Separation of cello-oligosaccharides up to G6 was obtained by using three Shodex OHpak SB-802.5 HQ columns in series (ø 8 × 300 mm; eluent, water at 0.5 mL min^{-1}; 328 K). The separated cello-oligosaccharides solutions were evaporated to remove water followed by addition of 1.1 mL of D_2O containing 0.1 mg of DSS and measuring the ^{1}H NMR spectrum in a JEOL ECX-600, ^{1}H 600 MHz instrument.

2.3 Results and discussion

2.3.1 Characterization of carbon catalyst

Activated carbon (AC) was oxidized under air at 698 K for10 h to prepare the carbon catalyst (AC-Air). The oxidation treatment reduced the surface area of AC from 1143 to 877 $m^2 g^{-1}$ without altering the microporous structure (Figure 2.3 a). A peak for C=O stretching of carboxyl groups appeared in the Fourier-transform infrared (FTIR) spectrum at 1710 cm^{-1} after oxidation, suggesting incorporation of weakly acidic functional groups (Figure 2.3 b).[27] The total amount of acidic functional groups was measured as 2560 μmol g^{-1} by titration.[28]

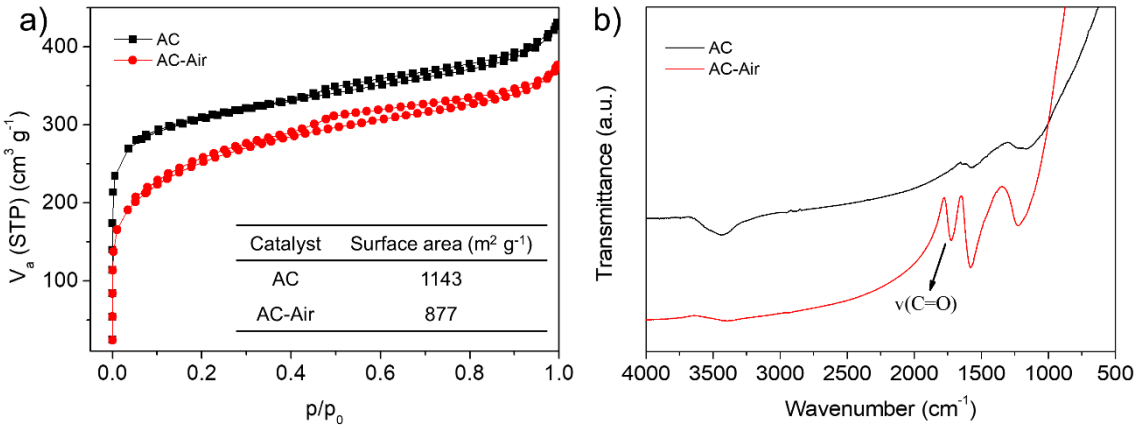

Figure 2.3. Characterization of AC and AC-Air, (a) N_2 adsorption isotherms, (b) FTIR spectra.

2.3.2 HPLC analysis of cellulose hydrolysis product

Cello-oligosaccharides were obtained by hydrolyzing cellulose adsorbed on carbon catalyst in the semi-flow reactor that extracted the soluble products as they were formed. HPLC analysis of a typical product solution using a Shodex Asahipak NH-2P-40 3E column showed distinct peaks of glucose, cellobiose (G2), cellotriose (G3), cellotetraose (G4), cellopentaose (G5) and cellohexaose (G6) (Figure 2.4 a). Celloheptaose (G7) and celloctaose (G8) were also detected in small amounts. During analysis, part of cello-oligosaccharides precipitated in the organic mobile phase and a linear calibration curve could not be obtained for quantification. Analysis using a Shodex Sugar SH-1011 column and a Phenomenex Rezex RPM-Monosaccharide Pb++ column with water as the mobile phase showed peaks of glucose, cellobiose and cellotriose. Remaining cello-oligosaccharides appeared as a single overlapped peak (Figure 2.4 b and c). The total yield of cello-oligosaccharides was calculated from these data according to the area of the peaks as the calibration factor showed a linear relationship with the degree of polymerization (DP) of cello-oligosaccharides. To avoid the influence of overlap of peaks, the glucose yield was calculated using the Phenomenex Rezex RPM-Monosaccharide Pb++ column and the cellotriose yield was

calculated using the Sugar SH-1011 column.

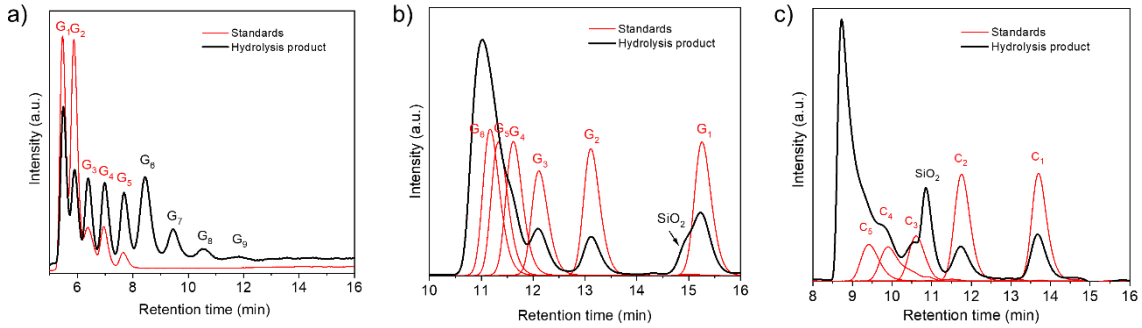

Figure 2.4. HPLC chromatogram of hydrolysis products and β-1,4 linked cello-oligosaccharide standards. a) Column: Amino NH 2P-40 3E; b) Column: Sugar SH-1011; c) Column: Phenomenex Rezex RPM-Monosaccharide Pb++. Reaction conditions: 0.175 g MMC (S/C = 6.5), 40 min, 0.75 mL min^{-1} water, 1 h mix milling.

2.3.3 Cello-oligosaccharides synthesis

In order to have a better understanding of cellulose hydrolysis in the semi-flow reactor, we investigated the evolution of products during the reaction. Formation rate of products during the hydrolysis at 453 K was plotted against reaction time, as shown in Figure 2.5. The hydrolysis of cellulose started when the temperature reached 423 K. Then the rate of cello-oligosaccharides formation gradually increased and reached the maximum at 20 min. Likewise, cellobiose and glucose formation rates also followed the same trend. After 30 min, the formation of all products simultaneously reduced and the reaction was complete within 40 min.

Cello-oligosaccharides were obtained in 71 % yield by hydrolysis of cellulose with AC-Air in the semi-flow reactor at 453 K with a space velocity (SV) of 70 h^{-1} [Figure 2.6, MMC AC-Air (cellulose mix-milled with AC-Air)]. Glucose (6.8 %) and cellobiose (5.0 %) were obtained as minor products. A trace amount of levoglucosan (0.2 %), a glucose degradation product, was also detected. The presence of acidic functional groups and the adsorption of cellulose on carbon by mix-milling were both

crucial for high cello-oligosaccharide yield.

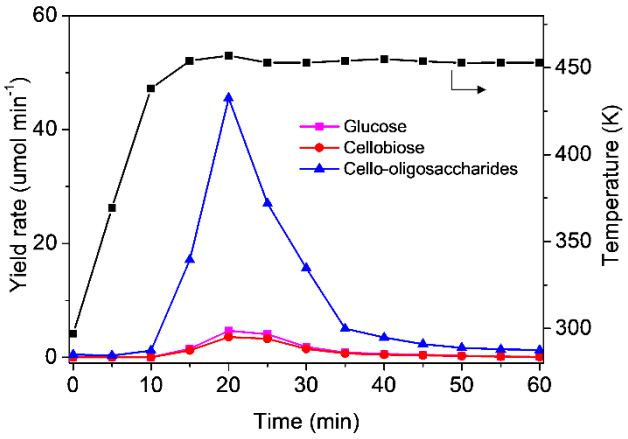

Figure 2.5. The evolution of products during the course of cellulose hydrolysis. Reaction conditions: 0.175 g MMC (S/C = 6.5), 453 K, 0.75 mL min^{-1} water.

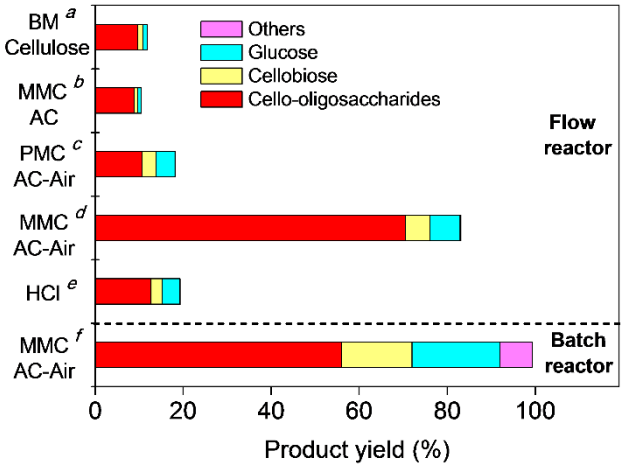

Figure 2.6. Yield of products after hydrolysis of cellulose. Reaction conditions for flow reactor: 453 K, 40 min, 0.75 mL min^{-1} distilled water. a) 0.150 g ball milled cellulose. b) 0.175 g cellulose mix-milled with AC (substrate to catalyst ratio S/C= 6.5). c) 0.175 g cellulose physically mixed with AC-Air (S/C = 6.5). d) 0.175 g cellulose mix-milled with AC-Air (S/C = 6.5). e) 0.150 g ball milled cellulose, 0.012 wt. % HCl aqueous solution instead of water. f) Reaction conditions for batch reactor: 0.374 g cellulose mix milled with AC-Air (S/C = 6.5), 40 mL distilled water, 453 K, 20 min.

In the absence of a catalyst with ball-milled (BM) cellulose as substrate, the yield was 9.7 % along with 2.2 % of glucose and cellobiose (Figure 2.6, BM cellulose). A

similar result was obtained if cellulose was adsorbed on AC by mix-milling. In addition, a homogeneous acid catalyst (0.012 wt % HCl, pH 2.5) only contributed 13 % yield of cello-oligosaccharides. If cellulose was physically mixed with AC-Air, the selectivity for cello-oligosaccharides was reduced. These results suggest that the catalytic activity is markedly increased by adsorbing the cellulose on the oxidized carbon catalyst through mix-milling.[29] In this context, we evaluated the effect of mix-milling on the yield of cello-oligosaccharides (Table 2.1). With an increase in mix-milling duration, the hydrolysis rate of cellulose was enhanced, which contributed to higher yield. XRD analysis of all mix-milled samples showed that the cellulose was amorphous, and the degree of crystallinity did not influence the rate of hydrolysis (Figure 2.7). Consequently, we concluded that the reactivity increased owing to better adsorption of cellulose on the carbon surface resulting from longer milling time. Adsorption resulting from 1 h of mix-milling was enough, and further increase in milling duration did not affect the yield or selectivity of cello-oligosaccharides. The semi-flow reactor, operating at an SV of 70 h^{-1}, prevented the secondary hydrolysis of cello-oligosaccharides. In the case of batch reactor, a large amount of dimer, monomer, and degradation compounds was obtained even under optimized conditions (Figure 2.6 f).

The advantage of the semi-flow reactor was further established by varying the hydrolysis temperature. At temperatures below 443 K, the total yield after 40 min was low because the rate of hydrolysis was slow (Table 2.1). Plotting the evolution of products showed that the hydrolysis was not complete within 40 min at lower temperature (Figure 2.8). The highest yield of cello-oligosaccharides was obtained as 72 % at 473 K (Table 2.1). Increase in temperature did not cause excessive hydrolysis, and the yield of glucose was 6.4 % even at 523 K.

Table 2.1 Hydrolysis of cellulose under different conditions.

Entry	Mix-milling duration (h)	T(K)	Yield based on carbon (%)				
			Oligosaccharides [a]	Cellobiose	Glucose	Others	Total
1	0	453	11	3.2	4.3	0.2	19
2	0.5	453	53	4.0	4.4	0.2	62
3	1	453	69	5.0	6.8	0.3	81
4	2	453	71	5.6	6.8	0.2	83
5	1	413	15	0.4	0.7	0.0	16
6	1	428	26	1.3	1.9	0.1	29
7	1	443	46	3.7	4.8	0.2	55
8	1	473	72	6.3	7.5	0.3	86
9	1	493	67	6.0	7.2	0.2	80
10	1	513	67	5.4	6.4	0.5	80
11	1	523	59	5.4	6.4	0.3	71

Conditions: 0.175 g MMC (S/C = 6.5), 40 min, water flow rate: 0.75 mL min^{-1} (SV = 70 h^{-1}); [a] cello-oligosaccharides with degree of polymerization more than 3.

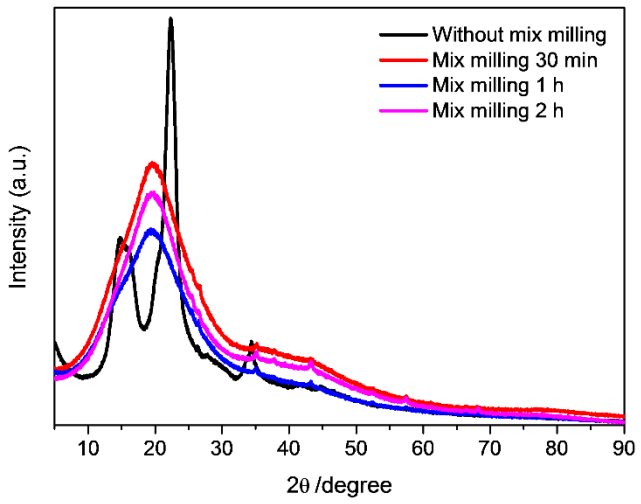

Figure 2.7. XRD patterns of mix-milled samples containing cellulose and AC-Air. S/C = 6.5

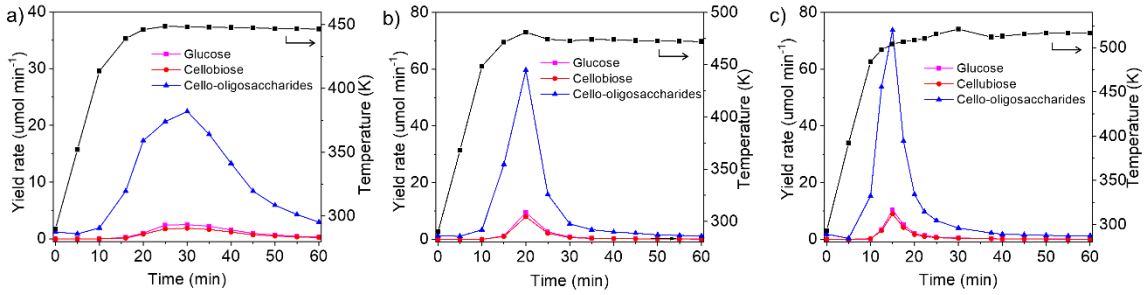

Figure 2.8. Time course of hydrolysis products at different temperatures: a) 448 K; b) 473 K; c) 513 K. Reaction conditions: 0.175 g MMC (S/C = 6.5), 0.75 mL min^{-1} water, 1 h mix milling.

The catalytic system was tested for hydrolysis of recycled paper and eucalyptus under identical reaction conditions. Carbohydrate composition of recycled paper and eucalyptus were determined by analysis protocols set by National Renewable Energy Laboratory (NREL/TP-510-42618), as shown in Table 2.2. The yield of cello-oligosaccharides from different substrates is shown in Figure 2.9 and it is calculated based on the initial glucan content of the substrate. When paper was used, only a minor reduction in cello-oligosaccharides yield was observed. The yield reduced to 50 % when eucalyptus was used as substrate. The decrease was ascribed to the presence of lignin that may partially deactivate the carbon catalyst. This result shows that replacing pure cellulose with recycled paper or eucalyptus biomass also produced cello-oligosaccharides as the main product.

Table 2.2 The compositions of cellulose materials measured by NREL/TP-510-42618 method.

Substrate	Glucan	Xylan	Acid insoluble lignin
Paper	69.7	11.8	11.0
Eucalyptus	41.4	12.8	21.3

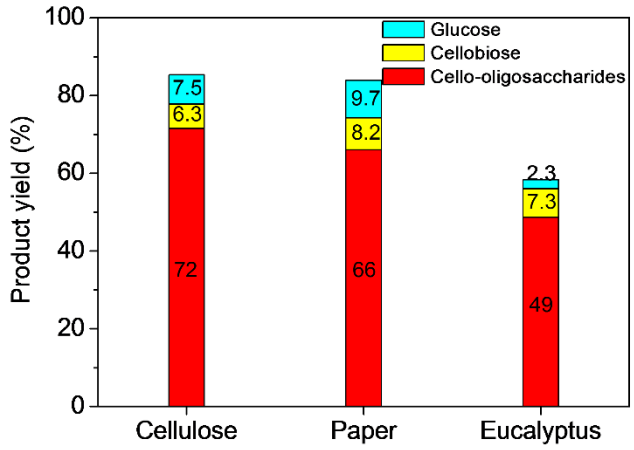

Figure 2.9. Product yields for real biomass hydrolysis. Reaction conditions: 0.175 g mix-milled substrate (S/C = 6.5), 473 K, 40 min, 0.75 mL min^{-1} water, 1 h mix milling.

2.3.4 Quantification of cello-oligosaccharides

To explore the distribution of products in the hydrolysis mixture, we developed a method for qualitative and quantitative analysis of individual cello-oligosaccharides by using MALDI-TOF MS method. The spectrum of freshly obtained product solution (Figure 2.10) revealed that the peaks were separated by m/z of 162, indicative of a polymer containing anhydro-glucose monomer units. Cello-oligosaccharides with a DP up to 13 were observed, which involved multiple peaks corresponding to $[M_w - H_2O + Na]^+$, $[M_w + Na]^+$ and its isotopes, and $[Mw + K]^+$ (e.g., cellopentaose, Figure 2.10 b). The total area of all these peaks was combined during analysis. For quantification, internal standards with different molecular weights, such as β-cyclodextrin[30] and xylo-oligosaccharides, did not work. However, cello-oligosaccharides showed an excellent correlation between concentration and peak area among themselves. Therefore, here we used cellotriose as a reference for the quantification. Firstly, the absolute concentration of cellotriose in the sample was measured. Secondly, the concentration of other cello-oligosaccharides was evaluated relative to cellotriose. For determination of cellotriose, the diluted sample (10 times) was spiked with increasing amounts of cellotriose and

then analyzed. The normalized area for cellotriose peaks was then plotted against the concentration of added cellotriose (Figure 2.10 c). The concentration of cellotriose in the unadulterated sample was determined as 0.038 mg mL^{-1} by extrapolating the plot to the point at which the value of ordinate became zero.[31] Based on this concentration, the carbon yield of cellotriose was calculated as 8.4 %, which was similar to the value calculated by HPLC (7.9 %).

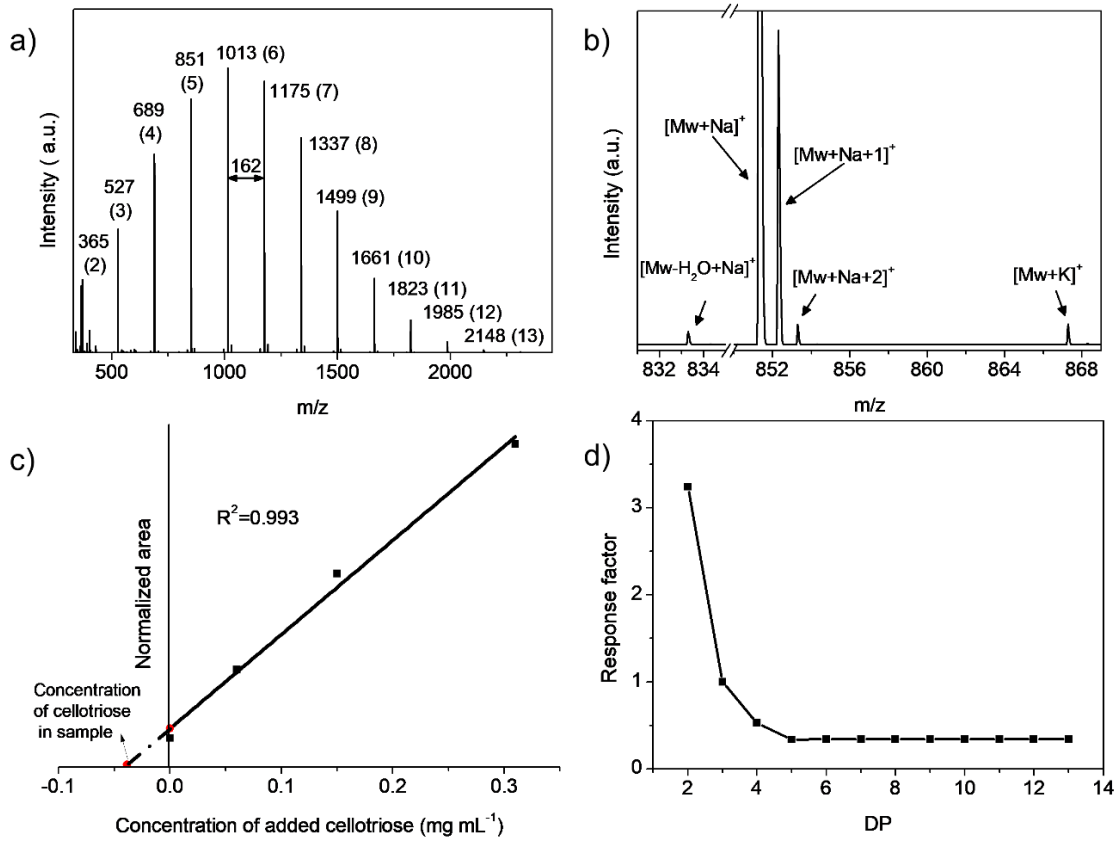

Figure 2.10. MALDI-TOF MS of cello-oligosaccharides. a) mass spectrum of product solution, b) expansion of the spectrum showing all peaks corresponding to cellopentaose, c) the relationship of normalized area with concentration of added cellotriose, d) plot showing relationship between response factor and DP of cello-oligosaccharides. Reaction conditions: 0.175 g (S/C = 6.5) MMC, 473 K, 40 min, 0.75 mL min^{-1} H_2O, 1 h milling.

The concentration of other cello-oligosaccharides was calculated by using Equation (2.2):

$$[Gx] = Rfx \times [G3] \times \frac{AGx}{AG3} \quad (2.2)$$

in which [*Gx*] is the concentration of cello-oligosaccharide with DP of x, and [*G3*] is the concentration of cellotriose measured in the first step. *AGx* and *AG3* are the peak areas for the respective cello-oligosaccharides. *Rfx* is the response factor for individual cello-oligosaccharides in comparison to cellotriose. It was calculated by preparing a solution of cellotriose and cello-oligosaccharide standards (G2-G6) with varying concentration ratios and determining the area in MALDI-TOF MS. A plot of the area ratio versus concentration ratio showed a linear relationship for all cello-oligosaccharides (Figure 2.11). The slope of the linear fit was set as *Rfx* and used to calculate the yield of G2 (9.9 %), G4 (9.0 %), G5 (8.8 %) and G6 (11 %). Concentration of higher cello-oligosaccharides was calculated by assuming that *Rfx* is constant for cello-oligosaccharides with a DP higher than 4 (Figure 2.10 d). The result calculated by MALDI-TOF MS is shown in Table 2.3. The total yield of cello-oligosaccharides (69 %) was in good agreement with the value calculated from HPLC (70 %). The quantification by MALDI-TOF MS revealed that cello-oligosaccharides with a DP below 10 were the primary products.

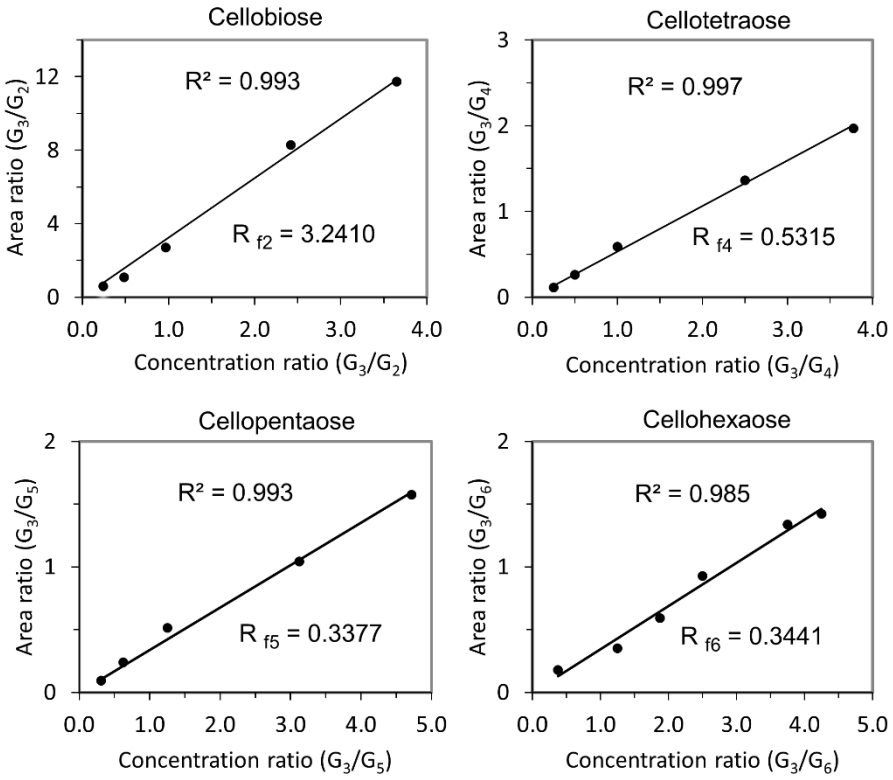

Figure 2.11. Relationship of area ratio of cellotriose and other cello-oligosaccharides against concentration ratio based on MALDI-TOF MS.

The distribution of cello-oligosaccharide was controlled by altering the SV of the reaction. At a high SV of 70 h^{-1}, G6 and G7 were the major components. The SV was reduced by increasing the reactor volume, which also increased the sample loading. The decrease in SV did not prolong the time required for completion of the reaction. Cellotriose was obtained as a major product at a SV of 20 h^{-1}. However, the composition remained unchanged by further reducing the SV to 13 h^{-1}. This result indicates that cello-oligosaccharides with lower DP undergo hydrolysis at a slower rate ascribed to their lower adsorption coefficient on the carbon surface.[24]

Table 2.3 The yield of cello-oligosaccharides at different SV calculated by HPLC and MALDI-TOF MS.

Component	Yield (%)			
	HPLC	MALDI-TOF MS		
	SV = 70 h^{-1}	SV = 70 h^{-1}	SV = 20 h^{-1}	SV = 13 h^{-1}
Glucose	6.9	-	-	-
G2	5.3	9.9	14	15
G3	7.9	8.4	14	13
G4	-	9.0	11	11
G5	-	8.8	7.7	7.4
G6	-	11	7.5	7.1
G7	-	11	6.1	5.8
G8	-	9.0	4.3	4.3
G9	-	6.0	2.7	2.6
G10	-	3.3	1.3	1.3
G11	-	1.4	0.10	0.40
G12	-	0.50	0.03	0.10
G13	-	0.10	0.01	0.10
G3+[a]	70	69	55	53

[a]Total yield of G3-G13 cello-oligosaccharides. Reaction conditions: 0.175 g MMC, 473 K, 20 min, 0.75 mL min^{-1}, 1 h mix-milling.

2.3.5 Characterization of cello-oligosaccharides mixture

The cello-oligosaccharide mixture was further characterized by FTIR and ^{1}H NMR analysis after precipitation in ethanol. The FTIR spectra of precipitated cello-oligosaccharides were compared with pristine cellulose (Figure 2.12 a). Peaks located at 3413 cm^{-1} and 2903 cm^{-1} were attributed to the stretching of O-H groups and aliphatic saturated C-H, respectively. The peak at 1639 cm^{-1} was assigned to the bending vibration of O-H. The peaks at 1465 cm^{-1} and 1380 cm^{-1} were attributed to the in-plane bending vibrations of C-H groups. The peaks at 1250 - 1000 cm^{-1} were assigned to the stretching vibration of C-O-C in pyranose ring of glucose. The peak of 897 cm^{-1} was associated to the β-glycosidic linkage between monomer units. The comparison of

FTIR spectra of cellulose and cello-oligosaccharides showed no additional peaks confirming the absence of any undesired modification in the cello-oligosaccharides structure. In addition, we used ^{1}H NMR spectroscopy to investigate the nature of glycosidic linkages present in cello-oligosaccharide mixture. The comparison of ^{1}H NMR spectra of cello-oligosaccharides and cellopentaose, used as reference, suggested that the cello-oligosaccharide was chemically identical to cellopentaose and lacked glycosidic bonds except β-1,4 linkages (Figure 2.12 b).

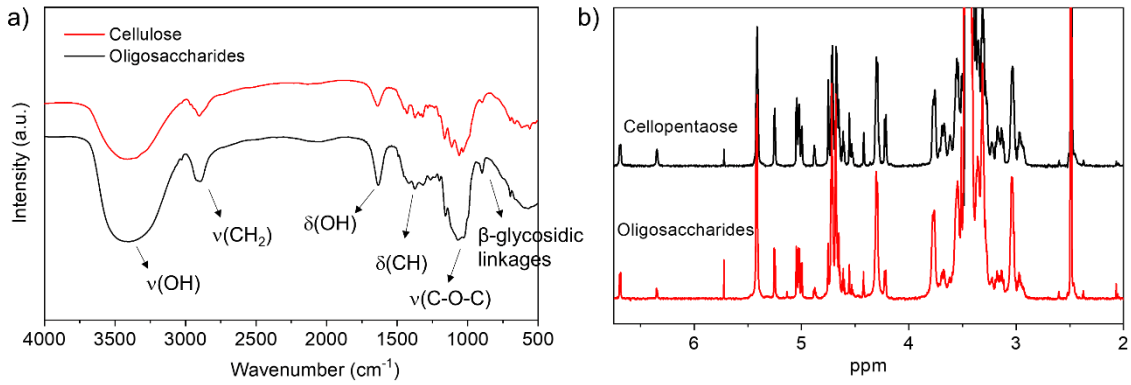

Figure 2.12. Characterization of precipitated oligosaccharides, a) FTIR spectra, b) ^{1}H NMR spectra in DMSO-d_6.

Individual cello-oligosaccharides (G3 to G6) were separated by preparative HPLC and were also evaluated by ^{1}H NMR spectroscopy with D_2O as solvent (Figure 2.13). The anomeric region showed a doublet at $\delta_H = 4.50$ (δ_H denotes ^{1}H chemical shift), which was assigned to the β-1,4 linked monomers with a non-reducing (nr) end.[32] The dominant doublet at $\delta_H = 4.52$ ppm was identified as β-1,4 internal (i) linkages. As the length of cello-oligosaccharides chain increased, the resonances of β-1,4-i also increased in relative intensity. The doublets detected between δ_H = 4.6 - 4.7 and δ_H = 5.2 - 5.3 ppm were characteristic of β reducing ends and α reducing ends, respectively. The chemical shifts at approximately δ_H = 5.0 ppm, indicative of branching α-1,6 linkages, were not detected. These findings revealed that monomers in oligosaccharides

were only linked by β-1,4 bonds. In addition, the number average DP (DP_n) of cello-oligosaccharides was calculated by using Equation (2.3)

$$DP_n = \frac{A_i + A_{nr}}{A_\beta + A_\alpha} + 1 \qquad (2.3)$$

in which A_i and A_{nr} are areas for peaks assigned to internal and non-reducing β-1,4-glycosidic bonds. A_β and A_α are areas for peaks assigned to the β and α reducing ends. The calculated DP_n values of 3.2, 4.3, 5.4, and 6.5 for G3-G6, respectively, were in good agreement with the expected values.

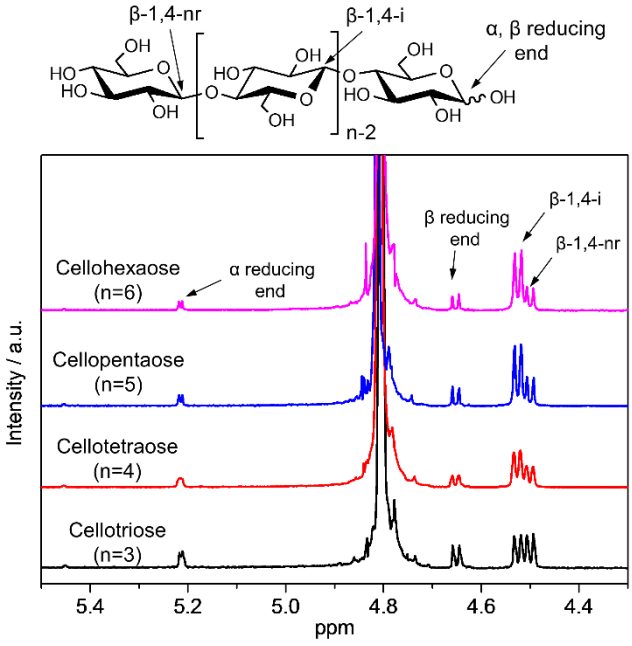

Figure 2.13. ^{1}H NMR spectra of the anomeric region of individual cello-oligosaccharides in D_2O.

2.4 Conclusions

High yields of cello-oligosaccharides from cellulose hydrolysis was achieved by using a weakly acidic carbon catalyst in conjugation with a semi-flow reactor. Presence of acidic functional groups on the carbon surface, adsorption of cellulose on catalyst, and high space velocity contributed to maximize the product yield. ^{1}H NMR and FTIR analysis confirmed the structure of β-1,4 linked straight-chain cello-oligosaccharides

and the absence of branching or impurities. It is expected that this method can be used for large-scale synthesis of cello-oligosaccharides for application in agricultural and healthcare industries, especially when combined with a clear understanding of their composition determined by MALDI-TOF MS. This process utilizes food-grade activated carbon as catalyst, which is oxidized using air. The avoidance of toxic chemicals during catalyst synthesis and the reaction ensures that the cello-oligosaccharide solution is compatible for use in agricultural and healthcare industries without the need for cost-intensive purification.

References

1. S. I. Mussatto and I. M. Mancilha, *Carbohydr. Polym.*, 2007, **68**, 587-597.
2. H. J. Flint, E. A. Bayer, M. T. Rincon, R. Lamed and B. A. White, *Nat. Rev. Microbiol.*, 2008, **6**, 121-131.
3. C. D. A. Souza, S. Li, A. Z. Lin, F. Boutrot, G. Grossmann, C. Zipfel and S. C. Somerville, *Plant Physiol.*, 2017, **173**, 2383-2398.
4. A. A. Gust, R. Pruitt and T. Nürnberger, *Trends Plant Sci.*, 2017, **22**, 779-791.
5. T. Hasunuma, K. Kawashima, H. Nakayama, T. Murakami, H. Kanagawa, T. Ishii, K. Akiyama, K. Yasuda, F. Terada and S. Kushibiki, *Anim. Sci. J.*, 2011, **82**, 543-548.
6. E. Billès, V. Coma, F. Peruch and S. Grelier, *Polym. Int.*, 2017, **66**, 1227-1236.
7. R. Rinaldi and F. Schüth, *ChemSusChem*, 2009, **2**, 1096-1107.
8. S. Suganuma, K. Nakajima, M. Kitano, D. Yamaguchi, H. Kato, S. Hayashi and M. Hara, *J. Am. Chem. Soc.*, 2008, **130**, 12787-12793.
9. A. Shrotri, H. Kobayashi and A. Fukuoka, *Acc. Chem. Res.*, 2018, **51**, 761-768.
10. A. T. To, P. W. Chung and A. Katz, *Angew. Chem. Int. Ed.*, 2015, **54**, 11050-11053.
11. Y.-B. Huang and Y. Fu, *Green Chem.*, 2013, **15**, 1095-1111.
12. R. Rinaldi, R. Palkovits and F. Schüth, *Angew. Chem. Int. Ed.*, 2008, **47**, 8047-8050.
13. Q. Chu, X. Li, Y. Xu, Z. Wang, J. Huang, S. Yu and Q. Yong, *Process Biochem.*, 2014, **49**, 1217-1222.
14. A. Martin-Mingot, K. D. O. Vigier, F. Jérômeb and S. Thibaudeau, *Org. Biomol. Chem.*, 2012, **10**, 2521-2524.
15. T. Liebert, M. Seifert and T. Heinze, *Macromol. Symp.*, 2008, **262**, 140-149.
16. F. Schüth, R. Rinaldi, N. Meine, M. Käldström, J. Hilgert and M. D. K. Rechulski, *Catal. Today*, 2014, **234**, 24-30.

17. L. Schneider, J. Haverinen, M. Jaakkola and U. Lassi, *Chem. Eng. J.*, 2017, **327**, 898-905.
18. N. Meine, R. Rinaldi and F. Schüth, *ChemSusChem*, 2012, **5**, 1449-1454.
19. A. Shrotri, L. K. Lambert, A. Tanksale and J. Beltramini, *Green Chem.*, 2013, **15**, 2761-2768.
20. A. Charmot, P.-W. Chung and A. Katz, *ACS Sustainable Chem. Eng.*, 2014, **2**, 2866-2872.
21. X. Zhao, J. Wang, C. Chen, Y. Huang, A. Wang and T. Zhang, *Chem. Commun.*, 2014, **50**, 3439-3442.
22. H. Kobayashi, M. Yabushita, T. Komanoya, K. Hara, I. Fujita and A. Fukuoka, *ACS Catal.*, 2013, **3**, 581-587.
23. A. Shrotri, H. Kobayashi, H. Kaiki, M. Yabushita and A. Fukuoka, *Ind. Eng. Chem. Res.*, 2017, **56**, 14471-14478.
24. M. Yabushita, H. Kobayashi, J.-Y. Hasegawa, K. Hara and A. Fukuoka, *ChemSusChem*, 2014, **7**, 1443-1450.
25. H. Kobayashi, M. Yabushita, J.-Y. Hasegawa and A. Fukuoka, *J. Phys. Chem. C*, 2015, **119**, 20993-20999.
26. O. M. Gazit and A. Katz, *J Am Chem Soc*, 2013, **135**, 4398-4402.
27. G. S. Foo and C. Sievers, *ChemSusChem*, 2015, **8**, 534-543.
28. H. P. Boehm, *Carbon*, 2002, **40**, 145-149.
29. M. Yabushita, H. Kobayashi, K. Hara and A. Fukuoka, *Catal. Sci. Technol.*, 2014, **4**, 2312-2317.
30. J. Wang, G. Jiang, T. Vasanthan, Peter Sporns, Edmonton and Alberta, *Food Sci. Technol.*, 1999, **51**, 243-248.
31. M. W. Duncan, H. Roder and S. W.Hunsucker, *Briefings Funct. Genomics*, 2008, **7**, 355-370.
32. L. A. Flugge, J. T. Blank and P. A. Petillo, *J. Am. Chem. Soc.*, 1999, **121**, 7228-7238.

Chapter 3

Unraveling the hydrolysis of β-1,4-glycosidic bond in cello-oligosaccharides over carbon catalysts

Abstract

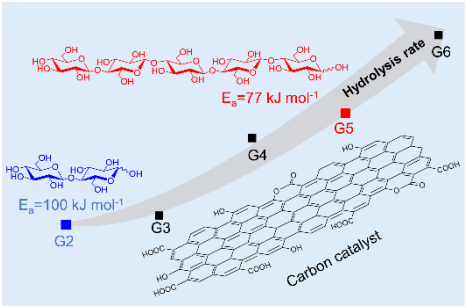

It is clear from the results in chapter 2 that high yield of cello-oligosaccharides can be obtained by employing a semi-flow reactor. But controlling the distribution of products by optimizing the reaction conditions is challenging. Therefore, this chapter plans to elucidate the reactivity of cello-oligosaccharides from a fundamental perspective. The approach aims to relate the results with the broader study of β-1,4-glycosidic bond hydrolysis in cellulose and tries to explain the unique ability of carbon materials to hydrolyze cellulose to cello-oligosaccharides. In this study, carbon catalysts favored hydrolysis of larger cello-oligosaccharides with an 11-fold increase in reaction rate constant from cellobiose to cellohexaose. Activation energy required to cleave the glycosidic bonds reduced concurrently with increase in molecule size. Based on these data, in conjugation with the stronger affinity of adsorption for larger cello-oligosaccharides, a plausible mechanism is proposed that axial adsorption within the micropores of carbon causes conformational change in the structure of cello-

oligosaccharide molecules, resulting in reduction of activation energy required to cleave the β-1,4-glycosidic bonds. Consequently, this translates to higher rate of reaction for larger cello-oligosaccharides and explains the high reactivity of carbon catalyst towards cellulose hydrolysis.

3.1 Introduction

Cellulose, the primary component of lignocellulosic biomass, is the most abundant carbon-based renewable resource on our planet. It is a biopolymer composed of anhydro-glucose units linked by β-1,4-glycosidic bonds.[1,2] Catalytic hydrolysis of the β-1,4-glycosidic bonds in cellulose is a crucial step in producing biofuels and value-added chemicals, which can reduce the dependence on fossil fuels and petroleum industry.[3-5]

Enzymes[6-8] and acid catalysts[9-12] are effective for hydrolysis of cellulose to oligosaccharides and glucose. Partial hydrolysis produces water-soluble cello-oligosaccharides as major component,[13,14] which possess the repeated β-1,4-glycosidic linkages but have a low degree of polymerization (DP). These oligosaccharides exhibit biological activity that can benefit the growth and health of plants, animals, and humans.[15-17] Complete hydrolysis of cellulose produces glucose, a precursor for value-added chemicals and fuels.[18-21]

Carbon catalysts are most active for hydrolysis of cellulose among heterogeneous acid catalysts. They are also benign and do not contaminate the product solution, making them ideal for synthesis of cello-oligosaccharide for use in agriculture and healthcare industries.[9,22,23] Carbon catalysts bearing weakly acidic functional groups such as hydroxyl (-OH) and carboxylic (-COOH) groups show comparatively high activity along with good hydrothermal stablity.[24,25] Owing to the insoluble nature of

cellulose, a strong interaction between catalyst and cellulose is essential in a heterogeneous reaction. The polyaromatic surface of carbon catalyst can adsorb cellulose molecules by CH-π and hydrophobic interactions[26], and it is believed that this adsorption promotes the interaction between acidic functional groups and β-1,4-glycosidic bonds.[5] The DP of the adsorbed molecules can affect their adsorption capacity and larger oligosaccharides show higher affinity towards carbon surface.[26-28] Katz's group found that there was a monotonical decrease in free energy of adsorption with increase in the chain length of oligosaccharides over mesoporous carbon nanoparticles.[28] Yabushita *et al*. observed a linear decrease in the adsorption enthalpy with an increase in chain length of oligosaccharides.[26]

The change in adsorption affinity with chain length of cello-oligosaccharide can affect their selectivity during cellulose hydrolysis. Chapter 2 showed that carbon can catalyze hydrolysis of cellulose in a semi-flow reactor to yield cello-oligosaccharides without forming large amounts of glucose. The distribution of DP, determined by quantitative MALDI-TOF MS analysis, suggested a decrease in rate of hydrolysis as the reaction progressed.[29] However, there is a lack of holistic understanding about the dependence of molecule size on the rate of hydrolysis and the influence of adsorption during reaction. Therefore, fundamental approach towards assessing the change in rate of hydrolysis from a kinetic and mechanistic perspective is essential to determine the underlying factors responsible for high activity of carbon catalysts.

This chapter reports the hydrolysis of a series of cello-oligosaccharides in the presence of heterogeneous and homogeneous catalysts. Kinetic analysis is done to compare the change in rate of hydrolysis over different catalysts. Investigation on the adsorption affinity of cello-oligosaccharides along with determination of apparent activation energy is used to ascertain the factors responsible for change in hydrolysis

rate. Based on the experimental results, a plausible mechanism is proposed which explains the hydrolysis behavior of large cellulose molecules over carbon catalysts.

3.2 Experimental Methods

3.2.1 Materials

Activated carbon (denoted as AC) was supplied from Ajinomoto Fine-Techno. Amberlyst 70 was purchased from Organo Corporation. H-beta was supplied from Catalysis Society of Japan. Cellotriose (G3, 95 %), cellotetraose (G4, 95 %), cellopentaose (G5, 95 %) and cellohexaose (G6, 94 %) were purchased from Megazyme. Glucose and cellobiose were purchased from Kanto Chemical Industries. 1,6-Hexanediol and sulfuric acid (H_2SO_4, 98 %) were purchased from Wako Pure Chemical Industries. DMSO was obtained from Tokyo Chemical Industry.

3.2.2 Air-oxidation of carbon catalyst

Air oxidation of carbon was performed using a method reported previously.[29] Briefly, activated carbon AC (4.0 g) was spread on a Pyrex dish of diameter 130 mm with a uniform thickness. The sample was then heated in a muffle furnace in air with the following program: 298 to 393 K at a rate of 10 K min^{-1} and then maintained at 393 K for 2 h to remove the physisorbed water, followed by heating to 698 K at a rate of 4 K min^{-1} and then maintaining at 698 K for further 10 h. The oxidized carbon catalyst was denoted as AC-Air. AC-Air-L was prepared via the same method except for lowering the oxidation temperature to 673 K.

3.2.3 Characterization of catalyst

Specific surface area of solid catalysts was determined by N_2 adsorption-desorption measurement (BEL Japan, BELSORP-mini) after vacuum drying at 393 K for 3 h. The total amount of acidic functional groups on solid catalysts were calculated by the titration.[30] The acidity of H-beta catalyst was also quantified by NH_3-temprature

programmed desorption (TPD) (BEL Japan, BELCAT-A coupled with a mass spectrometer).

3.2.4 Catalytic reactions

Hydrolysis of cello-oligosaccharides was performed in a glass tube placed inside a pressure-resistant hastelloy reactor (5 mL, TVS-1). For a typical reaction, 0.5 mL of water containing 1 μmol of cello-oligosaccharide substrate was added to the glass tube along with 5 mg of solid catalyst (in the case of H_2SO_4, 6.4 μmol of acid was used to replicate the acid content of 5 mg of AC-Air) and a magnetic stirrer bar. The glass tube was then placed in the reactor. The setup was purged and then pressurized to 0.5 MPa with argon (Ar) before immersing into a heated oil bath for a set period of time. After reaction, the reactor was cooled to room temperature and 0.1 mL of water containing 1 μmol of 1,6-hexanediol was added to the mixture to serve as internal standard. The catalyst was separated from the reaction mixture by centrifugation and then washed three times with DMSO (1 mL) to extract adsorbed sugar molecules. The reaction solution and the liquids obtained after washing were mixed and diluted to 5 mL using a volumetric flask. This obtained solution was analyzed to calculate the concentration of oligosaccharides by using a high-performance liquid chromatography (HPLC) system equipped with a refractive index detector (Shimadzu LC 10-ATVP) and a series of three Shodex Sugar SB 802.5HQ columns (ø 8 × 300 mm; eluent, water 0.5 mL min^{-1}; 328 K).

3.2.5 Adsorption of cello-oligosaccharides

Adsorption of cello-oligosaccharides on solid catalysts was performed at room temperature. Solid catalyst (5 mg) was added to a vial containing 0.5 mL aqueous solution of adsorbate. The mixture was equilibrated under stirring for a period of 30 min. The sample was subsequently filtrated, and the solution was analyzed by the HPLC

system described above. The amount of substrate adsorbed was calculated as the difference of sugar concentration in the liquid phase before and after adsorption.

3.3 Results and discussion

3.3.1 Characterization of catalysts

Carbon catalysts containing weakly acidic functional groups were prepared by air-oxidation of activated carbon (named AC) at elevated temperature. Amberlyst 70 (sulfonated resin catalyst), H-beta zeolite and homogeneous H_2SO_4 were used for comparing the activity with carbon materials. The N_2-adsorption isotherms for solid catalysts are shown in Figure 3.1. The Brunauer-Emmett-Teller (BET) surface areas of carbon catalyst prepared by oxidation at 698 K (named AC-Air) was calculated as 877 $m^2 g^{-1}$, which was lower than pristine AC (1143 $m^2 g^{-1}$) owing to collapse of some pores during the oxidation treatment (Table 3.1). AC-Air-L, a catalyst prepared by oxidation at milder condition (673 K), exhibited a similar surface area (1214 $m^2 g^{-1}$) to AC because of lower degree of oxidation. Zeolite H-beta had a surface area of 607 $m^2 g^{-1}$, a value typical for zeolite catalysts. The N_2 adsorption over Amberlyst 70 was negligible as the resin catalyst is not porous. However, the resin is permeable to reactants in aqueous solution allowing access to the acid sites.[31] The number of acidic functional groups on catalysts were calculated by titration with NaOH.[30] Amberlyst 70 showed the highest number of acid functional groups (3172 μmol g^{-1}) originating from $-SO_3H$ groups. Acidic sites originating from carboxyl, hydroxyl and lactone groups are known to be present over oxidized carbon catalysts.[25] The total number of acidic functional groups in AC-Air and AC-Air-L was determined as 2560 μmol g^{-1} and 2075 μmol g^{-1}, respectively. Lower oxidation temperature of AC-Air-L (673 K) introduced fewer functional groups as expected. Titration of H-beta showed a low concentration of acid sites of 296 μmol g^{-1}, consistent with the value (299 μmol g^{-1}) quantified using

NH_3-TPD.

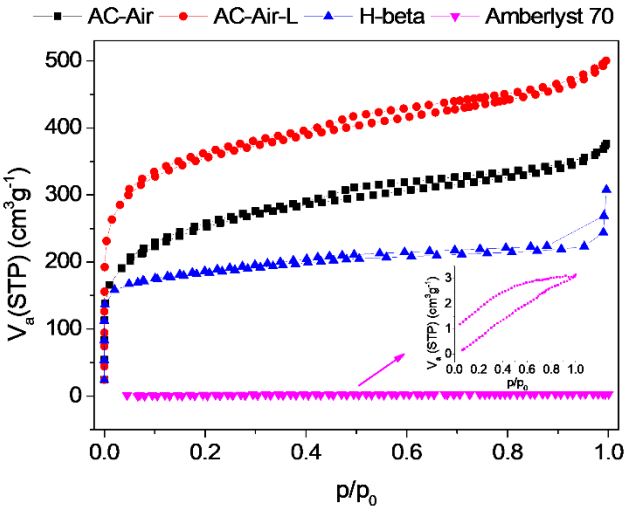

Figure 3.1. N_2 adsorption isotherms of solid catalysts.

Table 3.1 BET surface area and number of acid sites on solid acid catalysts.

Catalyst	BET surface area (m^2 g^{-1})	Total number of acid sites (μmol g^{-1})
AC	1143	355
AC-Air-L	1214	2075
AC-Air	877	2560
Amberlyst 70	-	3172
H-beta zeolite	607	296

3.3.2 Cello-oligosaccharides hydrolysis

Hydrolysis of cello-oligosaccharide with DP ranging from 2 - 6 was performed in the presence of AC-Air at 413 K to investigate the influence of chain length on the rate of hydrolysis. For cellobiose (G2) hydrolysis, 46 % conversion was achieved after 120 min of reaction (Figure 3.2 a). The hydrolysis pathway of cellobiose is shown in Scheme 3.1 and all steps were assumed to be first order reaction for kinetic analysis.[5,32] Accordingly, Equations (3.1) - (3.4) were used to represent the hydrolysis of cellobiose

and degradation of glucose:

$$\frac{d[G2]}{dt} = -k_2\,[G2] \tag{3.1}$$

$$[G2] = [G2]_0 e^{-k_2 t} \tag{3.2}$$

$$\frac{d[Glucose]}{dt} = -k_1\,[Glucose] + 2k_2\,[G2] \tag{3.3}$$

$$[Glucose] = \frac{2k_2[G2]_0}{k_1 - k_2}\left(e^{-k_2 t} - e^{-k_1 t}\right) \tag{3.4}$$

where [G2] and [Glucose] are concentrations of respective compounds. $[G2]_0$ is the initial concentration of cellobiose. *t* is the reaction time, and *k* is the rate constant. The rate constant k_2 for hydrolysis of cellobiose was determined as 0.38 h^{-1} (Figure 3.2 f) by simulating Equation (3.2) to fit the experimental data. Similarly, the rate constant for degradation of glucose (k_1) to other products was calculated as 0.03 h^{-1}. The high k_2/k_1 ratio indicated that the decomposition of glucose under the reaction condition was limited.

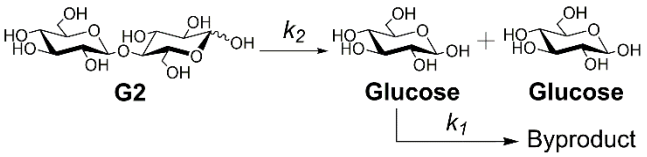

Scheme 3.1. Reaction pathway during hydrolysis of cellobiose.

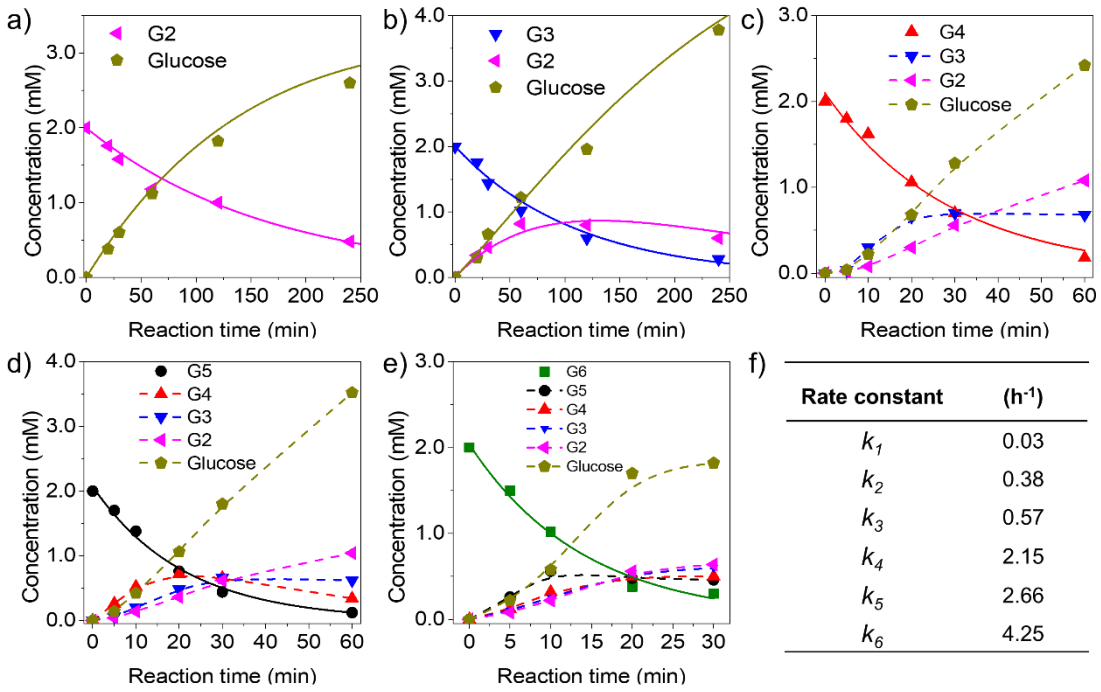

Figure 3.2. Time dependent conversion of cello-oligosaccharides and evolution of products in the presence of AC-Air. a) G2, b) G3, c) G4, d) G5, e) G6, f) Rate constant for hydrolysis of each cello-oligosaccharide. Reaction conditions: 1 μmol cello-oligosaccharides (G2-G6), 5 mg AC-Air, 0.5 mL H_2O, 0.5 MPa Ar, 413 K. Symbols denote experimental data points. Solid lines represent simulation of reaction using calculated rate constant and corresponding equations. Dashed lines show experimental trend for concentration of products during reaction.

Hydrolysis of cellotriose (G3) under the same reaction condition was faster than that of cellobiose and 50 % conversion was achieved in 60 min. The hydrolysis of cellotriose to cellobiose and its further hydrolysis to glucose is shown in Scheme 2. The degradation of glucose to by-products was ignored owing to the very low value of k_1 estimated previously. Therefore, the hydrolysis rate constant k_3 was evaluated by the following rate Equations (3.5) and (3.6).

$$\frac{d[G3]}{dt} = -k_3\,[G3] \tag{3.5}$$

$$[G3] = [G3]_0 e^{-k_3 t} \tag{3.6}$$

The rate constant k_3 for hydrolysis of cellotriose was calculated as 0.57 h^{-1}.

Simulation of reaction profile by Equations (3.6), (3.8) and (3.10) along with values of k_2 and k_3 fitted well with the experimental data (Figure 3.2 b).

$$\frac{d[G2]}{dt} = -k_2\,[G2] + k_3\,[G3] \tag{3.7}$$

$$[G2] = \frac{k_3[G3]_0}{k_2 - k_3}(e^{-k_3 t} - e^{-k_2 t}) \tag{3.8}$$

$$\frac{d[Glucose]}{dt} = 2k_2\,[G2] + k_3\,[G3] \tag{3.9}$$

$$[Glucose] = [G3]_0\left\{\frac{(k_3 - 3k_2)e^{-k_3 t} + 2k_3 e^{-k_2 t}}{k_2 - k_3} + 3\right\} \tag{3.10}$$

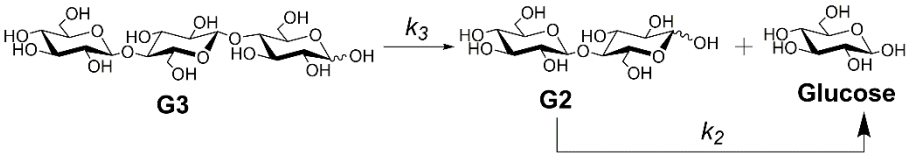

Scheme 3.2. Reaction pathway during hydrolysis of cellotriose.

Based on the good fit of rate equations for G2 and G3, the rate equation for hydrolysis of cello-oligosaccharide was generalized:

$$\frac{d[Gx]}{dt} = -k_x\,[Gx] \tag{3.11}$$

$$[Gx] = [Gx]_0 e^{-k_x t} \tag{3.12}$$

where Gx represents the cello-oligosaccharide with a DP of x and k_x represents the rate constant for hydrolysis of that cello-oligosaccharide.

The hydrolysis of cellotetraose (G4) was even faster (Figure 3.2 c) and k_4 was calculated as 2.15 h^{-1}. Furthermore, the rate constants for hydrolysis of cellopentaose (G5) and cellohexaose (G6) were calculated as 2.66 h^{-1} and 4.25 h^{-1}, respectively (Figure 3.2 d and 3.2 e). Consequently, kinetic analysis reveals that the rate of hydrolysis of cello-oligosaccharide increases dramatically with respect to its DP.

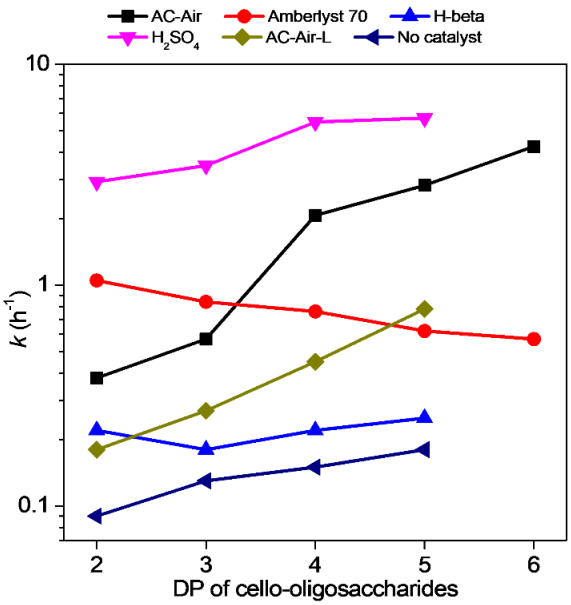

Figure 3.3. Comparison of change in rate constant for hydrolysis of cello-oligosaccharides in the presence of various acid catalysts. Reaction conditions: 1 μmol cello-oligosaccharides (G2-G6), 5 mg solid catalyst or 6.4 μmol H_2SO_4, 0.5 mL H_2O, 0.5 MPa Ar, 413 K.

To ascertain if the increase in rate of hydrolysis is caused by a favorable interaction between cello-oligosaccharide and carbon catalyst or it is an inherent property of cello-oligosaccharides, the hydrolysis of these compounds over other heterogeneous catalysts was performed (Figure 3.3). The time course for hydrolysis of cello-oligosaccharides over Amberlyst 70 is shown in Figure 3.4. The rate constant for hydrolysis of cellobiose on Amberlyst 70 was much higher (1.05 h^{-1}) in comparison to AC-Air (0.38 h^{-1}) owing to the higher abundance of acid sites along with high acid strength of -SO_3H group. However, unlike AC-Air, the rate constant for hydrolysis on Amberlyst 70 was not positively affected by increase in DP. In contrast, the rate constant gradually decreased with an increase in the chain length of cello-oligosaccharides. H-beta showed a significantly lower activity for the hydrolysis of cello-oligosaccharides (Figure 3.5) and the rate constant was not influenced by increase in DP. The reaction rate in the presence of H-beta was not much different in comparison

to a non-catalytic reaction (Figure 3.3), suggesting the inability of H-beta zeolite to interact with cello-oligosaccharides.

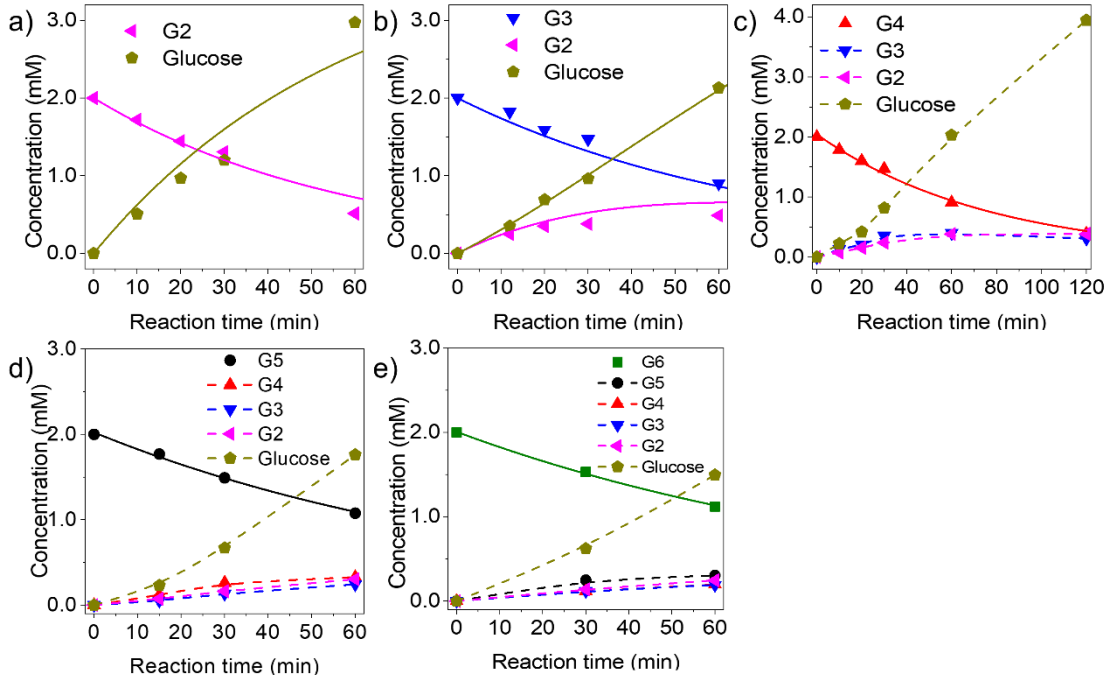

Figure 3.4. Time dependent conversion of cello-oligosaccharides and evolution of products in the presence of Amberlyst 70. Reaction conditions: 1 μmol cello-oligosaccharides (G2-G6), 5 mg Amberlyst 70, 0.5 mL H_2O, 0.5 MPa Ar, 413 K. a) G2, b) G3, c) G4, d) G5, e) G6.

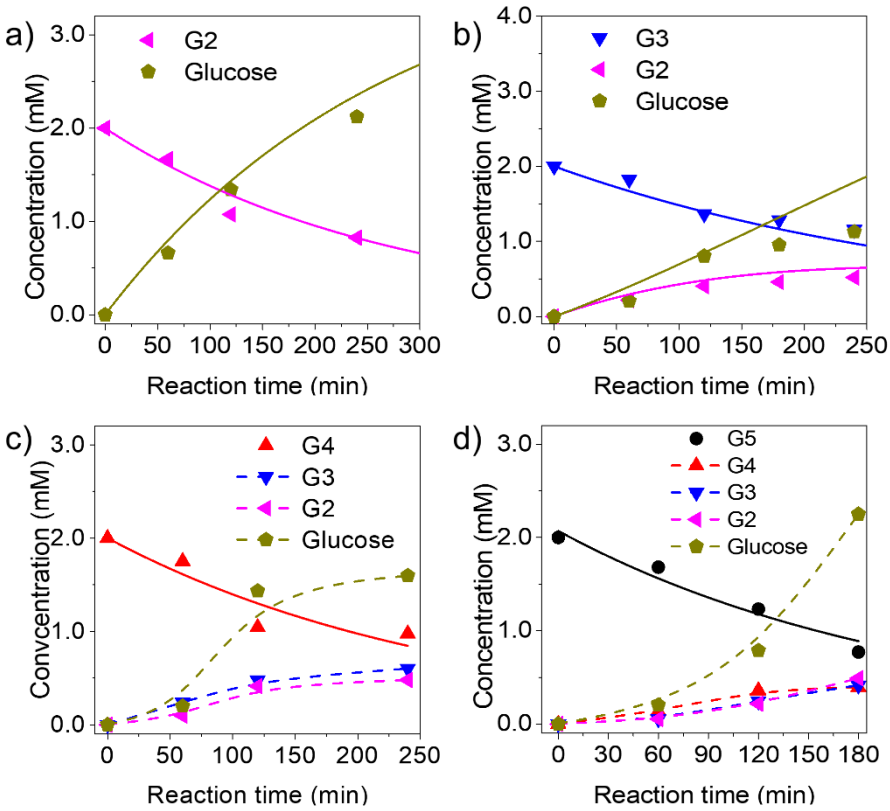

Figure 3.5. Time dependent conversion of cello-oligosaccharides and evolution of products in the presence of H-beta. Reaction conditions: 1 μmol cello-oligosaccharides (G2-G5), 5 mg H-beta, 0.5 mL H_2O, 0.5 MPa Ar, 413 K. a) G2, b) G3, c) G4, d) G5.

The rate constant of cello-oligosaccharide hydrolysis in the presence of homogeneous H_2SO_4 catalyst was also evaluated (Figure 3.6). The amount of H_2SO_4 used as catalyst was adjusted to match the total number of acid sites when AC-Air was used for the reaction. Hydrolysis in the presence of H_2SO_4 was much faster owing to its low pKa and homogeneous nature. The rate constant for hydrolysis of cellobiose was 2.94 h^{-1}, a value 7.7 times higher than that for AC-Air. A slight increase in rate constant of hydrolysis over H_2SO_4 was also observed with increasing DP of cello-oligosaccharides. However, the change in rate constant with DP was only 2.1 times from cellobiose to cellopentaose in comparison to 7 times for AC-Air.

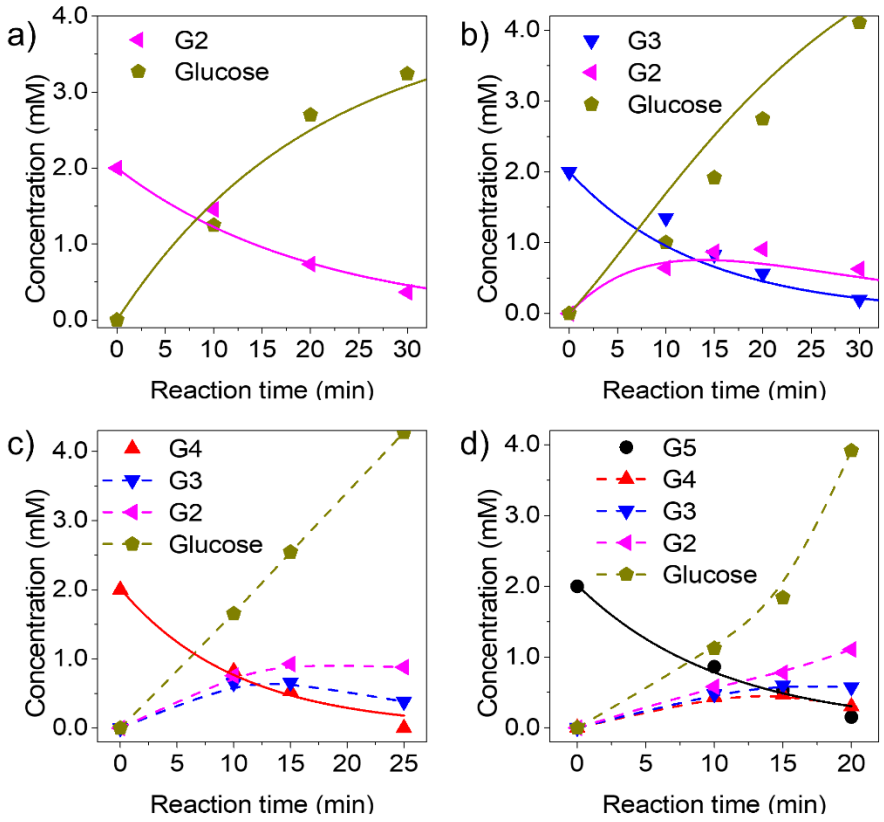

Figure 3.6. Time dependent conversion of cello-oligosaccharides and evolution of products in the presence of H_2SO_4. Reaction conditions: 1 μmol cello-oligosaccharides (G2-G5), 6.4 μmol H_2SO_4, 0.5 mL H_2O, 0.5 MPa Ar, 413 K. a) G2, b) G3, c) G4, d) G5.

The rate of hydrolysis over AC-Air-L was lower than that over AC-Air for all cello-oligosaccharides due to the less amounts of functional groups on the surface. However, a similar increasing trend for rate constant with DP of cello-oligosaccharide was obtained for AC-Air-L. From these results, we conclude that carbon materials show a uniquely preferential interaction with cello-oligosaccharides and the increase in DP favors this interaction causing an increase in their rate of hydrolysis.

It can be argued that the hydrolysis rate increased due to presence of more β-1,4-glycosidic linkages per molecule for larger cello-oligosaccharides. For example, cellobiose contains one glycosidic linkage whereas four linkages are present in cellopentaose. However, the rate constant increased 7 times from cellobiose to

cellopentaose in the presence of AC-Air, a value well above the increase in number of glycosidic linkages. Moreover, if the number of glycosidic linkages plays a crucial role, then its effect should be more prominent in the presence of H_2SO_4. However, the increase in rate constant was only 2.1 times in this case. This discrepancy further confirms the inherent ability of carbon catalysts to easily hydrolyze cello-oligosaccharides with higher degree of polymerization.

3.3.3 Adsorption of cello-oligosaccharides over solid catalysts

One distinct property of carbon materials is their ability to adsorb carbohydrates, which is likely to influence the rate of hydrolysis. It has been clarified that the adsorption of β-1,4-glucans on carbon surface occurs by CH-π and hydrophobic interactions.[26,28] Hydrolysis of cellulose is known to increase by 13 times when it is adsorbed on carbon surface by ball milling.[33] Therefore, the adsorption affinity of cello-oligosaccharides on all catalysts in this study was evaluated to elucidate its influence on rate of hydrolysis. Adsorption under reaction condition is expected to be lower than room temperature, but the change in adsorption capacity with respect to cello-oligosaccharide size is expected to the follow the same trend.

H-beta showed no adsorption of cello-oligosaccharides even though it had a relatively large surface area with micropores structure. The same phenomenon was observed in the case of Amberlyst 70 and there was no difference in the concentration of cello-oligosaccharides during adsorption.

The adsorption of cello-oligosaccharides on AC-Air was markedly different. The adsorption isotherms for G2-G5 cello-oligosaccharides over AC-Air are shown in Figure 3.7 a. They fitted well with the Langmuir adsorption model of type I isotherms in which the adsorption increased initially with change in concentration of reactant and then plateaus once the adsorption capacity was reached.[26,28] Accordingly, Langmuir

formula shown in Equation (3.13) was used to calculate the adsorption capacity (Q_{max}) and adsorption equilibrium constant (K_{ads}):

$$\frac{C}{Q_e} = \frac{1}{Q_{max}} C + \frac{1}{K_{ads} Q_{max}} \quad (3.13)$$

where C is the equilibrium concentration of cello-oligosaccharides after adsorption, Q_e (mg g $_{adsorbent}$ $^{-1}$) and Q_{max} (mg g $_{adsorbent}$ $^{-1}$) are the adsorption amount and the maximum adsorption capacity of cello-oligosaccharides, respectively. K_{ads} represents the adsorption equilibrium constant.

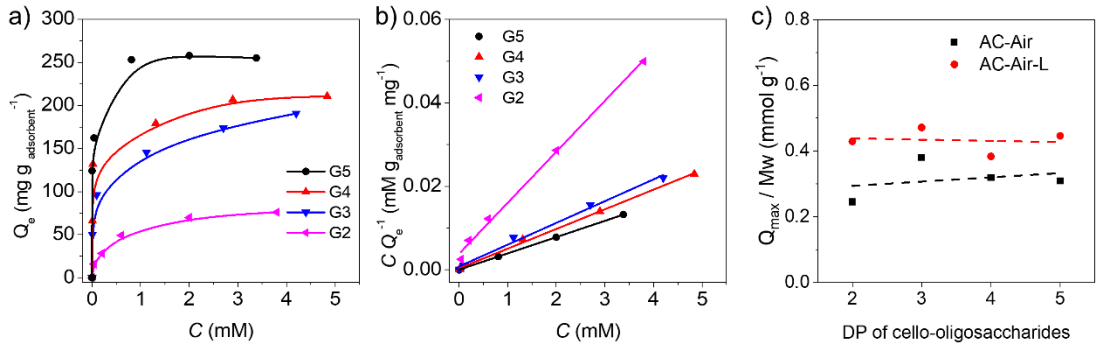

Figure 3.7. Adsorption of cello-oligosaccharides (G2-G5) on AC-Air: a) Adsorption isotherms, b) Langmuir plot derived from equation (3. 13). c) Plot showing maximum molar concentration of cello-oligosaccharides over AC-Air and AC-Air-L at saturation condition.

The Langmuir plots for each cello-oligosaccharide resulted in a good linear fit (Figure 3.7 b) and the calculated values for Q_{max} and K_{ads} are summarized in Table 3.2. The Q_{max} for cellobiose was 84 mg $g_{adsorbent}^{-1}$, which increased sequentially to 256 mg $g_{adsorbent}$ $^{-1}$ for cellopentaose. Similarly, the K_{ads} also increased 40-fold from G2 to G5. These parameters indicate that there is a stronger affinity for adsorption of larger cello-oligosaccharides on carbon surface. AC-Air-L showed higher Q_{max} and K_{ads} for all cello-oligosaccharides in comparison to AC-Air. AC-Air-L is expected to have a higher polyaromatic surface area owing to lower number of acidic functional groups and a larger surface area, which explains its higher adsorption capacity.

Table 3.2 Langmuir constants of cello-oligosaccharide adsorption over carbon catalysts at room temperature.

Substrate	AC-Air		AC-Air-L	
	Q_{max} (mg g^{-1})	K_{ads} (M^{-1})	Q_{max} (mg g^{-1})	K_{ads} (M^{-1})
G2	84	2429	147	4000
G3	192	6500	238	42000
G4	213	15667	256	195000
G5	256	97500	370	-

Figure 3.7 c shows a plot of number moles of cello-oligosaccharides adsorbed over carbon materials with respect to DP under saturation adsorption condition. For both carbon catalysts, the total molar adsorption of cello-oligosaccharides was not influenced with DP. Analysis of adsorption data reported by previous studies also shows that equivalent molar adsorption occurs over other carbon materials. Over K26, an alkali activated carbon, the molar adsorption of cellobiose and cellotriose was calculated as 1.2 and 1.0 mmol g^{-1}.[26] Similarly, over a mesoporous carbon surface, the molar adsorption for cellobiose, cellotriose and cellotetraose was calculated as 1.6, 1.1 and 1.0 mmol g^{-1}.[28] Therefore, It is concluded that although larger cello-oligosaccharides show a higher affinity to adsorb over carbon surface, this doesn't influence their surface concentration and this phenomenon is not linked with the type of carbon material used. Hence the increase in rate of hydrolysis cannot simply be a result of higher abundance of larger cello-oligosaccharide over the catalyst surface owing to stronger adsorption.

3.3.4 Affinity of cello-oligosaccharides and carbon catalyst

Adsorption can also influence the structure of large molecules, especially when they are adsorbed within narrow pores. To examine this possibility, the microporous structure of carbon materials was compared with the size of cello-oligosaccharide

molecules. The external surface area of AC-Air calculated by t-plot was only 45 m^2 g^{-1}. AC-Air-L had a similar structure with an external surface area of 55 m^2 g^{-1}. These surface areas are much lower than the minimum surface area required for adsorption of cello-oligosaccharides under equilibrium condition. This suggests that although adsorption may occur at any available surface area, the bulk of the cello-oligosaccharides are adsorbed within the micropores.

The pore size distribution of carbon catalysts was determined by NLDFT simulation (Figure 3.8). AC-Air and AC-Air-L catalysts showed a presence of micropores smaller than 2.0 nm, with the peaks centered at 0.98 nm and 1.0 nm, respectively. Their distributions of pore width became broader compared to pristine AC. In comparison, the cellobiose molecule has dimensions of 1.0×0.8×0.6 nm, whereas cellopentaose has dimensions of 2.5×0.7×0.6 nm. Therefore, the cello-oligosaccharides, especially the larger ones, must axially enter the micropores and adsorb within the micropore of the carbon catalysts.

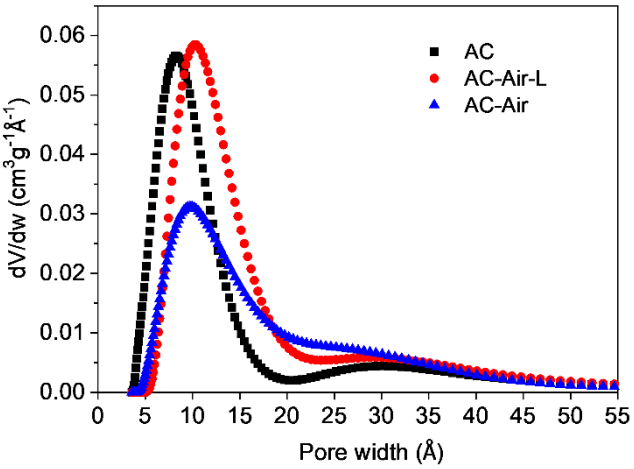

Figure 3.8. Pore size distribution of pristine and oxidized carbons determined by NLDFT simulation of N_2 adsorption isotherms.

The evolution of products during hydrolysis confirms this assertion. A closer inspection of hydrolysis data for cellotetraose (Figure 3.9 a) showed that the

concentration of cellotriose was same as glucose within the first 10 mins of reaction, which was twice than that of cellobiose. Preferential hydrolysis of terminal glycosidic bonds would cause a higher concentration of cellotriose and glucose (Figure 3.9 d). Axial adsorption of cello-oligosaccharides would favor the hydrolysis of terminal glycosidic bonds. A similar trend was also observed in the cases of hydrolysis of cellopentaose (Figure 3.9 b) and cellohexaose (Figure 3.9 c), in which cellotetraose and cellopentaose appeared as primary products along with equal amount of glucose. This observation is uniquely analogous to exoglucanase enzymes that sequentially cleave a glucose or cellobiose molecule from the chain end of cellulose.[34] Hence it reveals that the notion of heterogeneous carbon catalysts randomly cleaving the β-1,4-glycosidic bonds of adsorbed cellulose molecules, in a manner analogues to endoglucanase, is not entirely true.

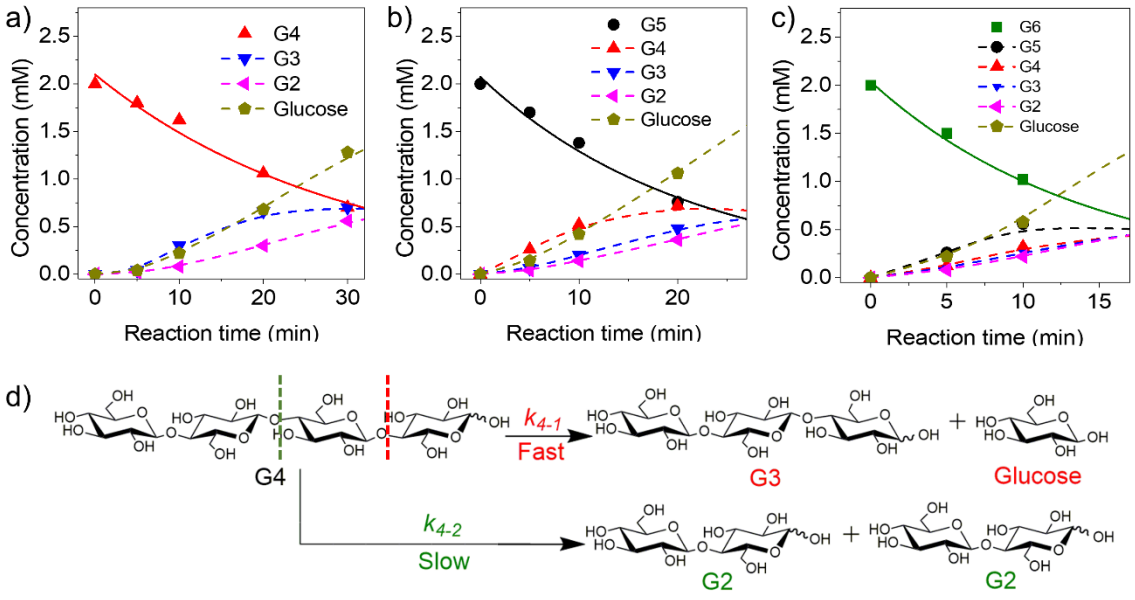

Figure 3.9. Close-up of reaction profiles shown in Figure 3.2 to illustrate the evolution of products from a) G4, b) G5, c) G6 over AC-Air catalyst. d) Scheme showing the pathway for hydrolysis of either the terminal glycosidic linkages or the internal glycosidic linkage in G4.

3.3.5 Activation energy of cello-oligosaccharides

Nevertheless, the axial adsorption and sequential cleavage of cello-

oligosaccharides also does not fully explain the increase in rate of hydrolysis. So the change in apparent activation energy during hydrolysis of cello-oligosaccharides over AC-Air was further evaluated. Arrhenius equation for the calculation is shown in Equation (3.14):

$$lnk = -\frac{E_a}{R}\frac{1}{T} + lnA \quad (3.14)$$

where k (h^{-1}) is the rate constant of cello-oligosaccharide hydrolysis, E_a (kJ mol^{-1}) represents the activation energy for cello-oligosaccharides hydrolysis. A (h^{-1}) and T (K) are the pre-exponential factor for the reaction and the absolute reaction temperature, respectively. R (kJ K^{-1} mol^{-1}) is the universal gas constant.

Hydrolysis of cello-oligosaccharides at other temperatures also conformed to the pattern of increase in rate constant with increase in number of glycosidic bonds (Table 3.3). The Arrhenius plots of these data fitted linearly with a high correlation coefficient (0.99, Figure 3.10). The apparent activation energy for cellobiose hydrolysis was calculated as 100 kJ mol^{-1}. A similar value of activation energy for cellotriose was obtained as 98 kJ mol^{-1}. The activation energy for hydrolysis of cellotetraose was 87 kJ mol^{-1} which further decreased to 77 kJ mol^{-1} for cellopentaose. This drastic reduction in the activation energy suggests a decrease in energy required to cleave the glycosidic bonds as the DP increases. Furthermore, it might be expected that the stronger adsorption of larger cello-oligosaccharides would lead to an increase in the pre-exponential factor (A). Instead, the value of A decreased, which could be attributed to the *compensation effect* observed when comparing E_a and A for reactions under similar conditions.[35]

Table 3.3 Rate constant of cello-oligosaccharide hydrolysis at varying temperatures over AC-Air and the calculated activation energy of hydrolysis for respective compounds.

Substrate	k (h^{-1})				E_a	A
	403 K	413 K	423 K	433 K	(kJ mol^{-1})	(h^{-1})
G2	0.17	0.38	0.72	1.38	100	1.74×10^{12}
G3	0.33	0.57	1.44	2.64	98	1.71×10^{12}
G4	0.81	2.15	3.37	5.13	87	2.16×10^{11}
G5	1.43	2.66	4.57	6.91	77	1.10×10^{10}

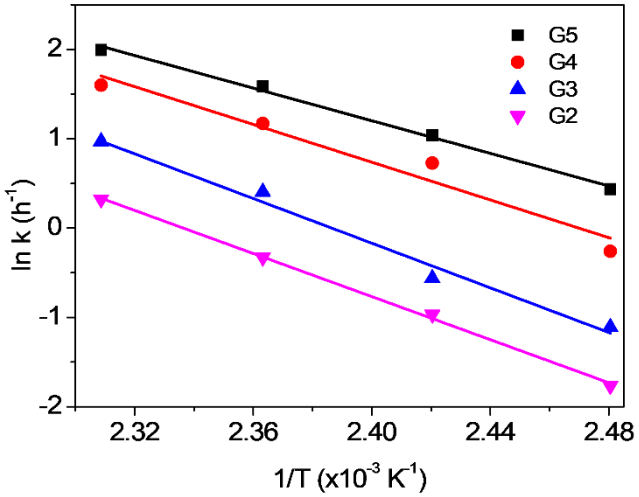

Figure 3.10. Arrhenius plot of cello-oligosaccharides (G2-G5) hydrolysis on AC-Air.

Moreover, the activation energy under the same reaction condition in the presence of H_2SO_4 catalyst was also calculated. The Arrhenius plots and calculated values of activation energy are shown in Figure 3.11. An identical value of 100 kJ mol^{-1} for activation energy of cellobiose hydrolysis was observed. This result was lower than previously reported value of 120-130 kJ mol^{-1} for cellobiose hydrolysis over concentrated H_2SO_4.[5] Lower concentration of cellobiose in our reaction mixture (2 mM) was the reason for this low value because activation energy of 139 kJ mol^{-1} was obtained when 50 mM solution of cellobiose was used in our reaction. A slight decrease in activation energy was also detected with the increase of DP of cello-oligosaccharides.

However, the activation energy decreased only by 11 kJ mol^{-1} from cellobiose to cellopentaose for H_2SO_4.

a)

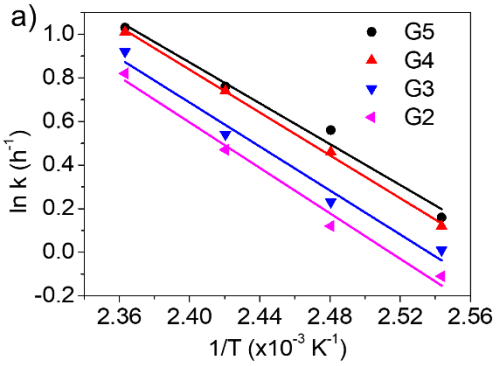

b)

Substrate	*Ea* (KJ mol $^{-1}$)
G2	100
G3	97
G4	94
G5	89

Figure 3.11. Arrhenius plot a) of cello-oligosaccharides hydrolysis on H_2SO_4 and the calculated activation energy b).

3.3.6 Proposed hydrolysis mechanism

Based on the above observations and in light of previous reports, it can be proposed that in addition to the presence of oxygenated functional groups, the adsorption and conformational change within the micropore influence rate of hydrolysis for cello-oligosaccharide. The increase in rate of hydrolysis with DP is caused by a decrease in activation energy required for hydrolysis of β-1,4-glycosidic bonds owing to their adsorption within the micropores of carbon. It is likely that the axial adsorption of a large molecule such as cellopentaose inside the micropores of carbon would cause a conformational change in its structure.[36] Cello-oligosaccharides conform to a stable twisted ribbon structure in aqueous solution.[37] Upon adsorption, this structure would untwist to accommodate itself within the pores and to achieve adsorption of multiple glucose units over the carbon surface (Figure 3.12). This deviation from the stable twisted form could cause a change in β-1,4-glycosidic bond angle, leading to reduction in activation energy required for its cleavage.

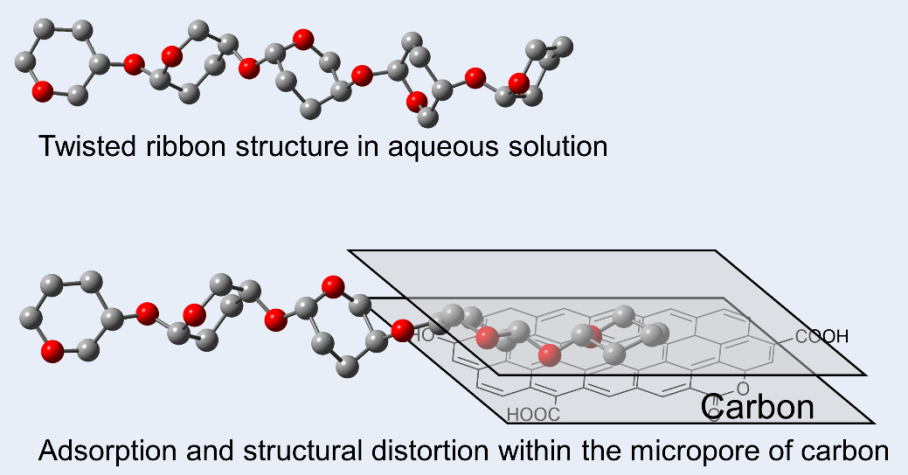

Figure 3.12. Illustration showing the twisted ribbon structure of cellopentaose in water and the proposed structural change during the adsorption on carbon surface. For clarity the hydroxyl groups are not shown and only the pyranose rings are depicted linked by β-1,4-glycosidic bond.

3.4 Conclusions

The hydrolysis of cello-oligosaccharides with increasing degree of polymerization in the presence of various catalysts was performed. Only in the presence of carbon catalysts the rate of hydrolysis was strongly dependent on their degree of polymerization. The hydrolysis rate constant increased 11 times with an increase in DP from 2 to 6. A simultaneous decrease in apparent activation energy for hydrolysis was also observed with respect to increase in DP. In addition, the larger oligosaccharide showed a stronger affinity towards adsorption over the narrow micropores of the carbon surface. A preference for hydrolysis of terminal over internal glycosidic bonds was observed, which was analogous to some enzymes in the cellulase family. Based on these observations, it is proposed that the increase in rate of hydrolysis is caused by reduction in activation energy which is the result of conformational changes in the oligosaccharide molecules when they adsorb within micropores of carbon.

References

1. G. W. Huber, S. Iborra and A. Corma, *Chem. Rev.*, 2006, **106**, 4044-4098.
2. D. Klemm, B. Heublein, H.-P. Fink and A. Bohn, *Angew. Chem. Int. Ed.*, 2005, **44**,

3358-3393.

3. A. J. Ragauskas, C. K. Williams, B. H. Davison, G. Britovsek, J. Cairney, C. A. Eckert, W. J. Frederick, Jr., J. P. Hallett, D. J. Leak, C. L. Liotta, J. R. Mielenz, R. Murphy, R. Templer and T. Tschaplinski, *Science*, 2006, **311**, 484-489.
4. E. Kontturi, T. Tammelin and M. Osterberg, *Chem. Soc. Rev.*, 2006, **35**, 1287-1304.
5. R. Rinaldi and F. Schüth, *ChemSusChem*, 2009, **2**, 1096-1107.
6. H. Zhao, C. L. Jones, G. A. Baker, S. Xia, O. Olubajo and V. N. Person, *J. Biotechnol.*, 2009, **139**, 47-54.
7. N. Kamiya, Y. Matsushita, M. Hanaki, K. Nakashima, M. Narita, M. Goto and H. Takahashi, *Biotechnol. Lett.*, 2008, **30**, 1037-1040.
8. Q. Chu, X. Li, Y. Xu, Z. Wang, J. Huang, S. Yu and Q. Yong, *Process Biochem.*, 2014, **49**, 1217-1222.
9. A. T. To, P. W. Chung and A. Katz, *Angew. Chem. Int. Ed.*, 2015, **54**, 11050-11053.
10. Y.-B. Huang and Y. Fu, *Green Chem.*, 2013, **15**, 1095-1111.
11. S. Suganuma, K. Nakajima, M. Kitano, D. Yamaguchi, H. Kato, S. Hayashi and M. Hara, *J. Am. Chem. Soc.*, 2008, **130**, 12787-12793.
12. A. Charmot, P.-W. Chung and A. Katz, *ACS Sustainable Chem. Eng.*, 2014, **2**, 2866-2872.
13. A. Martin-Mingot, K. D. O. Vigier, F. Jérômeb and S. Thibaudeau, *Org. Biomol. Chem.*, 2012, **10**, 2521-2524.
14. T. Liebert, M. Seifert and T. Heinze, *Macromol. Symp.*, 2008, **262**, 140-149.
15. T. Hasunuma, K. Kawashima, H. Nakayama, T. Murakami, H. Kanagawa, T. Ishii, K. Akiyama, K. Yasuda, F. Terada and S. Kushibiki, *Anim. Sci. J.*, 2011, **82**, 543-548.
16. C. D. A. Souza, S. Li, A. Z. Lin, F. Boutrot, G. Grossmann, C. Zipfel and S. C. Somerville, *Plant Physiol.*, 2017, **173**, 2383-2398.
17. E. Billès, V. Coma, F. Peruch and S. Grelier, *Polym. Int.*, 2017, **66**, 1227-1236.
18. A. Shrotri, H. Kobayashi and A. Fukuoka, *Acc. Chem. Res.*, 2018, **51**, 761-768.
19. X. Zhang, K. Wilson and A. F. Lee, *Chem. Rev.*, 2016, **116**, 12328-12368.
20. A. Onda, T. Ochi and K. Yanagisawa, *Green Chem.*, 2008, **10**, 1033-1037.
21. B. R. Caes, M. J. Palte and R. T. Raines, *Chem. Sci.*, 2013, **4**, 196-199.
22. A. Shrotri, H. Kobayashi and A. Fukuoka, *ChemCatChem*, 2016, **8**, 1059-1064.
23. G. S. Foo and C. Sievers, *ChemSusChem*, 2015, **8**, 534-543.
24. H. Kobayashi, T. Komanoya, K. Hara and A. Fukuoka, *ChemSusChem*, 2010, **3**, 440-443.
25. A. Shrotri, H. Kobayashi and A. Fukuoka, *ChemSusChem*, 2016, **9**, 1299–1303.
26. M. Yabushita, H. Kobayashi, J.-Y. Hasegawa, K. Hara and A. Fukuoka, *ChemSusChem*, 2014, **7**, 1443-1450.

27. P. Dornath, S. Ruzycky, S. Pang, L. He, P. Dauenhauer and W. Fan, *Green Chem.*, 2016, **18**, 6637-6647.
28. P. W. Chung, A. Charmot, O. M. Gazit and A. Katz, *Langmuir*, 2012, **28**, 15222-15232.
29. P. Chen, A. Shrotri and A. Fukuoka, *ChemSusChem*, 2019, **12**, 2576-2580.
30. H. P. Boehm, *Carbon*, 2002, **40**, 145-149.
31. J. Guilera, R. Bringué, E. Ramírez, M. Iborra and J. Tejero, *Ind. Eng. Chem. Res.*, 2012, **51**, 16525-16530.
32. L. Vanoye, M. Fanselow, J. D. Holbrey, M. P. Atkins and K. R. Seddon, *Green Chem.*, 2009, **11**, 390.
33. M. Yabushita, H. Kobayashi, K. Hara and A. Fukuoka, *Catal. Sci. Technol.*, 2014, **4**, 2312-2317.
34. K. Igarashi, T. Uchihashi, A. Koivula, M. Wada, S. Kimura, T. Okamoto, M. Penttil, T. Ando and M. Samejima, *Science*, 2011, **33**, 1279-1282.
35. W. C. Conner Jr., *J. Catal.*, 1982, **78**, 238-246.
36. P.-W. Chung, M. Yabushita, A. T. To, Y. Bae, J. Jankolovits, H. Kobayashi, A. Fukuoka and A. Katz, *ACS Catal.*, 2015, **5**, 6422-6425.
37. M. Umemura, Y. Yuguchi and T. Hirotsu, *J. Phys. Chem. A*, 2004, **108**, 7063-7070.

Chapter 4

Carbon catalyst with high density of carboxyl groups for the hydrolysis of cellulose to cello-oligosaccharides

Abstract

Short chain cello-oligosaccharides (G3-G6) exhibit high bioactivity as elicitors for improving the growth of plants. Controlled synthesis of these cello-oligosaccharides with narrow distribution is desirable for their effective utilization. Based on results from chapters 2 and 3, it is deduced that secondary hydrolysis of soluble cello-oligosaccharides over carbon catalyst preferentially produces glucose and reduces overall yield. Therefore, in order to obtain high yield of desired G3-G6 products, it is essential to improve the activity of catalyst to achieve one step direct conversion of cellulose to small cello-oligosaccharides. The desired carbon catalyst was synthesized by chemical oxidation of activated carbon to introduce high density of acidic sites. Oxidation with ammonium persulfate (APS) introduced 3.57 mmol g^{-1} of acidic functional groups on the carbon surface without altering the textual properties. This treatment enhanced the selectivity towards formation of carboxyl groups (1.72 mmol g^{-1}), which increased the hydrolysis activity. Cello-oligosaccharide with yield of 70 % was achieved from cellulose hydrolysis over this oxidized carbon catalyst in the semi-flow reactor. The mix-milling time reduced to 30 min owing to high activity of the catalyst. Quantification of individual products suggests that cello-oligosaccharides with low DP were obtained directly as major components with 50 % yield of G3-G6 cello-

oligosaccharides.

4.1 Introduction

Cello-oligosaccharides are obtained by the partial hydrolysis of cellulose. Preventing their further degradation to glucose is an essential step in order to achieve high yield of cello-oligosaccharides. Although conventional homogeneous acid catalysts are well-known for cellulose hydrolysis, the much faster hydrolysis rate of cello-oligosaccharides in comparison to cellulose hydrolysis hinders their use in this expected reaction. Hydrolysis rates are reversed in the presence of heterogeneous carbon catalysts when a suitable pretreatment method is employed. Under this condition, faster rate of cellulose hydrolysis in comparison to cello-oligosaccharides reduced the formation of unwanted glucose and cellobiose. In addition, the benign nature of carbon catalyst is essential to prevent contamination of cello-oligosaccharides products that finds application in agriculture and healthcare industries.

Chapter 2 reported that high yield of cello-oligosaccharides was obtained through cellulose hydrolysis in a semi-flow reactor over air-oxidized carbon.[1] Quantification using MALDI-TOF MS revealed that molecules with higher molecular weight were the primary products, which could be changed by adjusting the space velocity and temperature of the reaction. Low space velocity caused a shift of product distribution towards the desired smaller molecules (G3-G6). However, this phenomenon was accompanied with the formation of glucose, resulting in lower overall yield of these cello-oligosaccharides. The kinetic study in Chapter 3 revealed that glucose formation was due to higher rate of hydrolysis for terminal glycosidic bonds. Therefore, reducing space velocity causes sequential hydrolysis of dissolved oligosaccharides to glucose. Based on these considerations, it is crucial to directly synthesize desired low molecular

weight cello-oligosaccharides from cellulose rather than relying on secondary hydrolysis of larger oligosaccharides (G7+) (Figure 4.1). I postulate that using a catalyst with high density of acidic functional groups will improve the hydrolysis performance and lower cello-oligosaccharide selectivity. Moreover, the presence of carboxyl groups as predominant functional group will be helpful.[2] The position of these oxygenated groups is also a significant factor for the catalyst activity. It was reported that the synergy of adjacent carboxylic groups enhances the formation of hydrogen bond between the hydroxyl groups in cellulosic molecule and functional groups on catalyst. The hydrogen bond formation increases the frequency factor leading to higher catalytic activity.[3]

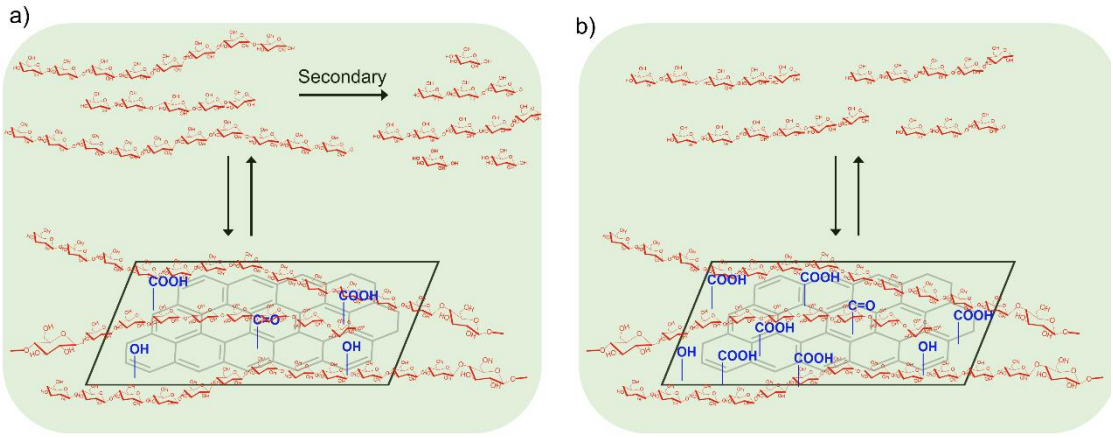

Figure 4.1. Scheme showing influence of surface acid site density on the surface of carbon catalyst over cello-oligosaccharide product distribution. a) Low density of acid sites leads to the formation of large oligosaccharides, which undergo secondary hydrolysis. b) High density of acid sites directly produces small cello-oligosaccharides and their secondary hydrolysis can be avoided.

Therefore, this study reports the synthesis of carbon catalysts with high density of weakly acidic functional groups by using different oxidation methods. And these catalysts are tested for hydrolysis activity towards the formation of water-soluble cello-oligosaccharides from cellulose.

4.2 Experimental Methods

4.2.1 Materials

Microcrystalline cellulose (Avicell PH-101) was purchased from Sigma Aldrich. Activated carbon (denoted as AC) and carbon black (denoted as CB) were supplied from Ajinomoto Fine-Techno. Granular SiO_2 (Q30, 100 - 200 mesh) was supplied from Fuji Silysia Chemical Ltd. Ammonium persulfate ($(NH_4)_2S_2O_8$, APS) and sulfuric acid (H_2SO_4) was purchased from Wako Pure Chemical Industries.

4.2.2 Oxidation treatment of carbon catalyst

Chemical oxidation of carbon catalyst was conducted in a round bottom flask. 1 M H_2SO_4 solution was prepared containing 2 mol L^{-1} of APS. For oxidation, 1.0 g carbon material (AC or CB) was dispersed in 20 mL of APS-H_2SO_4 solution. The mixture was heated and kept at 333 K for 3 h under stirring. After reaction the mixture was cooled to room temperature and the solid phase was separated by filtration. Copious amount of distilled water was used to wash the sample in order to remove the remaining H_2SO_4 and unreacted APS. Then the solid carbon catalysts were vacuum dried at 393 K for 3 h. The obtained catalysts were denoted as AC-APS and CB-APS. For comparison, AC-Air was prepared using the method described in Chapter 2.

4.2.3 Characterization of catalysts

The crystallinity of catalysts was analyzed by using X-ray diffraction (XRD; Rigaku Miniflex) measurement using CuKa radiation. FTIR spectra were measured by making a KBr pellet containing 0.1 wt. % of sample (0.05 wt. % in the case of CB and CB-APS). The pellet was then analyzed by using a PerkinElmer Spectrum 100 FT-IR Spectrometer. Specific surface area of catalysts was determined by BET analysis based on the N_2 adsorption-desorption isotherms (BEL Japan, BELSORP-min) after outgassing at 393 K for 3 h. The total amount of acidic functional groups on carbon

catalysts were calculated by the titration method described in Chapter 2. XPS analysis was performed by using a JEOL JPC-9010 MC instrument. Before analysis, the sample was spread on a copper tape with a thin layer and degassed in the preparation chamber overnight. Temperature-programmed desorption (TPD) was performed in a BELCAT-A coupled with a mass spectrometer (m/z 28 for CO and m/z 44 for CO_2). The elemental composition of catalysts was determined by using a CE440 CHN analyzer.

4.2.4 Ball-milling of cellulose and catalysts

For the mix-milling of cellulose and catalyst, 2.5 g microcrystalline cellulose and 0.38 g carbon catalysts (S/C=6.5) were milled together in an alumina pot with 100 g alumina balls of 5 mm diameter at 500 rpm in a Fritsch P-6 planetary ball mill. One milling cycle included 10 minutes of milling followed by 10 minutes of pause to allow dissipation of heat. In the case of AC-Air, 6 cycles were performed to give a total milling time of 1 h, whereas other catalysts were milled for only 3 cycles with a milling time of 30 min. After milling, the mixture was separated by sieving, followed by drying under vacuum at 393 K for 3 h. Mix-milled cellulose is denoted as MMC (S/C = 6.5).

4.2.5 Hydrolysis experiment

Hydrolysis experiments were performed in a semi-flow reactor shown in Figure 2.2 under similar reaction conditions reported in Chapter 2. The yield of products was calculated using the following (Equation 4.1):

$$\text{Yield of oligosaccharides (\%)} = \frac{\text{Moles of carbon in oligosaccharides}}{\text{Moles of carbon in cellulose}} \times 100 \qquad (4.1)$$

The product was analyzed using high performance liquid chromatography (HPLC) systems equipped with a refractive index detector (Shimadzu LC 10-ATVP) and a Shodex Sugar SB 802.5HQ×3 column (ø 8 × 300 mm; eluent, water at 0.5 mL min^{-1}; 328 K).

4.3 Results and discussion

4.3.1 Characterization of carbon catalysts

The abundance and nature of functional groups over carbon catalyst can be varied by using different oxidation treatment.[4] This variation can have a significant impact on the activity towards cellulose hydrolysis.[5] Here, air-oxidation and oxidation with ammonium persulfate (APS) were used for modification of activated carbon (AC). Carbon black, named as CB, was also used for the oxidation by APS. After air oxidation of AC, 51 wt. % of carbon was lost as a result of partial combustion of AC to CO and CO_2. In contrast, the mass loss was only 1 wt. % after treatment with APS. The concentration of oxygenated functional groups, which was determined by titration method reported previously,[6] and textural properties of these catalysts are summarized in Table 1. The total density of acidic functional groups on the carbon surface increased from 0.36 mmol g^{-1} in pristine AC to 2.56 mmol g^{-1} in AC-Air due to the concurrent increase in phenolic, lactone and carboxyl groups. Oxidation by APS introduced much higher amount of acidic functional groups totaling to 3.57 mmol g^{-1} in AC-APS. In addition, a higher proportion of acidic functional groups in AC-APS were composed of carboxyl groups (-COOH). This result was in agreement with previous result, which reported that the introduction of acidic functional groups onto carbon surface by using APS can selectively increase the density of carboxyl group.[7] The alkali treatment of CB-APS for the purpose of titration made it partially soluble in solution. Consequently, the number of acidic functional groups via titration in CB-APS could not be calculated.

Table 4.1. Properties of parent and modified carbon catalysts.

Catalyst	Oxidation method	Acidic functional groups (mmol g^{-1})				TPD (mmol g^{-1})		Surface area (m^2 g^{-1})	Total pore volume (cm^3 (STP) g^{-1})	Pore size (nm)
		OH	Lactone	COOH	Total	CO	CO_2			
AC	-				0.36	-	-	1143	256	0.80
AC-Air	Air	0.80	0.74	1.02	2.56	6.64	1.12	877	202	0.98
AC-APS	APS	0.66	1.19	1.72	3.57	4.30	1.39	838	192	0.68
CB	-	-	-	-	-			1093	251	1.50
CB-APS	APS	-	-	-	-	3.54	1.12	798	183	1.40

These carbon catalysts were characterized to understand the influence of oxidation on their physical and chemical properties. X-ray diffraction (XRD) spectra showed that all carbon materials were amorphous before and after oxidation treatment (Figure 4.2). Small peaks in AC and AC-Air were attributed to the presence of small amount of silica. Oxidation with any method caused a decrease in the BET surface area along with widening of pores (Figure 4.3 a). Parent AC has a surface area of 1143 m^2 g^{-1}, which decreased to 877 m^2 g^{-1} and 838 m^2 g^{-1} in AC-Air and AC-APS, respectively. Pore size distribution of carbon was calculated by NLDFT simulation. The pore size distribution for AC-Air shifted to a higher value with the peak center at 0.98 nm compared with 0.80 nm for AC (Figure 4.3 b). This was a result of pore widening and collapse owing to the burn off during air oxidation. In contrast, oxidation with APS caused a slight narrowing of pores as a result of formation of functional groups within the narrow pores of the carbon material. Surface area of carbon black (CB) also decreased from 1093 m^2 g^{-1} to 798 m^2 g^{-1} after APS oxidation. The N_2 adsorption isotherms for all carbons were type IV, indicative of a material containing irregular pore structure. AC had a hysteresis loop of type H4 and CB showed a type H3 kind of hysteresis loop (Figure 4.3 a and c). Type H4 is the typical form of hysteresis loop for activated carbon with slit type pores. The H3 type loop in CB is caused by presence of

interparticle spaces.[8,9] This assertion was also confirmed by the pore size distribution in Figure 4.3d, in which a broad peak appeared in the mesopore range along with a peak centered at 1.5 nm.

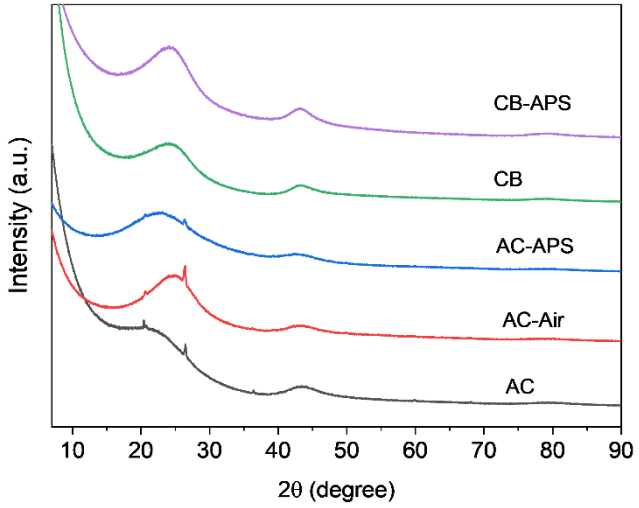

Figure 4.2. XRD patterns of carbon materials.

FTIR analysis was used to clarify the modification in structure of carbon, and the corresponding spectra of pristine and oxidized AC and CB materials were shown in Figure 4.4. The peak located at 3450 cm^{-1} was attributed to the stretching vibration of OH groups. The band appeared at 1600 cm^{-1} was attributed to ν (C=C) in the aromatic rings of carbon and δ (O-H) of adsorbed water. The broad band ranging from 1000 cm^{-1} to 1250 cm^{-1} was a result of multiple overlapping bands caused by ν (C-O) bonds. A prominent band appeared in oxidized carbon catalysts at around 1739 cm^{-1}, which was assigned to ν (C=O) in the O-C=O functional group. The presence of this vibration suggests the oxidation treatment successfully introduced the acidic functional groups on the carbon surface.

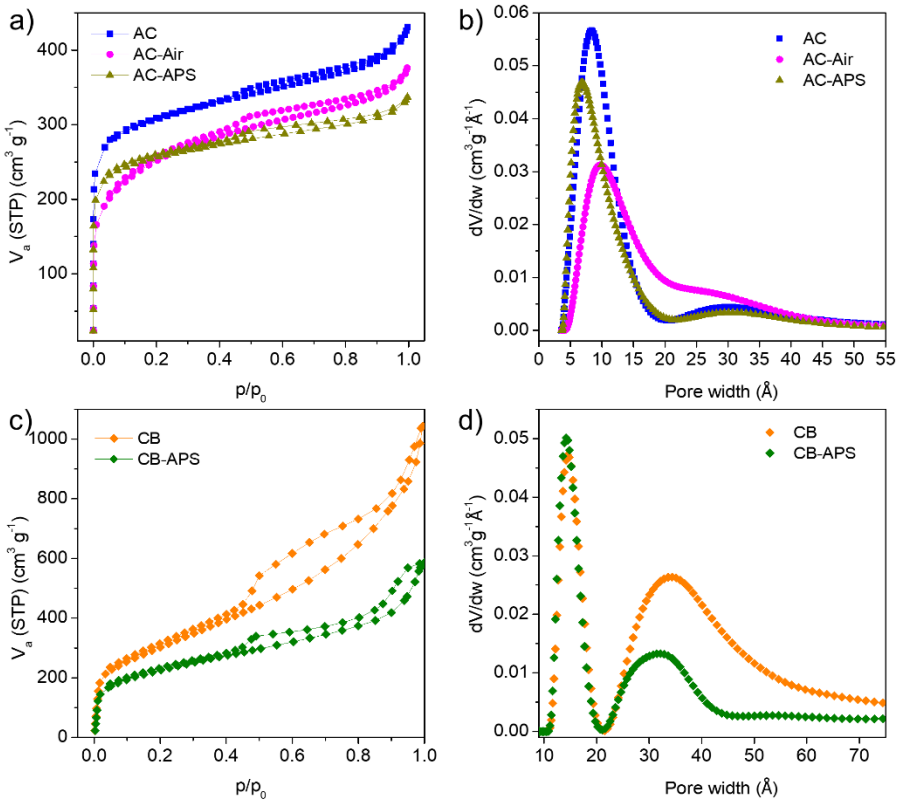

Figure 4.3. a) N_2 adsorption isotherms of parent and modified carbon AC materials, b) pore size distribution of parent and modified carbon AC materials, c) N_2 adsorption isotherms of parent and modified carbon CB materials, d) pore size distribution of parent and modified carbon CB materials.

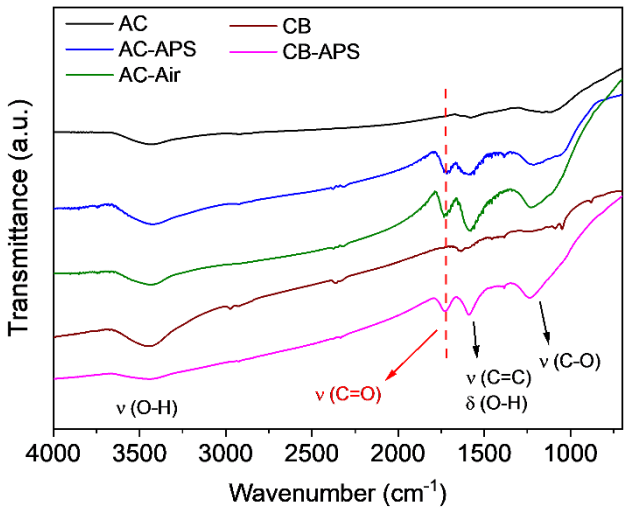

Figure 4.4. FTIR spectra of various carbon catalysts.

XPS analysis was performed to quantitatively differentiate the type of functional

groups on the carbon surface. The C 1s spectra for AC-Air, AC-APS and CB-APS are shown in Figure 4.5. All samples showed a dominant peak at 284.6 eV, assigned to aromatic carbon atoms inherent in carbon materials. The peaks with binding energy at 286.0 eV and 287.4 eV were assigned to carbon atoms with C-O bond and C=O bond present in hydroxyl group and carbonyl groups, respectively. AC-Air showed high proportions of these two functional groups. The peak appeared at 288.5 eV was attributed to the carbons present in the form of O-C=O bonds of carboxyl groups.[10] The presence of carboxyl groups in XPS spectra was in accordance with the result in FTIR analysis discussed above. However, the proportion of carboxyl groups in comparison to other functional groups was much higher in AC-APS than in AC-Air. This result indicates that AC-APS should have a higher activity for cellulose hydrolysis as it has higher density of reactive carboxyl groups. In addition, the lower density of hydroxyl and ketone groups will facilitate adsorption of cellulose.

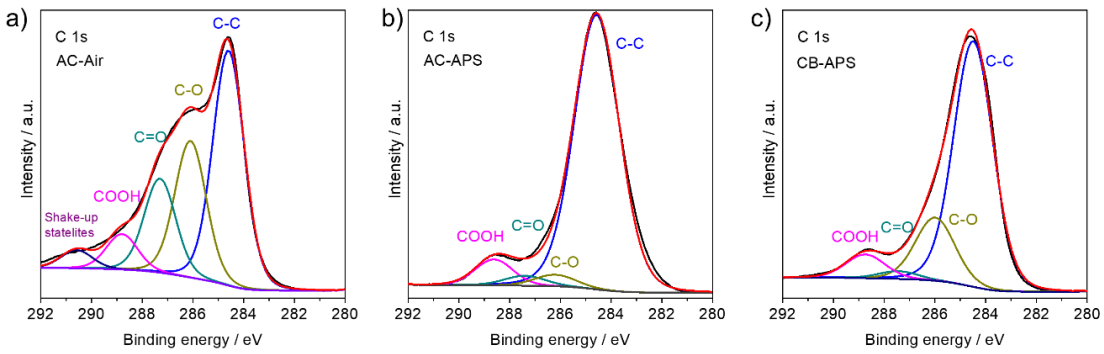

Figure 4.5. XPS spectra of carbon catalysts, a) AC-Air, b) AC-APS c) CB-APS.

In order to further understand the nature of these functional groups, TPD analysis was performed under the flow of He. Under this condition, CO, CO_2 and H_2O evolved as the functional groups decomposed at different temperatures based on their relative strength. The spectra are shown in Figure 4.6 and the quantification of gases evolved is summarized in Table 4.1. For AC-Air, the evolution of CO started at 500 °C with a

peak centered at 700 °C. The evolution of CO can be attributed to decomposition of hydroxyl, ketone, and ether type functional groups. The amount of evolved CO from AC-Air was quantified as 6.64 mmol g^{-1}, which was 2.6 times higher than the total acidic functional groups calculated by titration. This result suggests that there is a significant presence of nonacidic functional groups on AC-Air, such as carbonyl (C=O) as well as ether (C-O-C), which are not active for cellulose hydrolysis. This result is in agreement with XPS analysis. The evolution of CO_2 was detected in the similar temperature range with CO, which was caused by the decomposition of carboxyl groups and lactone. The amount of evolved CO_2 was calculated as 1.12 mmol g^{-1}, which was slightly higher than the expected amount based on titration data. The evolution of H_2O was not prominent for the AC-Air catalyst. The TPD result for AC-Air is in accordance with other reports.[11,12]

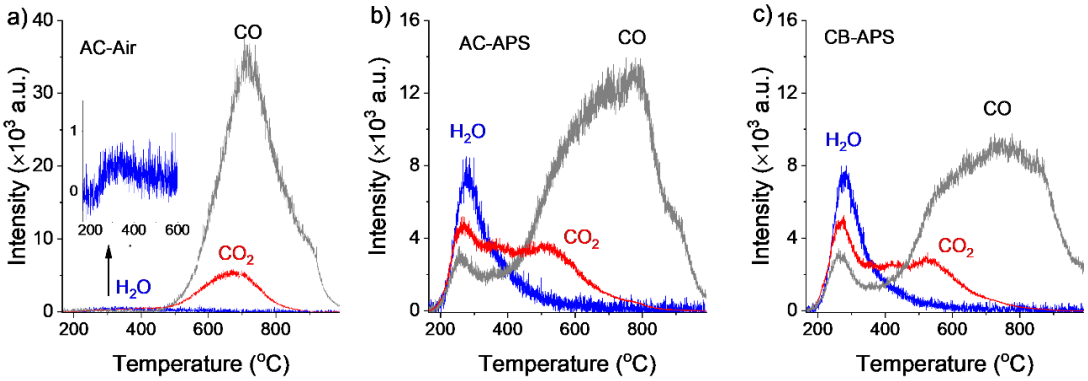

Figure 4.6. TPD mass spectra of carbon catalysts (50 mg), a) AC-Air, b) AC-APS, c) CB-APS.

The carbon catalysts synthesized by APS oxidation showed a very different TPD spectra (Figure 4.6 b and c). The evolution of CO_2 started at lower temperature compared with that of AC-Air. The CO_2 evolution peaks located at 290 °C, 345 °C and 500 °C were contributed to the strongly, weakly acidic carboxyl groups and carboxylic anhydrides/lactone, respectively. Evolution of CO showed two peaks centered at 290 °C and 790 °C. Moreover, obvious amount of H_2O was also released during the

decomposition of functional groups. The evolution of H_2O, CO and CO_2 was simultaneous, suggesting that they were part of the same decomposition mechanism. This type of behavior is expected during thermal decomposition of a dicarboxylic acid causing formation of an anhydride via dehydration followed by further decomposition to release CO and CO_2 (Figure 4.7).[13-15] Presence of dicarboxylic acid species over the carbon surface is expected to enhance the activity of the catalyst.

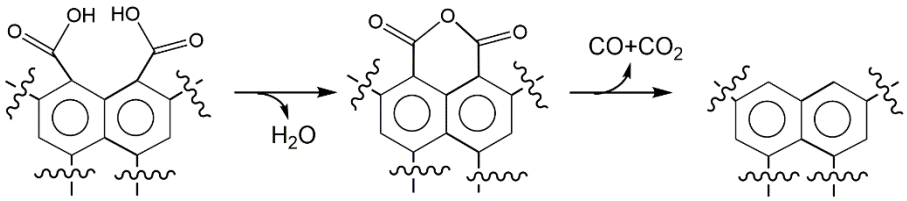

Figure 4.7. Decomposition process of two adjacent carboxylic acid on carbon catalyst during the thermal treatment.

The TPD of AC-APS released 1.39 mmol g^{-1} CO_2, which was again lower than the value of carboxyl groups calculated by titration. The amount of CO from TPD was determined as 4.30 mmol g^{-1}, which was slightly higher than the total acidic functional groups, indicating that nonacidic oxygenated groups were introduced on the carbon surface. The amount of CO_2 and CO evolved from CB-APS was 1.12 mmol g^{-1} and 3.54 mmol g^{-1}. However, the TPD spectrum and peak profile for CB-APS was similar to that of AC-APS, attesting formation of similar types of oxygenated functional groups.

In order to further identify the presence of vicinal carboxyl groups on oxidized AC-APS catalyst, the diffuse reflectance infrared fourier transform spectroscopy (DRIFTS) was used over a wide temperature range with the flow of He. The spectra of AC-APS catalyst at different temperatures are depicted in Fig. 4.8. As discussed above, infrared spectrum (IR) of AC-APS catalyst showed a prominent band at 1739 cm^{-1}, assigned as the ν (C=O) in the carboxyl groups or lactones. Once the temperature reached 200 ^oC, a new peak appeared at 1845 cm^{-1}, which corresponded to the

asymmetric C=O stretching in anhydrides (O=C-O-C=O). Concurrently, it was observed that the vibration band for ν (C=O) became broader with a new peak located at 1771 cm^{-1}, which was attributed to symmetric C=O stretching of anhydrides. This phenomenon suggests that anhydrides are formed on the carbon surface during the thermal treatment via the thermal decomposition of dicarboxylic acid, as shown in Fig. 4.7. Therefore, the presence of new peaks for anhydrides reveals the presence of vicinal carboxyl groups on oxidized AC-APS catalyst. After the temperature increased over 300 ºC, the signals for anhydrides gradually decreased and disappeared due to their further decomposition.

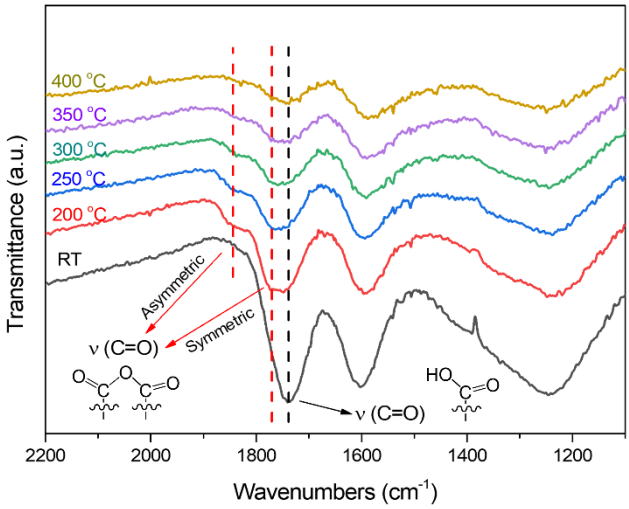

Figure 4.8. DRIFTS spectroscopy of AC-APS catalyst.

4.3.2 Cellulose hydrolysis on carbon catalysts

These catalysts were used for cellulose hydrolysis in a semi-flow reactor under a space velocity (SV) of 70 h^{-1} to evaluate their activity. Mix milling of cellulose and catalysts was done before hydrolysis to enhance the interaction between cellulose and catalyst.[16] In the presence of parent AC as catalyst, the total yield of hydrolysis products was 11 % including only 8.9 % yield of cello-oligosaccharides after reaction at 473 K for 40 min in the semi-flow reactor (Figure 4.8 a), which was ascribed to the low amount

of acid sites on carbon. The oxidized catalysts obviously showed high hydrolysis performance with the synthesis of high yield of products. Cello-oligosaccharides were obtained in a yield of 72 % by the hydrolysis over AC-Air after 1 h mix-milling treatment. When AC-APS was used as the catalyst, a similarly high yield (70 %) of cello-oligosaccharides was achieved with higher yield of dimer and monomer. It is important to note that this result was obtained only after 30 min mix-milling of cellulose and AC-APS in comparison to AC-Air for which 1 h of milling time is necessary. The higher density of acidic functional groups causes increase in catalytic activity and reduces milling time. CB-APS catalyst was also used for cellulose hydrolysis and similarly high yield of cello-oligosaccharides (67 %) was observed (Figure 4.9 a).

Although all catalysts exhibited similar total cello-oligosaccharide yield, the distribution of oligosaccharides was different as analyzed by MALDI-TOF MS.[14] The spectra showed that the peaks were separated by m/z of 162 as expected for cello-oligosaccharides. Cello-oligosaccharides with DP up to 13 were observed when cellulose was hydrolyzed by AC-Air and AC-APS, whereas the hydrolysis of cellulose over CB-APS produced cello-oligosaccharide with DP up to 11. Figure 4.9 b-d showed a plot of product yield with respect to DP. In the presence of AC-Air, cellohexaose and celloheptaose were obtained as major components. The distribution of product shifted to lower molecules with higher amount of cellotriose, as well as cellobiose and glucose, was produced over AC-APS catalyst, resulting in 50 % yield of desired G3-G6 cello-oligosaccharides (Figure 4.9 c). These results reveal that AC-APS catalyst increases the hydrolysis rate of β-1,4-glycosidic bonds in cellulose. Celloheptaose was produced as the major component when hydrolysis was performed by CB-APS catalyst and the hydrolysis products were evenly distributed in low molecular weight region (Figure 4.9 d).

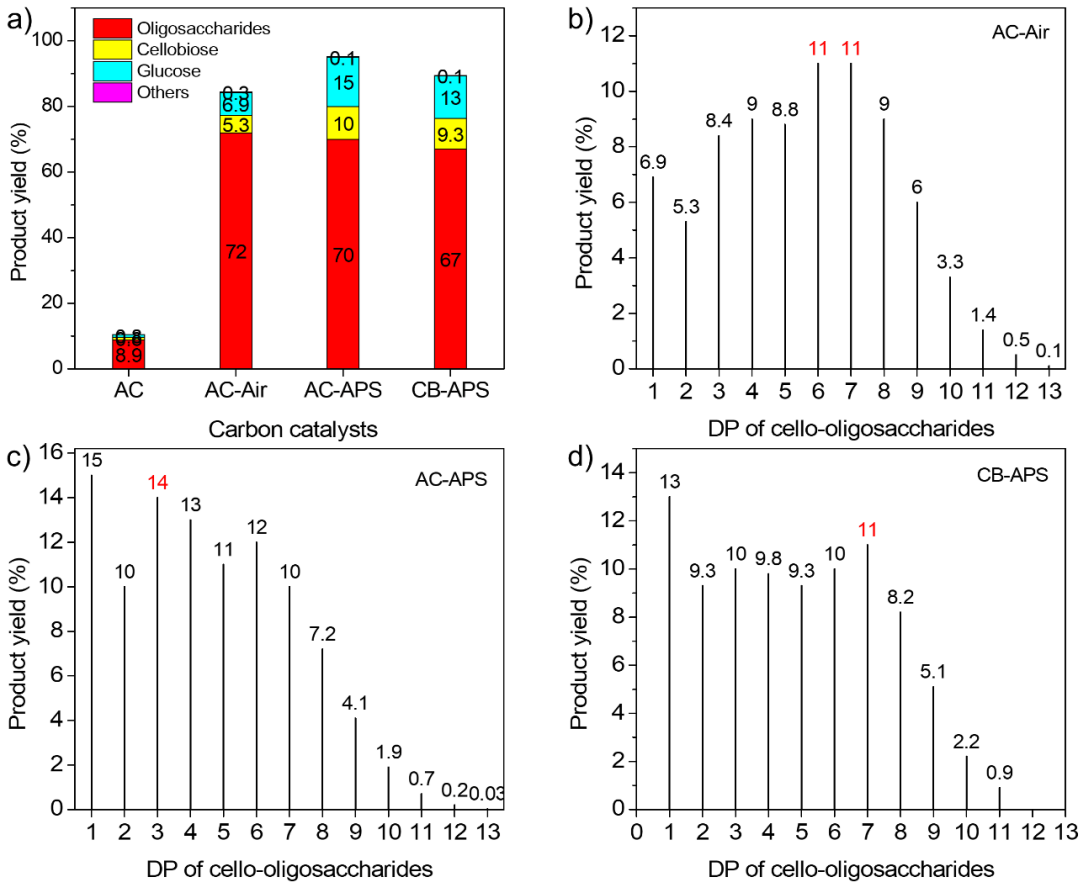

Figure 4.9. Total yield of products determined by HPLC analysis after cellulose hydrolysis by using different catalysts a). Products distribution measured by MALDI TOF MS over AC-Air b), AC-APS c), and CB-APS d). Reaction condition: 0.175 g MMC, 473 K, distilled water (0.75 mL min^{-1}), SV 70 h^{-1}.

Increasing the SV to 141 h^{-1} while keeping the other reaction conditions same resulted in 70 % yield of cello-oligosaccharides, whereas the product distribution shifted towards cello-oligosaccharides with higher molecular weight (Figure 4.10). Reduction in SV to 35 h^{-1} reduced the products yield to 53 % owing to incomplete elution of products from the reactor system. Increasing the reaction time to 2 h resulted in 62 % yield of cello-oligosaccharides along with large amounts of glucose. These results suggest that hydrolysis of cellulose over AC-APS catalyst with an SV of 70 h^{-1} favored the formation of desired cello-oligosaccharides.

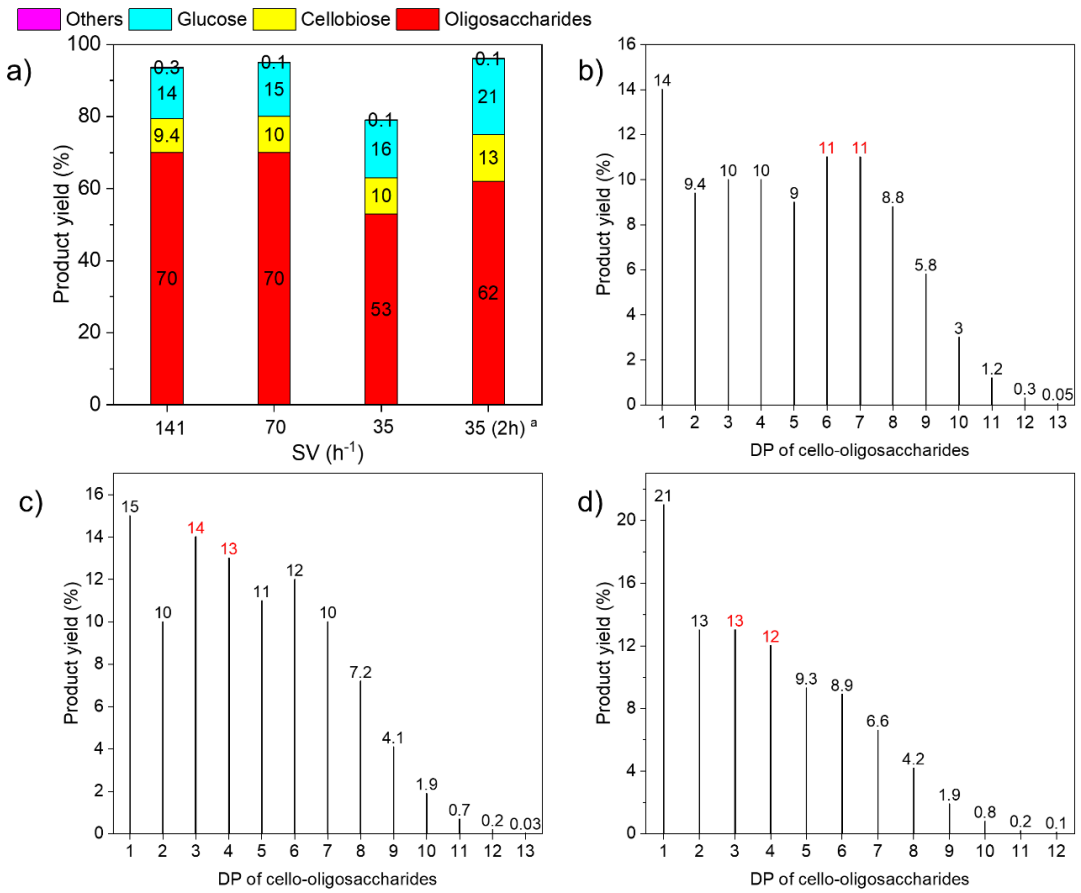

Figure 4.10. a) Cellulose hydrolysis HPLC results over AC-APS with different SV, b) Products distribution under SV of 141 h^{-1}, c) 70 h^{-1}, d) 35 h^{-1}. [a] Hydrolysis of cellulose was performed for 2 h. Reaction condition: 0.175 g MMC-AC-APS, 473 K, distilled water (0.75 mL min^{-1}).

4.4 Conclusions

This Chapter reports the synthesis of carbon catalysts with high density of weakly acidic oxygenated groups by the oxidation of activated carbon without altering inherent micropore structure. Treatment with ammonium persulfate (APS) introduced much higher amount of acidic functional groups in comparison with air-oxidation. APS treatment also resulted in higher proportion of carboxyl groups over the catalyst surface. TPD data suggested that vicinal di-carboxyl groups were present on the surface. AC-APS showed high activity for hydrolysis of cellulose, resulting in 70 % yield of cello-oligosaccharides with only 30 min of ball milling pretreatment. Quantification of

individual oligosaccharides showed increased yield (50 %) of smaller oligosaccharides G3-G6.

References

1. P. Chen, A. Shrotri and A. Fukuoka, *ChemSusChem*, 2019, **12**, 2576-2580.
2. H. Kobayashi, M. Yabushita, T. Komanoya, K. Hara, I. Fujita and A. Fukuoka, *ACS Catal.*, 2013, **3**, 581-587.
3. H. Kobayashi, M. Yabushita, J.-Y. Hasegawa and A. Fukuoka, *J. Phys. Chem. C*, 2015, **119**, 20993-20999.
4. J. L. Figueiredo, M. F. R. Pereira, M. M. A. Freitas and J. J. M. Orfao, *Carbon*, 1999, **37**, 1379-1389.
5. A. T. To, P. W. Chung and A. Katz, *Angew. Chem. Int. Ed.*, 2015, **54**, 11050-11053.
6. H. P. Boehm, *Carbon*, 2002, **40**, 145-149.
7. N. Li, X. Ma, Q. Zha, K. Kim, Y. Chen and C. Song, *Carbon*, 2011, **49**, 5002-5013.
8. C. M. Long, M. A. Nascarella and P. A. Valberg, *Environ. Pollut.*, 2013, **181**, 271-286.
9. P. Toth, T. Vikström, R. Molindera and H. Wiinikkaa, *Green Chem.*, 2018, **20**, 3981-3992.
10. A. Shrotri, H. Kobayashi and A. Fukuoka, *ChemSusChem*, 2016, **9**, 1299-1303.
11. A. Shrotri, H. Kobayashi, H. Kaiki, M. Yabushita and A. Fukuoka, *Ind. Eng. Chem. Res.*, 2017, **56**, 14471-14478.
12. L. Mahardiani, A. Shrotri, H. Kobayashi and A. Fukuoka, *Catal. Today*, 2019, DOI: 10.1016/j.cattod.2019.08.056.
13. H.P.Boehm, *Carbon*, 1994, **32**, 759-769.
14. M.Domingo-García, F. J. L. Garzón and M.J.Pérez-Mendoza, *J. Colloid Interface Sci.*, 2002, **248**, 116-122.
15. J. L. Figueiredo, M. F. R. Pereira, M. M. A. Freitas and J. J. M. Órfão, *Ind. Eng. Chem. Res.*, 2007, **46**, 4110-4115.
16. M. Yabushita, H. Kobayashi, K. Hara and A. Fukuoka, *Catal. Sci. Technol.*, 2014, **4**, 2312-2317.

Conclusions

Lignocellulosic biomass is a carbon-based renewable feedstock that is uniquely suited for the sustainable production of fuels and chemicals. The utilization of biomass is necessary to reduce the dependence of chemical industries on fossil fuels. Cellulose is the most abundant component in lignocellulosic biomass which is a polymer composed solely of repeated anhydro-glucose units (AGU) linked by β-1,4-glycosidic bonds. The transformation of cellulose is a promising approach to synthesize value-added chemicals. Cellulose is inedible by human beings, therefore, the large-scale processing of cellulose to fuels and chemicals will not cause a competition with food supplies. Cello-oligosaccharides are short chain linear polymers which can be produced by the partial depolymerization of cellulose. They are biologically active molecules that can provide multiple benefits to healthcare and agriculture industries. However, commercial use of cello-oligosaccharides is not possible due to the high cost of their synthesis. Therefore, the aim of this thesis is to selectively synthesize cello-oligosaccharides from cellulose. The first part of this thesis is concerned with survey of the reported technologies for partial depolymerization of cellulose. A major challenge in this process is that cello-oligosaccharides are always obtained as intermediates and undergo rapid hydrolysis to form glucose. The prevention of degradation of cello-oligosaccharides is significant to achieve high amounts of desired products. In addition, heterogenous catalysts, such as carbon material, are expected as the suitable catalyst for cellulose hydrolysis due to the advantages in cost reduction, catalyst separation and benign process.

In **Chapter 2**, the synthesis of cello-oligosaccharides from the hydrolysis of cellulose was performed by using a carbon catalyst. An innovative semi-flow reactor was developed for the reaction in which the products could be rapidly removed from

the reaction system, preventing their successive hydrolysis. Carbon catalyst (AC-Air) was synthesized by the air oxidation of activated carbon to introduce weakly acidic functional groups without altering the microporous structure. The catalyst showed high cellulose hydrolysis activity in combination with the semi-flow reactor to achieve a cello-oligosaccharide yield of 72 %. The presence of acidic functional groups and the adsorption of cellulose on carbon by mix-milling were both crucial for this high activity. In addition, a method for quantitative analysis of individual cello-oligosaccharides in the mixture was developed, which is difficult due to their very similar molecular structure. Cello-oligosaccharides with a DP up to 13 were observed with cellohexaose and celloheptose obtained as the major products at an SV of 70 h^{-1}. The product distribution was controlled by adjusting the space velocity of the reaction. For example, by reducing the space velocity, cellotriose can be obtained as the primary product instead of cellohexaose. ^{1}HNMR and FTIR analysis confirmed the structure of β-1,4-linked straight-chain cello-oligosaccharides and the absence of branching or impurities.

In order to understand the underlying mechanism that promotes rapid cellulose hydrolysis and reduces glucose formation from cello-oligosaccharides, a kinetic analysis of cello-oligosaccharide hydrolysis was performed in the presence of various catalysts in **Chapter 3**. The results showed that the rate of hydrolysis of individual cello-oligosaccharides was strongly dependent on their chain length in the presence of carbon catalyst. Larger cello-oligosaccharides underwent hydrolysis at a much faster rate. For example, carbon catalysts favored hydrolysis of larger cello-oligosaccharides with an 11-fold increase in reaction rate constant from cellobiose to cellohexaose. This behavior was unique to carbon catalyst, and other solid catalysts showed no such trend. The difference in rate constant of hydrolysis with chain length explains the accumulation of cello-oligosaccharides in the presence of carbon catalyst with low yield

of glucose during the cellulose hydrolysis in **Chapter 2**. Larger cello-oligosaccharide showed a stronger affinity towards adsorption over the narrow micropores of the carbon surface. This increase in adsorption affinity of cello-oligosaccharides alone was not sufficient to explain the change in hydrolysis rate. Further study revealed a decrease in apparent activation energy for hydrolysis with respect to increase in DP. Based on these observations, a plausible mechanism is proposed that larger molecules experience a greater degree of conformational distortion during their adsorption within the micropores of carbons. This leads to reduction in activation energy required to cleave the glycosidic bond and enhances the rate of reaction. In addition, a preference for hydrolysis of terminal over internal glycosidic bonds of cello-oligosaccharides was observed, which was analogous to some enzymes in the cellulase family.

The results in **Chapter 2** and **Chapter 3** reveal that carbon catalysts exhibit high activity for partial hydrolysis of cellulose to cello-oligosaccharides and the rate of hydrolysis increases with DP. Although reduction in space velocity can enhance the secondary hydrolysis of larger cello-oligosaccharides to low DP molecules, the formation of glucose also increases due to the preferred hydrolysis of terminal glycosidic bonds. Therefore, in order to produce high yield of low molecule cello-oligosaccharides (G3-G6), it is better to obtain the product directly from the depolymerization of cellulose rather than the successive hydrolysis of larger cello-oligosaccharides. Increasing the acidity of carbon catalyst can achieve this objective. Therefore, in **Chapter 4**, a novel oxidation method was developed for the modification of activated carbon with the aim of introducing high density of weakly acidic functional groups. Chemical oxidation with ammonium persulfate (APS) was an efficient method for introducing high amounts of acidic functional groups, especially carboxyl groups. This catalyst, named AC-APS, provided 70 % yield of cello-oligosaccharides after

reaction in a semi-flow reactor. Owing to the high density of acidic functional groups, the total yield of smaller oligosaccharides (G3-G6) increased to 50 %.

This work investigates the transformation of cellulose to versatile cello-oligosaccharides and elucidates the mechanistic insights β-1,4-glycosidic bond hydrolysis over carbon catalyst. Future work should focused on reducing the requirement of pretreatment to enhance the contact between cellulose and carbon catalyst. Current technology relies on mix milling to improve the contact and adsorb cellulose on carbon surface, which requires a substantial amount of energy. Development of a novel catalyst that can remove the requirement of mix milling and directly depolymerize crystalline cellulose to cello-oligosaccharides is promising approach for the large-scale application in industries. In addition, detailed study on the unique behavior of preferential hydrolysis of terminal glycosidic bonds over carbon catalyst is necessary to understand the similarities between enzymes and heterogeneous carbon catalysts during cellulose hydrolysis.

List of Publications

Journal publications

Pengru Chen, Abhijit Shrotri and Atsushi Fukuoka, Soluble cello-oligosaccharides produced by carbon-catalyzed hydrolysis of cellulose. *ChemSusChem*, **2019**, 12, 2576-2580.

Pengru Chen, Abhijit Shrotri and Atsushi Fukuoka, Unraveling the hydrolysis of β-1,4-glycosidic bonds in cello-oligosaccharides over carbon catalysts. *Catalysis Science & Technology*, **2020**, 10, 4593-4601.

Pengru Chen, Abhijit Shrotri and Atsushi Fukuoka, Carbon catalyst with high density of carboxyl groups for the hydrolysis of cellulose to cello-oligosaccharides. (In preparation)

Pengru Chen, Abhijit Shrotri and Atsushi Fukuoka, Catalytic synthesis of oligosaccharides from cellulose. (In preparation)

Journal publications (not related to this thesis)

Pengru Chen, Qi Zhang, Riyang Shu, Ying Xu, Longlong Ma and Tiejun Wang, Catalytic depolymerization of the hydrolyzed lignin over mesoporous catalysts. *Bioresource Technology*, **2017**, 226, 125-131.

Conference Contributions

Pengru Chen, Abhijit Shrotri and Atsushi Fukuoka, Carbon catalyzed hydrolysis of cellulose to cello-oligosaccharides in a semi-flow reactor, *The 125th Catalysis Society of Japan*, Tokyo, Japan, March 27, **2020** (Oral)

Pengru Chen, Abhijit Shrotri and Atsushi Fukuoka, Kinetic study of cello-oligosaccharides hydrolysis over carbon catalysts, *The 124th Catalysis Society of Japan*, Nagasaki, Japan, September 18, **2019** (Oral)

Pengru Chen, Abhijit Shrotri and Atsushi Fukuoka, Carbon catalyzed hydrolysis of

cellulose to synthesize cello-oligosaccharides in a semi-flow reactor, *The 14th European Congress on Catalysis*, *EuropaCat 2019*, Aachen, Germany, August 19, 2019. (Oral)

Pengru Chen, Abhijit Shrotri and Atsushi Fukuoka, Selective synthesis of cello-oligomers by hydrolysis of cellulose over carbon catalyst, *The 122th Catalysis Society of Japan*, Hakodate, Japan, September 27, **2018**. (Oral)

Pengru Chen, Abhijit Shrotri and Atsushi Fukuoka, Synthesis of cello-oligosaccharides by hydrolysis of cellulose in a semi-flow reactor, *ICAT-BIC Students' workshop*, Sapporo, Japan, November 21, **2018**. (Oral)

Pengru Chen, Abhijit Shrotri and Atsushi Fukuoka, Kinetics of β-1,4-glycosidic bond hydrolysis in cello-oligosaccharides over carbon catalysts, *IRCCS the 3rd Joint International Symposium*, Nagoya, Japan, January 31, **2020**. (Poster)

Pengru Chen, Abhijit Shrotri and Atsushi Fukuoka, Carbon catalyzed hydrolysis of cellulose to synthesize cello-oligosaccharides in a semi-flow reactor, *IRCCS The 5th Symposium*, Sapporo, Japan, November 11, **2019**. (Poster)

Pengru Chen, Abhijit Shrotri and Atsushi Fukuoka, Selective synthesis of cello-oligosaccharides by hydrolysis of cellulose over carbon catalyst in a semi-flow reactor", *IRCCS the 2rd Joint International Symposium*, Kyoto, Japan, January 25, **2019**. (Poster)

Pengru Chen, Abhijit Shrotri and Atsushi Fukuoka, Selective synthesis of cello-oligosaccharides by hydrolysis of cellulose over carbon catalyst in a semi-flow reactor", *The 14th Hokkaido University-Nanjing University-NIMS/FMCU Joint Symposium*, Sapporo, Japan, December 07, **2018**. (Poster)

Pengru Chen, Abhijit Shrotri and Atsushi Fukuoka, Selective synthesis of cello-oligosaccharides by hydrolysis of cellulose over carbon catalyst in a semi-flow reactor", *Hokkaido University-National Central University Joint Symposium on Materials Chemistry and Physics*, Sapporo, Japan, November 15, **2018**. (Poster)

Pengru Chen, Abhijit Shrotri and Atsushi Fukuoka, Selective synthesis of cello-oligosaccharides by hydrolysis of cellulose over carbon catalysts", *Pre-TOCAT 8*, Sapporo, Japan, August 03, **2018**. (Poster)

Acknowledgements

Time passes so fast without notice. Three-years journey for PhD degree is coming to the end. Within this period, I have improved not only in my research ability, but also the interpersonal skill, which cannot be achieved without the help and support of a lot of people. By this chance, here, I would like to express my gratitude to many of those who contributed to this thesis.

First and foremost, I want to thank my supervisor, Prof. Atsushi Fukuoka. Thank you for providing me this opportunity to pursue my PhD degree in this team. I really appreciate your kind guidance on my research topic with your broad and fruitful knowledge. You always tell us a good researcher should keep critical thought and attitude towards research and come up with new concept to expand the way of thinking. I learned a lot from your inspiring ideas and logical mind, which helped me to be a qualified PhD graduate. Moreover, thank you for offering me a lot of opportunities to attend many important conferences and present my study, from which I met many famous researchers worldwide and know more interesting work. I also improve my confidence from these wonderful experiences. Furthermore, I appreciate that you spent time on checking my papers and thesis and encourage me to do my best in my defense. Thank you very much.

I would like to thank Dr. Kiyotaka Nakajima as my sub-advisor. Thank you for giving me valuable suggestions in my study. You were always attentive towards my research progress and recommended me to obtain deeper insights on the reaction process. Discussions with you always enlightened and inspired me to explore more possibility in the research. I appreciate your help for checking my thesis and giving comments during my preparation for defense. Furthermore, I want to express my

sincere gratitude to you for the following encouraging words, “I am convinced of your great success as a scientist after PhD,” when I was confused about my future. It really inspired me, and I recognized what I want to do and which way I will go forward. I appreciate all your help and support during my job hunting. In addition, thank you for often inviting me to Chinese dumpling restaurant. It was really tasty. Thank you very much.

Deep thanks to my daily supervisor, Dr. Abhijit Shrotri. I am very grateful for all your guidance and help during these three years, especially the early time when I came here. You introduced to me the operating principle of all instruments for the study and taught me how to use them. You helped me to set up my reaction system and establish my study framework. You guided me to have a logical thought process to analyze experiment results. I learned a lot from you not only the capacity for scientific research, but also the technical skills. You gave me a lot of freedom to do my work, but when I faced problems or went in the wrong way, you helped me to solve it in time. Timely communication with you led me to the right direction and accelerated my progress. Your optimistic attitude towards research always encouraged me to be positive. Thank you for spending your time checking and correcting my papers and thesis. I enjoyed the time working with you and gratitude the knowledge and experience you shared with me. I will always remember that you told me, “you have the ability, you can do research independently”. Thank you very much.

I would like to thank Dr. Hirokazu Kobayashi. You have rich knowledge in cellulose utilization field. Every key question you asked during the discussion has prompted me to learn more and become fruitful. Thank you for spending time on my practice for PhD defense. All the comments and encouragement make me face it with more confidence. I also appreciate your recognition of my improvement in research

within these three years, which really inspired me. Thank you very much.

I would like to thank the committee members, Prof. Kei Murakoshi, Prof. Shin Mukai and Prof. Jun-ya Hasegawa. Thank you a lot for spending your time to review this work and attend my defense. I am grateful to AGS Office for providing me support for studying in Japan.

Many thanks to those in my group who provided me help from different aspects. At first, our awesome secretary, Hiromi Matsushima, thank you for dealing with all the forms and processes throughout my PhD. You always give me a hand when I feel confused or puzzled with Japanese documents. When I have difficulty with Japanese-speaking people, you always help me to communicate without hesitation. Talking with you made me really happy. To Dr. Takuya Sagawa, I enjoyed the time when you were in the team. You are so friendly and unassuming to everyone. My Japanese improved a lot by talking with you. You work very hard and always stay in office very late at night, which inspired me to work more. The time when we went to ARCS together after working would be my unforgettable memory. Dr. Shazia, thank you for all the awesome time and trips. You shared me a lot of life experience and gave me many advises. I really miss the time with you. Dr. Etty, happy to be together with you everyday. You always accompany me at night when I need to work late in office. I will never forget the time when we go to ARCS and go home together at night. All activities you organized making our life colorful. Dr. Daniele, the time with you is always full of laughing. Thanks for correcting my English pronunciation.

I would like to express my gratitude to Dr. Lingcong Li. Like my elder sister, you always encourage me when I have difficulty or depression. I enjoy the time talking with you, which is comfortable and happy. The Chinese food you cooked is amazing. Thank you always inviting me for meal. Because of you, I rarely feel lonely in Japan. To

Nazmul and Yayati, even though you are younger than me, you know more knowledge in chemistry. Thank you for sharing your knowledge with me and teaching me the instruments in the lab. Discussions with you always make me productive. I wish you great success in PhD period and future career. To Cheng Yang, thank you for your kind help in the early stage when I first came to Japan. Hope everything goes well with you. To Natsumi and Miyuki, I have a good time working and playing with you. You always take responsibility to do things in the lab and office. Thank you for teaching me Japanese, and the trips with you are unforgettable. To Kato, Yakuwa, Suzuki and Endo, it is pleased having you in the group. You are friendly to foreign members. I wish you success in your future career. Special thanks to Suzuki, thank you for being our driver for all trips, which made the journey convenient and relaxing. And I am so grateful for your help in dealing with all the Japanese phone calls and procedures for me.

Last but not least, I would like to express my appreciation to my friends in China and my dear family. To Xinyan Xie, Congcong Liu and Furong Han, I'm so lucky to have you as friends more than 15 years. Thanks for your concern and support. Looking forward the next trip with you. To Peipei Zhang, thank you always being my side no matter what happens. Your encouragement stimulates me to remain confidence and move forward. 对我亲爱的哥哥和嫂子，谢谢你们对我到国外留学的支持和理解。感谢你们对我的惦记和关怀。有你们在国内照顾爸妈才让我放心的投身于我的学业。对我亲爱的爸妈，忠心的感谢你们给与我如此和谐温暖幸福的家庭，谢谢你们对我一如既往的支持和鼓励。感谢你们默默的付出。我爱你们。

Pengru Chen

2020.08.28